Summer 1977

Optimal Control of a Large Space Telescope Using an Annular Momentum Control Device

Arun Anant Nadkarni
Old Dominion University

OPTIMAL CONTROL OF A LARGE SPACE TELESCOPE USING AN ANNULAR MOMENTUM CONTROL DEVICE

by

Arun Anant Nadkarni
B.E., June 1966, Bangalore University, India
M.E., Aug. 1968, Indian Institute of Science, India
M.S., May 1975, Pennsylvania State University

A Dissertation Submitted to the Faculty of
Old Dominion University in Partial Fulfillment of the
Requirements for the Degree of

DOCTOR OF PHILOSOPHY

MECHANICAL ENGINEERING AND MECHANICS

OLD DOMINION UNIVERSITY
August 1977

Approved by:

ABSTRACT

OPTIMAL CONTROL OF A LARGE SPACE TELESCOPE
USING AN ANNULAR MOMENTUM CONTROL DEVICE

Arun Anant Nadkarni
Old Dominion University, 1977
Director: Dr. W. J. Breedlove, Jr.

Application of a new development in the field of momentum storage devices, the Annular Momentum Control Device (AMCD), to the twin problems of large angle maneuvers and fine pointing control is considered. The basic concept of the AMCD consists of a spinning rim, with no central hub area, suspended by a minimum of three magnetic bearings, and driven by a noncontacting electromagnetic spin motor. The dissertation considers in detail the design of an optimal controller to achieve both the large angle maneuvers and the fine pointing control of a Large Space Telescope (LST) with a single configuration, consisting of a single AMCD mounted in a single gimbal.

The problem of designing an optimal controller is accomplished in two parts: (1) an optimal controller for generating the open-loop, control law for the nonlinear maneuvering problem was designed using a modified Gradient technique with penalty functions, and (2) an optimal stochastic controller for generating the constant gain, state estimate feedback control law for the stochastic linear fine pointing problem was designed using the Newton-Kleinman iterative procedure.

The open-loop, optimal control law for the high order (15)

maneuvering problem was derived iteratively incorporating "hard" constraints on the magnitudes of the state and control variables. A general, readily available, user oriented computer program was developed to derive the open-loop, optimal control law history using this procedure for a general, high order (up to 25), nonlinear system. The program was used to achieve the design objective of deriving the open-loop, optimal control law to retarget the LST from one stellar target to another with a minimum expenditure of energy. A specific example problem involving a maneuver of the LST through a prescribed reorientation ($\simeq 20^{o}$) was solved. It was shown that the convergence of the iterative procedure to a local minima was highly dependent on 1) the initial control history chosen, 2) the initial choice of weighting matrices, and 3) the choice of the elements of these weighting matrices during the convergence.

The fine pointing stochastic linear problem was shown to be uncontrollable. The optimal state estimate feedback control law for the fine pointing controller was derived using Linear-Quadratic-Gaussian (LQG) optimal regulator theory. Structurally, this controller consists of an optimal regulator and a Kalman-Bucy filter. Existing techniques to compute the initial stabilizing gains and iterative procedures to solve the algebraic Riccati equation were extended to the present problem which is uncontrollable. This extension was made by modifying the state equations in order to make the regulator problem stabilizable. It was shown that initial errors in the states can be nulled satisfactorily by the optimal regulator designed. The performance of the fine

pointing controller was investigated by performing a linear covariance analysis to obtain the RMS pointing errors. The analysis indicated that fine pointing accuracies of less than 1 arcsecond can be achieved.

ACKNOWLEDGEMENT

I wish to express my sense of gratitude to Dr. Willard W. Anderson and Nelson J. Groom of NASA Langley Research Center, for suggesting the problem for my doctoral dissertation. The problem turned out to be an extremely interesting one, enabling me to gain an extensive insight into both the dynamics and the control aspect of the spacecraft attitude control. I had many discussions with both of them which provided me with a clearer view of the dynamics of the problem. I owe the interesting derivation of the expressions for torque outlined in Appendix B to Dr. Anderson. The derivation of the expressions for forces in Appendix C is based on this.

I also wish to thank Dr. W. J. Breedlove, Associate Professor of Engineering, Department of Mechanical Engineering and Mechanics, for serving as the Chairman of the Dissertation Committee and taking keen interest in the problem throughout the course of this work.

My sense of gratitude and indebtedness to Dr. Suresh M. Joshi, Research Assistant Professor, ODU Research Foundation, cannot be expressed in words. I consider myself very fortunate to have been able to associate with Dr. Joshi throughout the course of this work. He introduced me very patiently to the interesting field of Modern Control Theory and its applications. His valuable experience in a related field of Annular Suspension and Pointing System (ASPS) was of tremendous help to me while formulating the Optimal Controller design problem in the present case. I could always draw upon his

extensive experience in the design of Kalman-Bucy filter and he would always, without hesitation, and cheerfully discuss various aspects of the filter theory with which I had no prior familiarity. In addition to the close professional relationship, we also developed a close personal friendship. This sense of personal friendship helped me to a great extent during the difficult days of student life.

Messrs. Ralph Will, Gerald Sisson, and Ms. Carolyn Grantham helped me to a great extent in debugging the tedious computer programs. Their extensive experience in this field would greatly simplify the problem of finding a mistake in the program, specially of the magnitude involved in the nonlinear problem. I wish to acknowledge their help and express my grateful thanks to them.

I also wish to thank my wife, Aparna, for giving me constant companionship during the difficult days of student life. Even though she herself was equally busy, she would always, and without my knowledge, reduce the domestic burden on me so that I could devote myself fully to the work. Inspite of this, however, the writing of this dissertation was slowed down a little because of my deep involvement with another sweet girl who appeared in our life during the final period of this work. But for Arti, our daughter, the work would have been completed earlier, but nobody seems to have any regrets.

Last, but not least, I owe my deepest sense of gratitude and indebtedness to my parents, Anant and Anasooya, who, without any complaints or inhibitions whatsoever, stood firmly behind me all these years and patiently waited for the completion of the work. In

appreciation, I wish to dedicate this work to them.

Finally, I wish to thank Old Dominion University for granting financial support during the major portion of this work under ODU-NASA Aeronautics Research Participation Program (Grant No. NGR 47-003-052). I also wish to thank Mr. Nelson J. Groom for granting financial support during the final phase of the work (Grant No. NAS1-14193-20) for developing a general, user-oriented computer program for nonlinear optimization problem, a specific example of which was solved in the present dissertation as an optimal maneuvering problem.

TABLE OF CONTENTS

List of Figures

List of Tables

Notation and Abbreviations

Symbols

A	Coefficient matrix premultiplying the state vector x in the linear state equation,
B	Coefficient matrix premultiplying the control vector u in the linear state equation,
C	Coefficient matrix premultiplying the state vector x in the linear measurement equation,
E	Expected value of,
F	Force vector,
f	Right hand side of the nonlinear state equation,
G	Optimal controller gain matrix; also, weighting matrix for terminal deviation,
g	Control variable inequality constraints; also, nonlinear measurement equation,
H	Optimal filter gain matrix; also, Heaviside function; also Angular Momentum vector,
h	State variable inequality constraint,
I	Inertia matrix; also, identity matrix,
J	Performance index or cost function,
J_d	Cost function for the deterministic problem,
J_s	Cost function for the stochastic problem,
ΔJ	Decrease in J,
K_o	Time Varying Riccati matrix,
K	Constant value of K_o,
K_a	Spring constant for axial bearings

Symbols

K_a	Damping constant for axial bearings
K_c	Weighting constants of Heaviside functions to penalize control constraints,
K_R	Spring constant for radial bearings
K_R	Damping constant for radial bearings,
K_s	Weighting control constraints, state constraints,
K_λ	Defined as $= 1.5\ r^2\ K_a$ (App. B)
K_λ	Defined as $= 1.5\ r^2\ K_a$ (App. B)
ℓ_1	Distance of the center of mass of gimbal 0_g from 0_{gs}
m	Mass; also, order of the control vector u,
N	Terminal state manifold for the target set; also, covariance intensity matrix,
n	Order of the state vector x; also, white noise vector,
o	Origin of the coordinate frame,
Q	Weighting matrix for integral state penalty,
R	Weighting matrix for integral control penalty,
r	Order of the output vector y or the measurement vector z; also, distance $0_{gs}0_g$ (Fig. 14),
T, t_f	Final time,
Tg	Gimbal torquer torque,
Ts	Spin torque,
t	Independent variable, time,
u	Control vector of dimension m,
v	Actuator control voltages,

Symbols

x	State vector of dimension n; also, inertial motion of the subscripted body,
x'	Reduced state vector used for controller design, Eqn. (134),
y	Output vector of dimension r,
z	Measurement vector of dimension r,

Coordinate Frames

$O_a X_a Y_a Z_a$	A nonrotating frame centered at the center of mass of the rim,
$O_g X_a Y_g Z_g$	A body fixed frame centered at the center of mass of the gimbal ring,
$O_{gs} X_{gs} Y_{gs} Z_{gs}$	A reference frame centered at the center of mass of LST-gimbal and parallel to $O_g X_g Y_g Z_g$

Greek Symbols

α	A constant, = 2 for minimum time problem, = 0 for minimum energy problem,
β_o, β_1	The angle by which bearing station 1 is offset from $O_g Y_g$,
β_2	Defined as $(60^o - \beta_1)$,
β_3	Defined as $(60^o + \beta_1)$,
γ	Angle defined in Appendix B, C,
δ, δ_1	Angle defined as $\theta_{g_1} - \beta_1$; also, impulse function,
δ_2	Defined as $(60^o - \delta_1)$,
δ_3	Defined as $(60^o + \delta_1)$,
ε	Relative displacement vector between gimbal ring and rim, = $x_a - x_g$,

Greek Symbols

ζ	Modified state vector of equation (101),
η	Actuator noise vector in the control voltages v,
Θ	Covariance intensity matrix of θ,
θ	Measurement noise vector; also, Euler angles,
λ	Costate vector (Lagrange multipliers) of dimension η,
Ξ	Covariance intensity matrix of ξ,
ξ	Plant noise vector (actuator noise, disturbance etc.),
Σ	Covariance intensity matrix of the initial state x_o,
τ	Torque vector,
ϕ	Functional form of integral penalty of cost function,
χ	Modified state vector of equation (108),
ω	Angular velocity vector.

Special Symbol

$[\omega]$	Cross product matrix of form defined in equation (2),

Superscripts

$\cdot$	Differentiation with respect to time,
$-$	Average value,
$\hat{}$	Optimal estimate

Subscripts

a	Axial or rim
g	Gimbal
gs	LST-gimbal
o	Nominal value or steady state value
r	radial
sat	Saturation value
f	Final value

Abbreviations

AMCD	Annular Momentum Control Device
C-G	Conjugate Gradient
DFP	Davidon-Fletcher-Powell
LQG	Linear-Quadratic-Gaussian
LQ	Linear-Quadratic (regulator problem)
LG	Linear-Gaussian (estimator problem)
MMS	Minimum-mean-squared
RMS	Root-mean-squared

Chapter 1

INTRODUCTION AND SUMMARY

From a comparatively early stage in the history of the "space age," the concept of using stored angular momentum for the purpose of controlling the attitude of artificial satellites has been applied almost universally. This concept has proven advantageous when extreme pointing precision is required and when either environmental contamination or excessive fuel use prohibit reaction jet usage. Applications of (the stored angular momentum) concept include spinning spacecraft (e.g., TIROS), dual-spin spacecraft (e.g., OSO), momentum wheel stabilized spacecraft (e.g., ITOS), reaction wheel stabilized spacecraft (e.g., OAO), and the control moment gyro (CMG) system, (e.g., SKYLAB). Many other concepts for stabilization and attitude control of spacecraft have been suggested, such as chemical thrusters, cold gas jets, magnetic torquers, electric ion engines, reaction spheres, gravity gradient and reaction booms stabilization, solar pressure panels, and aerodynamic surfaces.

Most of the "active" stabilization methods mentioned above, i.e. those using power or fuel (e.g., chemical thrusters, cold gas jets, etc) impose a payload penalty on the spacecraft due to the weight of fuel carried aboard. In addition, after the expenditure of this fuel, there is no means of either stabilizing or controlling the spacecraft attitude. The method of employing aerodynamic surfaces for attitude control suffers from the obvious limitations that it can only

be used for very low-orbit satellites. The method of gravity gradient stabilization, although a very tempting candidate, can produce only limited pointing accuracies. This, along with the incessant oscillations of the spacecraft, rule out this method for all spacecraft, but those requiring very crude stabilization.

The major disadvantages of the "active" control and stabilization methods indicate that the only viable method of attitude stabilization of spacecraft - which are required to operate for a long duration of time or which require stringent limitations on the attitude history - should utilize the concept of stored angular momentum.

It may seem that all satellites may be inertially stabilized using the simple technique of spin stabilization by imparting a nominal spin to the satellite. This method proves quite satisfactory for many scientific and meteorological satellites. Almost all textbooks on classical mechanics discuss the stability of a rigid body nominally rotating about a principal axis. Classical stability theorems show that rotation of a rigid body about the axis of maximum or minimum moment of inertia are stable while rotation about the axis of intermediate moment of inertia is unstable. On the basis of this widely accepted stability criteria, Explorer I was spin "stabilized" by spinning it about its "long axis" i.e. its axis of minimum moment of inertia. The unfortunate instability and subsequent tumbling of Explorer I in orbit brought to light a fundamental error made in the design process in which the effect of energy dissipation on the above stability criteria was ignored.

A theorem due to Liapunov [1] states that, if the potential energy of a conservative holonomic system has a maximum (or has no minimum) in an equilibrium position, then that equilibrium position is unstable. This theorem can be extended to nonconservative systems to prove that if damping is present, then the equilibrium position remains unstable. It can also be shown that the equilibrium position is unstable, even in the presence of gyroscopic stabilizing forces, when dissipative forces are present [1]. It can be proven using the above theorems that pure spin about a principal axis of minimum moment of inertia for a freely rotating rigid body represents an unstable equilibrium state. In addition, pure spin about the principal axis of maximum moment of inertia represents a stable equilibrium state [2].

In view of the above realization, it became mandatory that any satellite, intended to be stabilized by this simple technique, be spun about its axis of maximum moment of inertia. This may not always be practical. This undesirable constraint, along with the need to provide specific acceleration environments such as 1) an unaccelerated (zero g) laboratory area for instrument packages or 2) an artificial gravity environment for the crew members of manned spacecraft, led to a new concept, viz., dual-spin (or multi-spin) spacecraft. The concept of dual-spin spacecraft was discussed by Landon and Stewart [3] and Iorillo [4]. A stability analysis for dual-spin spacecraft has been presented by Likins [5] and Mingori [6], in which Routh and Floquet analyses were made utilizing some specific types of energy dissipation mechanisms. The stability criterion was obtained through an

approximate energy-sink analysis in a compact form. In 1955, Stuhlinger [7] discussed the use of reaction wheels for attitude control. Methods using stored angular momentum also have major disadvantages as well as advantages as pointed out e.g., by Anderson and Groom, [8]. Thus, spinning a spacecraft (or portion of it, as in dual-spin satellites) to achieve attitude stability is simple and reliable, yet the spacecraft itself cannot be utilized fully because of its rotation. Also, any momentum axis reorientation maneuvers require external torques for momentum precession and the artificial gravity produced may run counter to payload requirements for zero gravity. Stabilizing the spacecraft by utilizing a momentum wheel which provides gyroscopic stiffness equivalent to spinning the vehicle itself allows a nonspinning spacecraft and permits arbitrary orientations about the roll axis for the purpose of pointing onboard experiments. However, this technique does not overcome the inability to reorient or maneuver the spacecraft about all three axes without external torques since the spin axis of the momentum wheel is fixed with respect to the spacecraft. The use of three reaction wheels aligned with the spacecraft axes allows complete spacecraft active attitude control. However, reaction wheel momentum must be limited to relatively low amounts because of an excessive requirement for power when directly producing a torque on a rapidly spinning flywheel. The limitation on reaction-wheel momentum can be overcome by using a control moment gyro (CMG) system, which uses constant speed wheels and developes precession torques through controlled slewing of gimballed

flywheels. However, to achieve the smooth low-level torques necessary for fine pointing requires precise control of very low gimbal slew rates. These low rates are inherently limited by the requirement for high servo stiffness and thus, high friction torque. These difficulties cannot be overcome unless extreme mechanical precision and resultant high costs are involved.

A new development in the field of momentum storage devices, the Annular Momentum Control Device (AMCD) [9] was recently formulated and patented at the NASA Langley Research Center. The basic concept consists of a spinning rim, with no central hub area, suspended by a minimum of three magnetic bearings, and driven by a noncontacting electromagnetic spin motor, Figure 1. A detailed description of the AMCD is given in reference [8]. Thus, this spin assembly configuration design is based on space usage (vacuum and zero gravity) rather than of conventional terrestrial design of using shaft driven steel flywheels with ball bearings.

The major advantages of this device used as a momentum storage unit, are described in detail in reference [8], and are as follows:

"1) The rotating element (spinning rim) approaches a thin rim which is the optimum shape for a given stress-limited material when maximizing momentum for a given mass of material and for a given maximum radius.

2) The thin rim configuration allows a unidirectional filament layup of composites; thus, allowing the maximum usage of these high strength-weight materials.

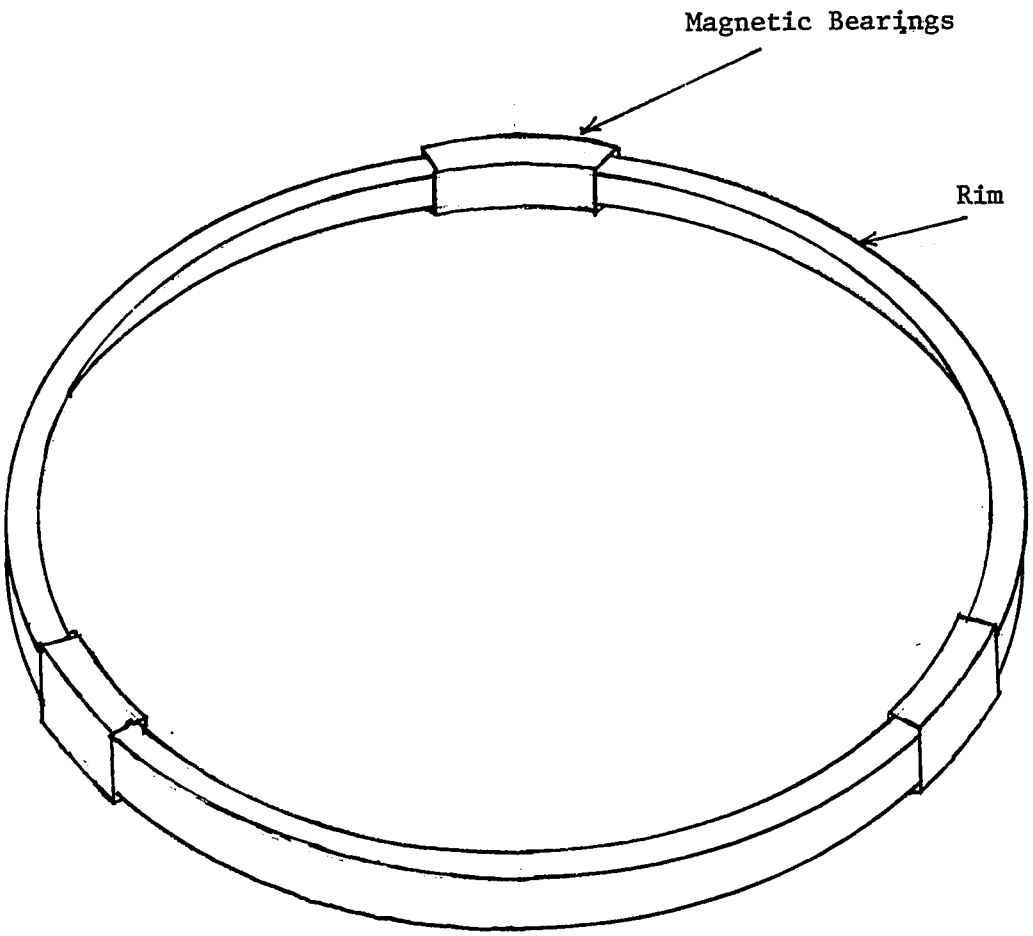

Figure 1. Annular Momentum Control Device Concept

3) The configuration allows, where possible and desirable, the use of a large rim diameter with the inherent additional increase in momentum-mass (H/m) ratio.

4) The noncontacting magnetic bearings and drive motor eliminate mechanical friction and wear and should yield a device reliability equal to that of the solid state circuits.

5) The isolation of the rotating rim from the spacecraft affords an effective control over the transmittal of rim vibration to the spacecraft when active magnetic bearings with no permanent magnetism are used.

6) The magnetic bearings also provide the capability for directly producing torques on the spacecraft with no mechanical or electrical breakout torques involved.

7) For the "passive" mode of spacecraft control (when compared with single-spin, dual-spin, or gyrostat control), much improved precessional damping can be shown theoretically.

8) For the "passive" mode of spacecraft control, smaller attitude errors caused by environmental torques will result from the higher momentum allowed by the AMCD for a given momentum storage weight.

9) For the "active" mode of spacecraft control, extreme precision fine pointing is projected since extremely low spacecraft control torques can be easily generated

with the magnetic bearings used as spacecraft torquers driven by spacecraft attitude sensors.

10) The configuration of spinning rim, with no central hub area, also allows the mounting of this unit outside the spacecraft, thus releasing the much needed payload space within the spacecraft," Figures 2 and 3.

The purpose of this dissertation is to design an optimal controller, using the AMCD concept, to provide fine pointing control and the capability for large angle maneuvers for a spacecraft such as the Large Space Telescope (LST). These maneuvers can be accomplished in a variety of ways by using one or more AMCD's [8]. A particular potential configuration, utilizing a single AMCD mounted in a single gimbal is considered in this dissertation. The configuration is shown in Figure 3. This particular configuration was chosen since both fine pointing control and large angle maneuvers can be achieved effectively with a single configuration. In addition, utilizing a single gimbal results in a considerable savings in weight, which would otherwise be added with the addition of each outer gimbal. The mounting of the gimbal on extended arm as shown also makes it very convenient to be stowed at the end of the circular face of the spacecraft at the time of launching and deployed after insertion in the proper orbit.

The design of the optimal controller is accomplished in two parts:

1) An open-loop optimal controller for the large angle

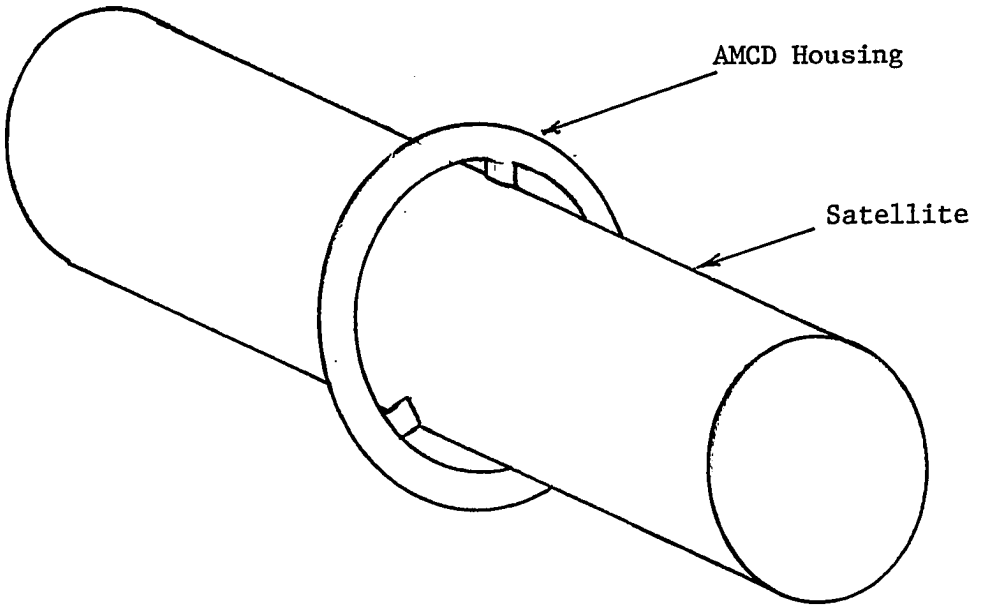

Figure 2. Fine Pointing AMCD Application

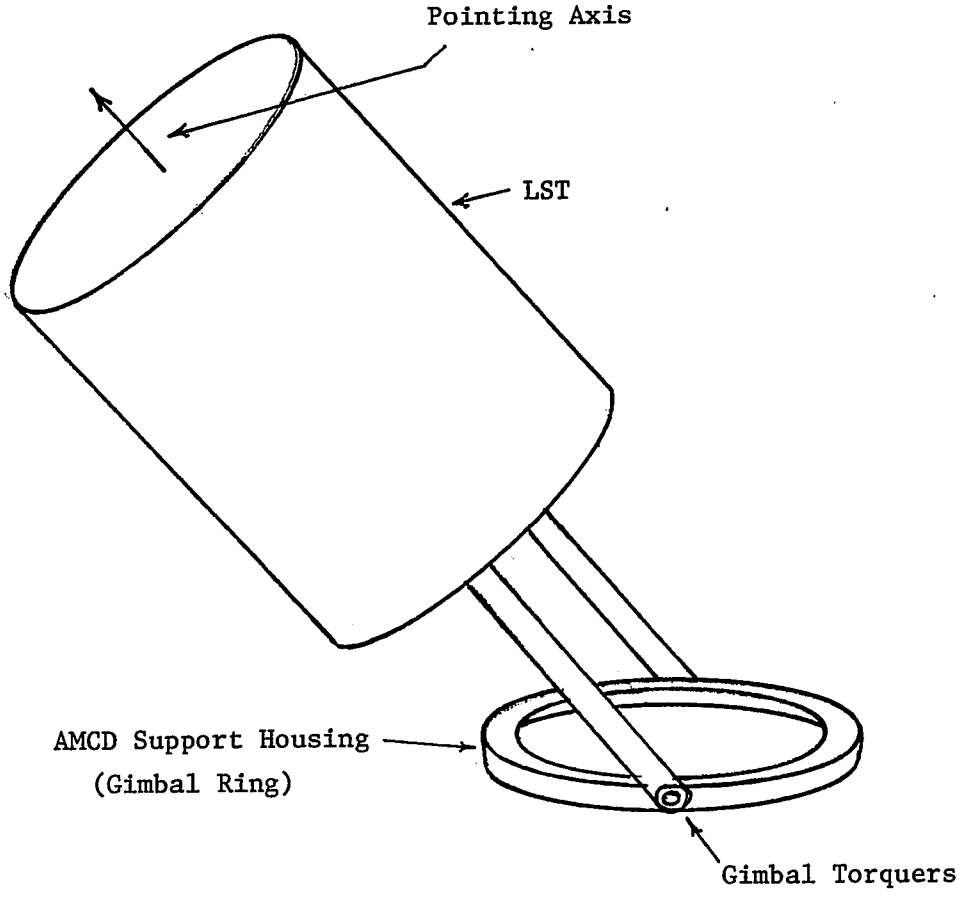

Figure 3. Single Gimbal AMCD Application

maneuvers is designed by using a numerical first-order gradient method incorporating penalty functions extended to function space,

2) A linear, time-invariant, stochastic, dynamic compensator for fine pointing control is designed by cascading a Kalman-Bucy filter design with an optimal regulator design produced independently.

In the design of the optimal controller for large angle maneuvers, the design objective is to derive the open-loop time history of the control forces and torques, which will retarget the LST from the given initial target to the next known target, with a minimum expenditure of energy. Thus, the performance criterion to be minimized for this mission includes an integral penalty on the power used (assumed to be proportional to the square of the control used) and a term to penalize the terminal deviation from the desired final target state manifold.

The presence of "hard" constraints on the magnitudes of both the state and the control variables are accounted for in this design.

In the design of the optimal stochastic controller for fine pointing, the design objective is to derive the control forces and torques as a closed-loop state feedback function, which will nullify the pointing errors with a minimum expenditure of energy. The performance criterion to be minimized, therefore, is the integral penalty on the power used (assumed proportional to the square of the control used).

The design allows for the presence of uncertain and unknown errors in actuator voltages (used to control the forces and torques) and in the measurement of states by instruments such as star trackers, rate gyros, proximity sensors, etc.

In Chapter 2, a detailed qualitative analysis of the motion of the LST-Gimbal-Spinning rim is done. The general equations of motion for the rigid bodies (LST-gimbal and the rim) are derived under the following assumptions:

1) The spacecraft momentum is limited to a small fraction (<1%) of the AMCD momentum; hence, the planes of the spinning rim and the gimbal ring remain nearly fixed in inertial space. Thus, small angle approximations can be made in terms involving the transverse angles,

2) The LST can rotate relative to the gimbal only about the gimbal torquer axis. This eliminates some of the terms containing the products of inertia,

3) Except for the relative motion about the torquer axis, the LST and the gimbal rotate as a single rigid body, i.e., both the bodies have the same angular velocities about the other two axes.

The general optimization problem for both the nonlinear case and the stochastic linear case is formulated in Chapter 3. A critical survey of the various numerical techniques available for the nonlinear problem is presented in Appendix L and the reasons for selecting the modified Gradient technique (in function space) with penalty functions

are pointed out. The iterative procedure to derive the optimal, open loop control law is outlined in sec. 3.1. The general stochastic Linear-Quadratic-Gaussian control problem is formulated in sec. 3.2. The problem is decoupled into two simpler problems, the Optimal Regulator and Estimator problems, utilizing the Separation Theorem presented in sec. 3.3. The solution of the Optimal Regulator problem is presented in sec. 3.4. Existing techniques to solve the resulting algebraic Riccati equation are discussed and extension of these techniques to the present problem, which is uncontrollable, is discussed by indicating the modifications of the state equations required to make the problem stabilizable. The solution of the optimal estimator (Kalman-Bucy filter) is presented in sec. 3.5 and the cascading of the Regulator and the Estimator is indicated in sec. 3.6. Finally, a linear covariance analysis required to evaluate the performance of the linear controller is outlined in sec. 3.7.

The final form of the equations of motion for the large angle maneuver case is presented in sec. 4.1 and the explicit form of the "hard" constraints on the state and the control variables are formulated in sec. 4.3. A specific example maneuver problem involving a reorientation of $\simeq 20^{\circ}$ is solved and the numerical results are discussed in sec. 4.3.

The final form of the equations of motion for the fine pointing case is presented in sec. 5.1. A specific example fine pointing problem is solved and the numerical results are discussed in sec. 5.2.

The computed open-loop, control law as applied to the LST-AMCD configuration considered here is capable of providing minimum energy large angle maneuvers to reorient the LST through approximately 20^{o}. The computed linear state estimate feedback control law is capable of nulling the initial errors in the angles and the rates in about 6-8 seconds, again using minimum energy.

Computation of these optimal control laws was found to be very expensive in terms of computer time and difficult in terms of implementation. Hence, a more simplified procedure for the design of the sub-optimal controllers for practical implementation is outlined in Chapter 6.

Chapter 2

DYNAMICAL SYSTEM MODEL

2.1 Qualitative Study of Spacecraft Motions and Control.- The spacecraft configuration consists of a single AMCD, suspended in a single gimbal. The gimbal in turn is mounted on an extendable yoke from the LST as shown in Figure 3. The coarse pointing or the large angle maneuvering of the LST is produced in an analogous manner to an Earth based telescope. Changes in the azimuth angle are generated by varying the spin rate of the spinning rim through controlling the electromagnetic spin motor. Changes in the elevation angle are generated by producing internal reactive torques between the AMCD and the spacecraft with the gimbal torquers. If the spacecraft angular momentum is limited to a small fraction of the AMCD angular momentum, then it can be seen that the momentum vector of the AMCD is nearly fixed in inertial space and the LST moves in a fashion similar to that of an Earth based telescope when subjected to the above controls. When the LST pointing axis is approximately aligned with the target, the gimbal torquer is locked and fine pointing is accomplished by torquing the gimbal ring (and hence the LST which is now locked with the ring) in the air gaps using electromagnetic actuators in the magnetic bearings against the AMCD momentum.

Tremendous simplification in the analysis can be achieved by noting that two of the bodies, viz., the gimbal ring and the

spinning rim are physically separated by magnetic actuator gaps. This allows the development of the equations of motion in two phases considering the gimbal ring (with the LST) and the spinning rim as two rigid bodies. After deriving the equations of motion for each body, the equations are coupled via the common magnetic forces and torques taken to be "external" for each body. Accordingly, consider the LST-gimbal as one body, with an additional degree of freedom in rotation about the gimbal torquer axis, and the spinning rim as the second body. No flexibility effects are considered. Now, the "external" forces and torques exerted by the axial and radial magnetic bearing actuators, the gimbal torquer and the spin torquer, impart translational accelerations to the centers of mass of both the bodies. In addition, since these forces do not pass through the mass centers of either body, both bodies would rotate. As examples of possible motions, consider first a pure spin maneuver about the AMCD spin axis and then a pure pitch maneuver about the torquer axis.

To perform a pure spin torquer maneuver as shown in Figure 4a, the spin torquer controls the spin rate of the rim to impart a spin rate to the gimbal ring. The LST/AMCD/gimbal system center of mass is unaffected since this applied torque is internal. The resulting rotation of the LST-gimbal is shown by the dotted lines in Figure 4a. Since the AMCD radial servos generate control forces to keep the rim centered in the gaps, a translational acceleration is imparted to the rim.

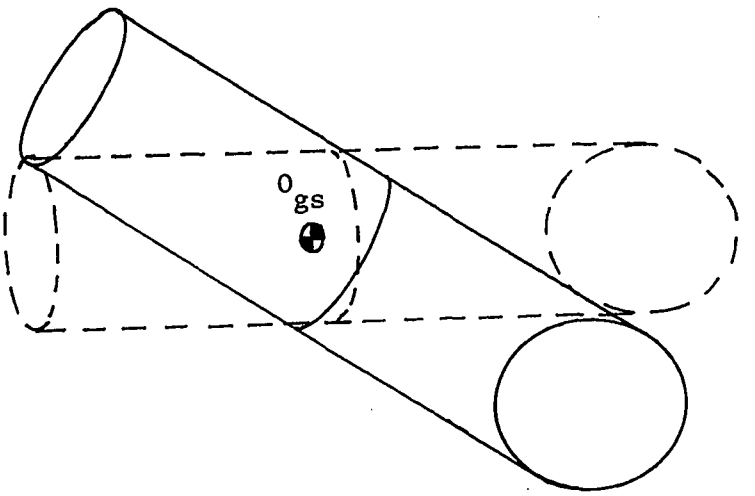

a) pure spin torquer maneuver

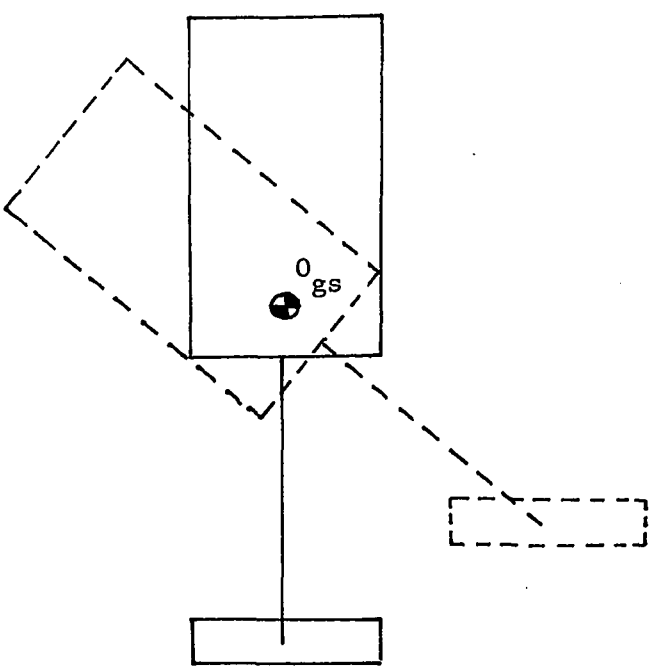

b) pure gimbal torquer maneuver

Figure 4. Examples of Possible LST-AMCD Maneuvers

Similarly, to perform a pure gimbal torquer maneuver (about the torquer axis) as shown in Figure 4b, the gimbal torquer torques the LST (and hence the gimbal ring) to impart a pitch rate on the LST. The resulting rotation of the LST-gimbal is shown by dotted lines in Figure 4b. Again, the AMCD servos (both axial and radial) generate control forces to center the rim in the gaps and a translational acceleration is imparted to the rim. In actual maneuvers, both the spin torquer and gimbal torquer maneuvers are performed simultaneously and so, the resulting motion will be extremely complex.

2.2 Formulation of the Dynamical System Model

General Equations of Motion.- The differential equations of motion for a system of rigid bodies can be derived using either the vectorial approach of Newton's Laws or the analytical approach embodied in the methods of Lagrange and Hamilton. In the second approach the equations of motion are derived from Lagrange's equations after formulating expressions for the system kinetic energy, the system potential energy, and any nonconservative generalized forces. Both approaches have been utilized leading to equivalent results for the systems dynamics model. Only the vectorial approach is presented here. Thus, the equations of motion for the system are derived using Euler's equations for the rotational motion of the bodies and the Newton's laws for the translational motion of the mass center of each body.

The translational equations of motion for the center of mass of a rigid body are given in vector form as

$$m_b \ddot{\bar{x}}_b = F_b \qquad (1)$$

where subscript b refers to the body under consideration.

The rotational equations of motion of a rigid body with reference to a body fixed frame with origin at the center of mass of that body can be expressed in vector-matrix form as follows:

$$[I_b]\,\omega_b + [\omega_b][I_b]\,\omega_b = \tau_b \,. \qquad (2)$$

In the above equation, the notation of references [1, 10]was utilized where

$$[\omega_b] = \begin{bmatrix} 0 & -\omega_z & \omega_y \\ \omega_z & 0 & \omega_x \\ -\omega_y & \omega_x & 0 \end{bmatrix}$$

$$[I_b] = \begin{bmatrix} I_{xx} & I_{xy} & I_{xz} \\ I_{yx} & I_{yy} & I_{yz} \\ I_{zx} & I_{zy} & I_{zz} \end{bmatrix}$$

and τ_b is a vector of torque components along the body axes.

Equations (1) and (2) represent complete equations of motion, translational and rotational, of a rigid body. These two vector-matrix equations can be solved independently if and only if the forces are not functions of the angular motion and the torques are not functions of the center of mass position and velocity. However, in the present case, the electromagnetic forces are functions of the relative orientation of the gimbal and the spinning rim. Hence, the translational and rotational equations of motion cannot be solved independently of each other.

The equations of motion can now be written for each of the two bodies under consideration, viz., the LST-gimbal (gs) and the spinning rim (a), based on equation (1) and equation (2).

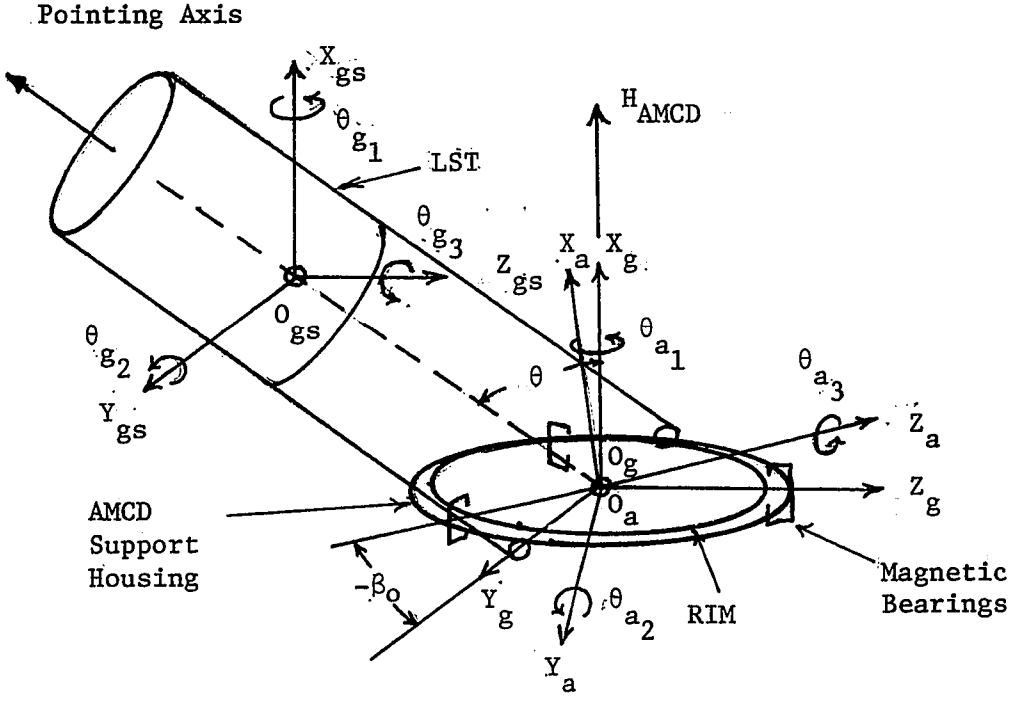

Figure 5. LST-AMCD Axis System

2.3 Coordinate Frames.- Two "body" frames are introduced, one for the LST-gimbal assembly (O_{gs}, X_{gs}, Y_{gs}, Z_{gs}) and the other for the spinning rim (O_a, X_a Y_a, Z_a). The origins of these frames, O_{gs} and O_a, are taken at the center of mass of the respective body as shown in Figure 5. The X_{gs} axis is taken nominally parallel to the nominal spin axis of the AMCD. The Y_{gs} axis is parallel to the gimbal torquer axis and the Z_{gs} axis completes the right-handed frame (note that this frame is not fixed to either the LST or the gimbal). The Euler angles θ_{g_1}, θ_{g_2}, and θ_{g_3} as generated by an XYZ rotation sequence locate the O_{gs} frame with respect to its nominal orientation. Note that the O_{gs} axes frame is always parallel to the frame O_g which is a body fixed frame in the gimbal ring. The additional degree of freedom in rotation for the LST with respect to the gimbal torquer axis is given by the angle θ, which is the angle made by the LST pointing axis with the X_{gs} axis. The composite LST-gimbal body thus has seven degrees of freedom represented by the generalized coordinates X_{gs}, Y_{gs}, Z_{gs}, θ_{g_1}, θ_{g_2}, θ_{g_3}, and θ. The first six variables locate the center of mass O_{gs} of this body and the orientation of a frame parallel to a gimbal fixed frame. The last variable θ describes the relative motion of the LST with respect to the gimbal.

The X_a axis coincides with the spin axis of the rim. The Y_a axis is nominally coincident with the gimbal torquer axis and the Z_a axis completes the right-handed frame. The Euler angles

θ_{a_1}, θ_{a_2}, and θ_{a_3} as generated by an XYZ rotation sequence locate the O_a frame with respect to its nominal position. This non-spinning frame has the advantage that the transverse moments of inertia of the spinning rim are time invariant due to axial symmetry as they would be in a strictly body fixed (spinning) frame.

2.4 Equations of Motion for the Spinning Rim.- The coincidence of the body axes, O_a, with the principal axes of the rim eliminates the products of inertia terms in equation (2) and the equations simplify considerably. Thus, those equations become:

$$H_x = I_{xx_a} (\omega_o + \omega_x), \tag{3a}$$

$$H_y = I_{yy_a} \omega_y , \tag{3b}$$

$$H_z = I_{zz_a} \omega_z , \tag{3c}$$

where ω_o is the nominal spin frequency of the rim, and the subscript "a" refers to the rim inertias. Neglecting the products of ω_x, ω_y, and ω_z (<0.05 rad/sec) which are small compared to ω_o (200 rad/sec), the equations of motion for the rim reduce to the following form in the nonspinning reference frame:

$$I_{xx_a} \dot{\omega}_{a_x} = \tau_{a_x} \tag{4a}$$

$$I_{yy_a} \dot{\omega}_{a_y} + H_o \omega_{a_z} = \tau_{a_y} \tag{4b}$$

$$I_{zz_a} \dot{\omega}_{a_z} - H_o \omega_{a_y} = \tau_{a_z} \tag{4c}$$

where $H_o = I_{xx_a} \omega_o$.

The body rates ω_{a_x}, ω_{a_y}, ω_{a_z} may be expressed in terms of the Euler rates $\dot{\theta}_{a_1}$, $\dot{\theta}_{a_2}$, $\dot{\theta}_{a_3}$ as shown in Appendix A. Since the angles θ_{a_2} and θ_{a_3} are small (<0.3°), the transformation equations become $\dot{\theta}_{a_1} \simeq \omega_{a_x}$, $\dot{\theta}_{a_2} \simeq \omega_{a_y}$, $\dot{\theta}_{a_3} \simeq \omega_{a_z}$ and the rotational equations of motion of the rim are given by

$$I_{xx_a} \ddot{\theta}_{a_1} = \tau_{a_x} , \tag{5a}$$

$$I_{yy_a} \ddot{\theta}_{a_2} + H_o \dot{\theta}_{a_3} = \tau_{a_y} , \tag{5b}$$

$$I_{zz_a} \ddot{\theta}_{a_3} - H_o \dot{\theta}_{a_2} = \tau_{a_z} . \tag{5c}$$

The translational accelerations of the center of mass of the rim are given by the vector equation

$$m_a \ddot{x}_a = F_a \tag{6}$$

where F_a are the electromagnetic forces exerted on the rim by the bearing stations located in the gimbal ring.

Equations (5) and (6) describe the motion of the spinning rim under the assumptions stated above.

2.5 Equations of Motion for the LST-Gimbal Body.- Some simplification can be made in equation (2) for describing the motion of the LST-gimbal. First of all, since the LST can rotate relative to the gimbal only about the gimbal torquer axis (which is parallel to the body-fixed Y_{gs} axis), it can be seen that of the terms containing products of inertia in equation (2), only those terms containing I_{xz} need be retained. Secondly, since the reference coordinate frame is oriented such that its $Y_{gs}\,Z_{gs}$ plane coincides nominally with $Y_a Z_a$ plane of the spinning rim and does not deviate much from it (because of the magnitude limits on gaps), small angle approximations can be made in terms involving products of θ_{g_2}, θ_{g_3}. The LST itself may rotate relative to the gimbal plane through a large angle θ. Thirdly, it is observed that the LST and gimbal rotate as a single rigid body about the X_{gs} and Z_{gs} axes, but as two different rigid bodies about the Y_{gs} axis. This latter rotation can be considered to occur about their common center of mass O_{gs}. Fourthly, the offset of the center of mass of the LST-gimbal from the center of the gimbal ring produces an additional torque due to the forces acting on the gimbal ring at the magnetic bearing stations.

From the above observations and, after substituting for the body rates in terms of Euler rates from Appendix A, the equations of motion for the LST-gimbal simplify to the following form:

$$I_{xx_{gs}}\ddot{\theta}_{g_1} - I_{xz_{gs}}\ddot{\theta}_{g_3} = \tau_x\,, \qquad (7a)$$

$$I_{yy_g}\ddot{\theta}_{g_2} = \tau_y\,, \qquad (7b)$$

$$I_{zz_{gs}} \ddot{\theta}_{g_3} - I_{xz_{gs}} \ddot{\theta}_{g_1} = \tau_z \,, \qquad (7c)$$

$$I_{yy_s}' \ddot{\theta} = \tau_g \,, \qquad (7d)$$

where the subscript gs refers to the combined LST-gimbal body and the primed inertia terms are the moments of inertia transferred to the composite center of mass O_{gs}.

The translational equations of motion for the combined body are given by

$$m_{gs} \ddot{x}_{gs} = F_{gs} = - F_a \,. \qquad (8)$$

The LST-gimbal system has seven degrees of freedom represented by the generalized coordinates X_{gs}, Y_{gs}, Z_{gs}, θ_{g_1}, θ_{g_2}, θ_{g_3} and θ. The first six coordinates locate the center of mass O_{gs} of the LST-gimbal combination and describe the orientation of that body with respect to inertial space. The last variable specifies the LST orientation relative to the gimbal. Equations (5), (6), (7), and (8) completely describe the motion of the two bodies, spinning rim and LST-gimbal, in inertial space, as subject to the assumptions. The total system thus has thirteen degrees of freedom.

These general nonlinear equations of motion can be written in a standard first order form, viz.,

$$\dot{x}(t) = f(x(t), u(t)) \quad \text{with} \quad x(t_o) = x_o. \qquad (9)$$

where x is an n-state vector and u is an m-control vector containing the electromagnetic control forces and torques. It may be that the state vector x is not directly measurable so an

r-measurement vector

$$y(t) = g(x(t)) \qquad (10)$$

is introduced.

It is pointed out here that the external torques on the LST-gimbal body, such as the gravity gradient torques, were neglected in the equations of motion, since they were found to be an order of magnitude less than the control torques involved.

2.6 Reduction in the Order of the Equations.- It is seen from the detailed discussion and derivation of the equations of motion in previous sections, that the motion of the complete system (LST-gimbal-spinning rim) is described by thirteen second-order nonlinear differential equations. It is also noted that, for the purpose of simplification of the derivation only, the system was considered to be made up of two bodies (LST-gimbal and spinning rim) with the magnetic forces exerted by the bearing stations being considered as the external forces, acting on each of the two bodies. However, the complete system of LST-gimbal spinning rim has a net resultant force and torque of zero magnitude since these interbody magnetic forces are equal and opposite and all orbital and environmental torques are neglected. The center of mass of the complete system therefore is unaccelerated. Hence, the translational motion of the two individual bodies considered is not independent of each other. The motion of only one body need be considered since the motion of the other can be calculated from the knowledge of this motion. Thus, it is possible to reduce the number of equations by three, and, only ten second-order nonlinear equations are considered for integration. This results in a significant saving in the computer core requirements and computational time requirements.

In view of the above observation, the differences in the inertial positions and velocities of the center of the spinning rim from those of the center of the gimbal ring are considered as the state variables. This facilitates the computation of the

magnetic gaps, since these gaps are functions of the differences in the inertial positions of the ring and the rim. The magnetic forces generated by the bearing stations are derived as the functions of these differential positions and the velocities (Appendix C).

Large Angle Maneuver Controller Design.- A preliminary analysis of the linearized version of equation(9) indicated the presence of five negative eigenvalues of large magnitude. These eigenvalues were found to be associated with the three degrees of freedom in translational and two degrees of freedom of the rim in transverse rotation, i.e., in the θ_{a_2} and θ_{a_3} directions. The two eigenvalues associated with the transverse rotational motion of the rim were found to be of highest magnitude being equal to twice the nominal spin frequency of the rim.

The existence of these large (negative) eigenvalues necessitated the choice of computational interval for integration of the nonlinear equations to be 0.001 sec in order that the solution did not diverge. This extremely small integration interval, together with a high order of nonlinear system equations to be solved (n = 21 x 21 for adjoint system), made it impossible to get any appreciable maneuvers in reasonable computer times. Hence, a standard technique of increasing the step size for integration was applied as discussed below.

Since the largest eigenvalues were associated with the large linear acceleration of the system and the large rotational

acceleration of the spinning rim, these second order acceleration components were eliminated by defining the mass and the moments of inertia of the spinning rim to be identically equal to zero. This has the effect of instant transfer of velocities (both linear and angular) to the rim, i.e., with (theoretical) infinite accelerations. The resulting equations for velocities were solved. In case of angular velocities, however, the substitution of zero inertia resulted in a pair of simultaneous equations for $\dot{\theta}_{a_2}$, $\dot{\theta}_{a_3}$, the transverse angular velocities. The solution of these simultaneous equations was necessary to obtain individual angular velocities.

The modified system, with the five high acceleration components of the rim thus removed, was again analyzed. The eigenvalues of the modified system were compared with those of reference [8] and also with another program developed independently at Langley Research Center in order to have a check on the system. The eigenvalue plots of this system duplicated all the eigenvalues of small magnitude of the original system, the large eigenvalues being eliminated. The time histories of the states (position and angles) were plotted for both the original system and the new modified system without the high acceleration components. The values of the states matched within 2 percent of each other. Thus, the modified system of equations were used for calculating the time responses of the nonlinear equations of Chapter 4 with a tenfold increase in the step size used for integration (0.01 sec).

Thus, in the final form, fifteen nonlinear, coupled, first

order, ordinary differential equations of motion are utilized in the integration of the system equations and the adjoint equations for the nonlinear optimization problem.

Optimal Fine Pointing Controller Design.- As was pointed out in section 2.1, after the LST pointing axis is approximately aligned with the given stellar target, the gimbal torquer is locked and fine pointing control is accomplished by torquing the gimbal ring in the gaps against the AMCD momentum vector. Since the torquer is now locked, both LST and gimbal ring now rotate as a single rigid body and hence the system now has only nine degrees of freedom.

It is also to be noted that application of any spin torque (which is small in magnitude for the fine pointing problem) along the X_a axis makes the spinning rim spin up while exerting an equal and opposite reactive torque on the LST-gimbal body. While the resulting small motion of the LST-gimbal is of interest from the viewpoint of accuracy of the pointing, the small spin up of the rim is of no direct interest to the problem. Thus, the angular motion of the spinning rim about the spin axis is ignored in this case. This reduces the number of degrees of freedom of interest to eight in the fine pointing problem.

However, as is discussed in Section 3.4, in detail, it turns out that inclusion of angles θ_{a_2}, θ_{a_3} in the state vector, makes the pair of coefficient matrices A,B uncontrollable, giving rise to subsequent difficulty in the convergence of the solution of the Riccati equation. For computation of the optimal control gains, therefore, these two angles are dropped from the state

vector. However, these angles are considered in the optimal estimator (observer) problem and the complete LQG controller design.

Thus in the final form, fourteen nonlinear, first order, ordinary differential equations are used to derive the linearized model about the target pointing angles and the target (zero) velocities. The derivation of the linearized model is outlined in Sec. 2.8 and the complete analysis of the stochastic Linear-Quadratic-Gaussian Control System is presented in Chapter 5.

2.7 Control Forces and Torques.- The external forces and torques on each of the two bodies (LST-gimbal and spinning rim) as indicated in deriving the equations of motion for the two bodies (Sec. 2.4, 2.5) are the interacting magnetic forces and torques due to the magnetic bearing stations. In practice, the three bearing stations each generate an axial force and a radial force at the station and an electromagnetic spin motor generates a tangential force on the rim, thus providing the spin axis torque. Finally, the gimbal torquer motor generates the torque which torques the LST against the (inertially stable) gimbal to move it relative to the gimbal ring (when the gimbal is not locked). Thus, there are eight control variables, six forces (three axial and three radial, one at each bearing station), a spin torque and a gimbal torque.

The magnetic forces generated by the bearing stations are made up of 1) "passive" forces, i.e., the centering forces generated by assuming a spring-dashpot system for bearings, and 2) "active" forces, i.e., the additional forces generated by command inputs to the servo-loops of the electromagnets.

In the design of the controller for LST fine pointing, it is desired to align the LST pointing axis with the target as accurately as possible. This is done by forcing and torquing the LST-gimbal (locked) combination within the gaps against the momentum of the spinning rim. In this case, both types of forces mentioned above are collected together in the control vector. The optimal closed

loop feedback control law obtained aligns the pointing axis with the target

In the design of the controller for large angle maneuvers, however, the main concern is that of retargeting the telescope from one target to another through a large angle. In this case, the centering "passive" forces and torques were separated from the "active" control forces and torques. These "passive" forces and torques were expressed in terms of the states (Appendix B and C). The control vector now consists of the spin torque, the gimbal torque and the "active" forces at the bearing stations required to center the rim in the gaps, to nullify the motion due to the maneuvering of the gimbal.

The derivation of the control forces and torques expressions is outlined in Appendix D. The derivation of the passive forces and torques in terms of the states is summarixed in Appendices B, C, D, and E.

2.8 Linearization for the Fine Pointing Case.- The linearized perturbation model for the fine pointing is derived from the general nonlinear equations (9) and (10). The linearization is accomplished by expanding f and g about the nominal (or desired) values of $x_o(t)$, $u_o(t)$ in a Taylor series expansion and dropping the higher order terms (second order and higher) in this expansion. In the present case, the linearization is to be performed about a set of desired constant target angles $\theta_{g_o} = (\theta_{g_{1_o}}, \theta_{g_{2_o}}, \theta_{g_{3_o}})$ and about the nominal constant spin frequency of the rim ($\omega_{x_o} = \omega_o$). This is adopted as the reference solution for the expansion and is an equilibrium state of the motion. The linearized perturbation model can therefore be written as:

$$\dot{x}(t) = Ax(t) + Bu(t) \qquad \text{with } x(t_o) = x_o \qquad (11)$$

$$y(t) = Cx(t) \qquad (12)$$

where

$$A \triangleq \frac{\delta f}{\delta x}\Big|_{\substack{x_o \\ u_o}}, \quad B \triangleq \frac{\delta f}{\delta u}\Big|_{\substack{x_o \\ u_o}}, \quad C \triangleq \frac{\delta g}{\delta x}\Big|_{x_o}$$

In the present case, the linearization is performed as indicated before, about the equilibrium state of the target angles θ_{g_o}, about the nominal spin frequency of the rim ω_o, and about the central position of the rim in the gaps. Hence, the elements of the coefficient matrices A, B, and C are time-invariant and the analysis is considerably simplified. Also, the linearization is performed about the equilibrium position of the states, which can be taken to be the zero state without loss of generality.

Chapter 3

DESCRIPTION OF THE OPTIMAL CONTROLLER DESIGN METHODS

With the development of the mathematical model described in section 2.2 completed at this stage, it is now possible to describe the optimal controller design techniques utilized for (1) the fine pointing (linear) case, and (2) the large angle maneuvers (nonlinear) case for the LST/AMCD.

3.1 Optimal Control for the Large Angle Maneuver Case by a Modified Gradient Technique Using Penalty Functions.- This section is concerned with the formal design of an optimal controller for the case of large angle maneuvers of the LST/AMCD. The design objective here is to find the optimal open-loop control law to retarget the LST (i.e., the pointing axis of the LST) from one stellar object, after completing the necessary observations of this object, to another stellar object which may not be in the vicinity of the first. The performance index to be minimized here is the final pointing error and energy usage. Since the power used by the spin and the torquer motors is proportional to the square of the magnitudes of the torques provided by these motors, the time integral of the square of the torques can suitably be taken as a measure of the performance index to be minimized along with the final pointing errors. The nonlinear, coupled, second order differential equations of motion for this case are of the form given in section 2.5.

Additionally, there are "hard" constraints on the magnitude of the control vector u and the state vector x which cannot be exceeded in any case. This is due to the fact that there are physical limits on the magnetic gaps and the value of the forces and torques provided by the actuators. Since the problem as stated cannot be solved in closed form, an iterative numerical method must be utilized. This method, a modified gradient procedure, incorporates the "hard" constraints as penalty terms in the performance index ("cost") and an additional differential equation. This iterative numerical procedure, when convergence is achieved, provides an open loop control law as a function of time, to minimize the modified performance index (including the penalty terms).

An extensive critical analysis of many available techniques and variations was made in arriving at the conclusion that the modified gradient method using penalty functions was the best technique in this case. This critical review of existing techniques is presented in Appendix L.

In the modified gradient method, the given inequality constraint on the control variables is converted to an equality constraint (either differential equation or algebraic equation). This technique is similar to the penalty function technique of Kelley [11,12] and was apparently first proposed by Valentine [13] and extended by Berkovitz [14]. The constraint is then included in the integral penalty term. A slightly different

approach is needed to handle state inequality constraints. An additional differential equation defines a new state variable x_{n+1} with the help of the Heaviside step function. The value of the new variable at $t=t_f$ is a measure of the penetration of the state variable inequality constraint. The method is described by Sage [15] and is outlined in detail below.

The design problem may be posed as one of minimizing the performance index (cost function)

$$J = \theta\,[x(t_f),\ t_f] + \int_{t_o}^{t_f} \phi\,[x(t),\ u(t),\ t]\,dt \qquad (13)$$

for the system

$$\dot{x} = f(x(t),\ u(t),\ t),\quad x(t_o) = x_o \quad \text{where x is an n-vector} \qquad (14)$$

with the terminal manifold

$$N(x(t_f),\ t_f) = 0 \qquad (15)$$

by proper choice of control $u(t)$.

The control inequality constraints are

$$g_i(x(t),\ u(t),\ t) \geq 0 \quad i = 1,\ 2,\ \ldots\ r, \qquad (16)$$

and the state inequality constraints are

$$h_i(x(t),\ t) \geq 0 \qquad i = 1,\ 2,\ \ldots\ s. \qquad (17)$$

The control constraints are incorporated into the performance index by converting these inequalities into equivalent equality constraints with Heaviside step functions defined as follows:

$$H(g_i) = \begin{cases} 0 , & g_i \geq 0 \\ K_{c_i} , & g_i < 0 \end{cases} \qquad (18)$$

where K_{c_i} are arbitrary constraints.
The constraints can then be included inside the performance index as a penalty term as

$$J' = \ldots + \int_{t_o}^{t_f} \sum_{i=1}^{r} |g_i(x,u,t)|^2 \, H(g_i) \, dt . \qquad (19)$$

A slightly different treatment is necessary to incorporate the state constraints. The procedure based on a modification of the method of Kelley [11] by McGill [16] is as follows.

The state constraint equation is replaced by the additional differential equation

$$\dot{x}_{n+1} = f_{n+1} = \sum_{i=1}^{s} |h_i(x,t)|^2 \, H(h_i) \qquad (20)$$
$$\text{with } x_{n+1}(t_o) = x_{n+1}(t_f) = 0,$$

or equations

$$\dot{x}_{n+1} = |h_1(x,t)|^2 \, H(h_1), \quad x_{n+1}(t_o) = x_{n+1}(t_f) = 0$$
$$\dot{x}_{n+2} = |h_2(x,t)|^2 \, H(h_2), \quad x_{n+2}(t_o) = x_{n+2}(t_f) = 0$$

$$\dot{x}_{n+s} = |h_s(x,t)|^2 \, H(h_s), \quad x_{n+s}(t_o) = x_{n+s}(t_f) = 0. \qquad (21)$$

The Heaviside step functions are defined as

$$H(h_i) = \begin{cases} 0 , & h_i \geq 0 \\ K_{s_i} , & h_i < 0 \end{cases} \qquad (22)$$

where K_{s_i} are arbitrary constants.

In the present problem, the constraints are proposed to be replaced by only one differential equation, to keep the total system to the lowest possible order, as the order of the original problem itself is high (n=15).

Since the violation of these equations is almost certain to occur during the trajectory, the final values of the x's are included in the performance index as penalty function. The final reformulated cost function to be minimized is

$$J = [N^T G N + |x_{n+1}(t_f)|^2 K_s] + \int_{t_o}^{t_f} [\phi(x,u,t) + \sum_{i=1}^{r} |g_i(x,u,t)|^2 H(g_i)] \, dt \qquad (23)$$

for the modified unconstrained system

$$\dot{x}(t) = f(x,u,t) \qquad (24)$$

with $x(t_o) = x_o$, and

$$\dot{x}_{n+1}(t) = f_{n+1}, \qquad (25)$$

with $x_{n+1}(t_o) = x_{n+1}(t_f) = 0$.

The form of ϕ is generally chosen to be a quadratic function of state and control variables as follows

$$\phi = \tfrac{1}{2} (x^T Q x + u^T R u + \alpha) \qquad (26)$$

where $Q \geq 0$, $R > 0$, and

$$\alpha = \begin{cases} 0 & \text{for minimum energy problem} \\ 2 & \text{for minimum time problem.} \end{cases}$$

The Hamiltonian for the above system is defined as

$$H(x,u,\lambda,t) = \phi(x,u,t) + \lambda^T(t)\, f(x,u,t). \quad (27)$$

The adjoint equation and the terminal condition is

$$\frac{\partial H}{\partial x} = -\dot{\lambda} = \frac{\partial \phi}{\partial x} + \frac{\partial f}{\partial x}^T \lambda \quad (28)$$

$$\text{and } \lambda(t_f) = \partial\theta[x(t_f),\, t_f]/\partial x(t_f). \quad (29)$$

From the Maximum Principle, the condition for optimality is

$$\frac{\partial H}{\partial u} = \frac{\partial \phi}{\partial u} + \frac{\partial f}{\partial u}^T \lambda = 0. \quad (30)$$

Since the initial guess of u_o will, in general, not be optimal, this condition will not be satisfied.

The given system (24, 25) is integrated forward (in time) with the initial guess, u_o and the adjoint system (28) is solved backward (in time) utilizing the terminal conditions (29). To achieve the largest decrease in the performance index J, the correction Δu is directed opposite to the gradient of the Hamiltonian and is proportional to it. Thus,

$$\Delta u(t) = -K \frac{\partial H}{\partial u} \quad (31)$$

and the new corrected control history is computed for the next iteration.

The constant K is calculated as follows. The improvement in the cost function is given by [15],

$$\Delta J = - \int_{t_o}^{t_f} \left\{\frac{\partial H}{\partial u}\right\}^T \Delta u \, dt . \qquad (32)$$

where negative sign indicates the decrease in the cost function. Substituting for Δu,

$$\Delta J = K \int_{t_o}^{t_f} \left\{\frac{\partial H}{\partial u}\right\}^T \left\{\frac{\partial H}{\partial u}\right\} dt, \qquad (33)$$

and

$$K = \Delta J \Big/ \int_{t_o}^{t_f} \left\{\frac{\partial H}{\partial u}\right\}^T \left\{\frac{\partial H}{\partial u}\right\} dt. \qquad (34)$$

The value of the integral in the denominator is calculated while computing $\partial H/\partial u$. A reasonable value of ΔJ, say 10 percent, is assumed and the corresponding value of K is computed. As the solution approaches the minimum value of the cost function, it may be necessary to decrease the value of ΔJ. This is done automatically in the program by halving the previous value of ΔJ when an increase in the cost function is encountered at any iteration. The iterative procedure is repeated until one of the following convergence criteria is met during the N+1st iteration:

1) $J_{N+1} \geq J_N$. In this case, further study may be required by reducing the step size K appropriately,

2) $\Delta u_N \leq 0.01\, u_N$, i.e., the correction vector is less than 1 percent (or any other suitable factor) of the control vector.

3.2 A Steady State Stochastic LQG Controller for the Fine Pointing Case.- This section is concerned with the design of an optimal controller for the fine pointing case. The design is accomplished in the following manner:

a) Solve the steady-state linear quadratic (LQ) optimal regulator problem to get the deterministic optimal gains matrix,

b) Solve the steady-state linear Gaussian (LG) optimal estimator or filting problem to get the minimum mean square (MMS) estimate of the state vector,

c) Solve the steady-state stochastic linear quadratic Gaussian (LQG) control problem by cascading the deterministic control of step (a) and stochastic estimator step (b)

d) Calculate the covariance or RMS error matrix to get the accuracy of the design.

Deterministic Fine Pointing Controller Design Problem.- The design objective in this case is to keep the actual states $x(t)$ (i.e., magnetic actuator gaps, LST pointing angles) "near" their ideal desired values $x_o(t)$ for all $t \in [t_o, t]$. The linearized perturbation model for this case was described in Section 2.8.

The design problem can be stated as one of determining the control vector $u(x(t), t)$ so as to minimize

$$J_d = \tfrac{1}{2}\, N^T G N + \tfrac{1}{2} \int_{t_o}^{t_f} (\alpha + x^T Q x + u^T R u)\, dt \qquad (35)$$

for the system with the differential constraints

$$\dot{x}(t) = A\, x(t) + B\, u(t) \qquad (36)$$

with $x(t_o) = x_o$ and,

$$y(t) = C x(t)\,. \qquad (37)$$

The practical disadvantage of the deterministic system given above is that it requires exact measurement of all of the state variables. This cannot always be achieved. Even if, in the ideal situation, one could measure all the state variables, one has to use physical sensors to carry out these measurements and this introduces a certain degree of uncertainty in the measurements. This uncertainty in measurement must somehow be taken into account. In addition, although the deterministic approach admits errors in the plant modeling (necessitating feedback) it did not explicitly take into account errors introduced by actuators and disturbance inputs that are not generated by the control system, and are almost always acting upon the physical process. Also, if one cannot measure the state variables exactly (due to actuator noise), one can no longer assume the initial state of the plant $x(t_o) = x_o$.

It is common engineering practice to use a probabilistic approach to the modeling and implications of physical

uncertainties. The reason is that a probabilistic approach is characterized by the existence of an extensive mathematical theory which has been already developed. In the design of dynamical system, therefore, the continuous existence in time of plant disturbances, sensor errors and initial state estimate errors are modeled by representing these uncertainties ("noise") by means of random processes, more particularly by means of "white" noise. A random process modeled as a continuous time white noise views the uncertainty as the most unpredictable one. This prevents the designer from "second guessing" the future values of noise from past measurements. This "guessing" not only required tremendous online computational effort (as in Monte-Carlo Techniques), but also might give the designer a "wrong" estimate of the noise since in practical design situations the random processes are almost always uncorrelated.

Two useful statistical parameters, characterizing continuous time white noise $n(t)$ (which is a Gaussian process) are its mean and covariance. The mean value, $\bar{n}(t)$ and the covariance are defined as:

$$E\{n(t)\} = \bar{n}(t) = 0 \quad \text{for all } t \quad \text{(for white noise)}$$

$$\text{cov}[n(t); n(\tau)] = E\{n(t)\, n^T(\tau)\} = N(t)\, \delta(t-\tau)$$

where

$$N(t) = N^T(t) \geq 0$$

where $N(t)$ is called the covariance intensity matrix of the

vector valued white noise $n(t)$. If $N(t) = N$ = constant, the noise is called stationary white noise.

With the brief qualitative treatment of the white noise given above, it is now possible to give the quantitative description of noises involved. Accordingly, the initial state uncertainty, the plant noise uncertainty and the measurement uncertainty are modeled as follows:

1) The initial state vector is assumed to be Gaussian with the known mean $\bar{x}_o$ and covariance matrix, Σ_o, i.e.,

$$E\left\{x_o\right\} \triangleq \bar{x}_o;\ \text{cov}\,[x_o;\bar{x}_o] \triangleq E\left\{(x_o-\bar{x}_o)(x_o-\bar{x}_o)^T\right\} = \Sigma_o;$$

$$\text{and}\quad \Sigma_o = \Sigma_o^T \geq 0$$

where E is the expected value operator and the $\geq$ sign implies that Σ_o must be positive semi-definite.

2) The plant driving noise (due to disturbance inputs and the actuator errors) $\xi(t)$ is assumed to white, Gaussian with zero mean and known covariance matrix, i.e.,

$$E\left\{\xi(t)\right\} = 0 \quad \text{for all} \quad t > t_o;\ \text{cov}\,[\xi(t);\ \xi(\tau)]$$
$$\triangleq E\left\{\xi(t)\ \xi^T(\tau)\right\} \triangleq \Xi(t)\ \delta(t-\tau);\quad \text{and}$$
$$\Xi(t) = \Xi^T(t) \geq 0, \quad \text{for all} \quad t \geq t_o$$

3) The measurement noise (due to sensor errors) $\theta(t)$ is assumed white, Gaussian, with zero mean and known covariance matrix, i.e.,

$$E\left\{\theta(t)\right\} = 0;\ \text{cov}\,[\theta(t);\ \theta(\tau)] \triangleq$$

$$E\{\theta(t)\ \theta^T(\tau)\} = \Theta(t)\ \delta(t-\tau);\ \text{and}$$

$$\Theta(t) = \Theta^T(t) > 0 \quad \text{for all} \quad t \geq t_o.$$

Furthermore, it is also assumed that the random processes x_o, $\xi(t)$, and $\theta(t)$ are mutually independent. This assumption is reasonable in most physical processes. The matrices Σ_o, $\Xi(t)$, and $\Theta(t)$ are the intensity matrices of the respective white noises.

It is now appropriate to incorporate the uncertainties (noises) defined above in the deterministic controller design problem statement as presented before. It is first necessary to incorporate the uncertainty in the nonlinear model as follows:

$$\dot{x}(t) = f(x(t),u(t)) + \xi(t), \qquad \bar{x}(t_o) = E\{x_o\} \tag{38}$$

$$y(t) = g(x(t)) \tag{39}$$

$$z(t) = y(t) + \theta(t) = g(x(t)) + \theta(t) \tag{40}$$

A repetition of the procedure involving a Taylor series expansion about $x_o(t)$, $u_o(t)$, and $y_o(t)$ outlined before, is now applied to the stochastic nonlinear model (38) - (40). The assumption (without loss of generality) that the equilibrium trajectories $x_o(t)$, $u_o(t)$, $y_o(t)$ are zero, yields the following linearized, time invariant perturbation stochastic model of the system.

$$\dot{x}(t) = A\,x(t) + B\,u(t) + \xi(t) \tag{41}$$

$$z(t) = C\,x(t) + \theta(t) \tag{42}$$

It is noted here that the design objective for the deterministic problem was to determine a commanded control history $u(t)$ so that the state deviation vector $\delta x(t) = x(t) - x_o(t)$ ($= x(t)$, if $x_o(t) \triangleq 0$) is small for $t \in [t_o, t_f]$ and the performance index J_d is minimized. The design objective is still the same, except that now $x(t)$, $u(t)$ etc. are random processes. This results in the performance index being a scalar-valued random variable. To formulate a meaningful problem, however, one needs to minimize a nonrandom scalar. Since the cost functional (i.e., performance index) in the stochastic problem formulated above is random, a natural criterion is to minimize the expected value of J_d conditional on the past measurements up to its present value at time t.

Thus, the controller design problem involves minimizing the cost functional

$$J_s \triangleq \bar{J}_d \triangleq E\left\{ J_d \mid \delta z(\tau);\ t_o \le \tau \le t \right\} \qquad (43)$$

where $J_s = E\left\{ \frac{1}{T} \int_o^T [x^T(t)\ Q\ x(t) + u^T(t)\ R\ u(t)]\ dt \right\}$

The states are now random variables (rather than deterministic variables) and this fact has to be taken into account when defining the cost functional J_d accordingly.

The stochastic fine pointing controller design problem can now be stated. Given the completely controllable and observable, linear, time-invariant system

$$\dot{x}(t) = A\,x(t) + B\,u(t) + \xi(t); \quad \bar{x}(o) = E\{x_o\} \qquad (44)$$

and the time-invariant measurements

$$z(t) = C\,x(t) + \theta(t) \qquad (45)$$

where the noises $\xi(t)$, $\theta(t)$ are both Gaussian, white, zero-mean, mutually independent (uncorrelated), and stationary such that

$$\text{cov}\,[\xi(t);\ \xi(\tau)] = \Xi\,\delta(t-\tau);\ \Xi = \Xi^T > 0$$

$$\text{cov}\,[\theta(t);\ \theta(\tau)] = \Theta\,\delta(t-\tau);\ \Theta = \Theta^T > 0$$

$$\text{cov}\,[\xi(t);\ \theta(\tau)] = 0$$

find a linear time varying gain, feedback control $u(t)$ for all $t \in [o,\ t_f]$, such that the cost functional

$$\hat{J}_s = E\left\{\frac{1}{T}\int_o^T x^T(t)Q\,x(t) + u^T(t)R\,u(t))\,dt\right\} \qquad (46)$$

is minimized where the constant weighting matrices Q and R are such that

$$Q = Q^T \geq 0$$

$$R = R^T > 0$$

The design problem formulated above is referred to as a steady state stochastic linear-quadratic Gaussian (LQG) control problem.

3.3 The Separation Theorem.- The controller design problem stated in section 3.2 may be decoupled into two simpler design problems if the separation theorem of reference [15] is invoked.

For a particular class of this problem, which has linear system dynamics with white noise disturbances, and the cost functions are quadratic in nature, a decoupling of the design procedure is possible due to a very powerful theorem called the Separation Theorem. This theorem is stated without proof below:

> The optimal linear solution of the stochastic linear optimal output feedback regulator is the same as the solution of the corresponding stochastic optimal state feedback regulator problem except that in the control law the actual state $x(t)$ is replaced with its MMS (minimum mean square) linear estimator $\hat{x}(t)$, that is the input control is chosen as
>
> $$u(t) = - G_o \hat{x}(t) . \qquad (47)$$
>
> The MMS estimator $\hat{x}(t)$ is the output of the optimal observer or filtering problem.

The theorem in essence states, that, for linear systems with quadratic cost functional and subjected to additive white Gaussian noise inputs, the optimum stochastic controller is realized by cascading an optimal estimator with a deterministic optimum controller. The decoupling is partly due to the fact that the random noises are white with zero mean and, since they

are completely unpredictable and therefore cannot be taken into account in the design of the optimal controller. It must be noted here that the formulation of the cost functional (which is to be minimized) as a quadratic is indeed to maximize the average validity of the linearized models, both deterministic and stochastic. The proof of this important theorem can be found in the literature references[17] - [20].

The solution indicated above by the theorem is the optimal linear solution. It can be proved that,[21] - [25], if the initial state $\bar{x}_o$ is Gaussian and the noise inputs (both inputs and measurement) are Gaussian white noise processes, then the optimal linear solution is indeed the optimal solution.

The state estimator $\hat{x}(t)$ in the theorem above is the conditional expectation of the true state $x(t)$, viz.,

$$\hat{x}(t) \triangleq E\{x \,|z(\tau);\ t_o < \tau < t\} \qquad (48)$$

given all the measurements $z(\tau)$ up to the present time t. It is to be noted that if all noises are Gaussian white noises, this conditional mean of $x(t)$ is the same as the MMSE (minimum mean square error) estimate, which also is equal to the Kalman estimate of $x(t)$. If all noises are not Gaussian, however, then the Kalman estimate is only the linear MMSE estimate of the state $x(t)$, [15].

The separation theorem thus guarantees that for a particular class of problems the LQG problem can be separated into

two parts, viz.,

1) Linear Quadratic Optimal Regulator LQ Problems

To calculate the commanded control u(t) so as to minimize the cost functional

$$J = x^T(t_f)G\,x(t_f) + \int_o^{t_f} [x^T(t)Q\,x(t) + u^T(t)R\,u(t)]\,dt$$

$$G = G^T \geq 0;\ Q = Q^T \geq 0;\ R = R^T > 0$$

for the deterministic time invariant system described by

$$\dot{x}(t) = A\,x(t) + B\,u(t) \qquad \text{where } x(t_o) = x_o \text{ is an n-vector}$$

2) Linear Gaussian Optimal Estimator Problem

For the linear dynamics stochastic system

$$\dot{x}(t) = A\,x(t) + B\,u(t) + \xi(t)$$

and the linear stochastic measurement equation

$$z(t) = C\,x(t) + \theta(t)$$

where $x(t)$ is a Gaussian random variable with the mean

$$E\{x(t_0)\} \triangleq \bar{x}_o \quad \text{(known)}$$

and the measured signal $z(\tau)$ for all $\tau \in [t_o, t]$, find a vector $\hat{x}(t)$, an estimate of the true state vector $x(t)$, which is "optimal" in the well defined statistical sense of the minimum mean square error.

The complete stochastic problem is seen to be a time-varying problem, and the control matrix gains G_o and the filter matrix gains H_o therefore will be functions of time. In principle, these time functions can be calculated, albeit with trememdous increase in the computational effort. In addition, from the viewpoint of the practical design of the control system, it is difficult to generate the control vector using a time varying control gain matrix or to generate the state estimate using a time varying filter gain matrix. Thus, the design problem of interest is reformulated by replacing the cost function with

$$J_s = \lim_{T\to\infty} E\left\{\frac{1}{T}\int_o^T [x^T(t)\ Q\ x(t) + u^T(t)\ R\ u(t)]\ dt\right\} \quad . \quad (49)$$

This modification ignores the transient behavior of the states, and the gains (both control and filter) are computed as constants as shown in next section.

3.4 Linear Quadratic Optimal Regulator Problem.- The deterministic steady state linear quadratic optimal regulator problem, which is the controller part of the stochastic control problem defined in section 3.2 is stated as follows:

Given the linear deterministic time invariant system

$$\dot{x}(t) = A\,x(t) + B\,u(t) \qquad (50)$$

$$\text{with } x(o) = x_o$$

$$y(t) = C\,x(t) \qquad (51)$$

find a linear constant gain feedback control vector $u(t)$ (an m-vector) $t \in [t_o, T]$ so as to minimize the following deterministic quadratic cost functional (performance index)

$$J_o = x^T(T)\,G\,x(T) + \int_o^T [x^T(t)\,Q\,x(t) + u^T(t)\,R\,u(t)]dt \qquad (52)$$

where $G = G^T \geq 0$ nxn matrix

$Q = Q^T \geq 0$ nxn matrix

$R = R^T > 0$ mxm matrix

for all $t \in [0, T]$

The solution to the above time invariant problem is given by the linear time varying feedback relationship

$$u(t) = -G_o(t)\,x(t) \qquad (53)$$

where $G_o(t)$ is a mxn control gain matrix. The value of $G_o(t)$ is given by

$$G_o(t) = R^{-1}\,B\,K_o(t) \qquad (54)$$

where the nxn time varying matrix $K_o(t)$ is the solution of the nonlinear matrix differential equation, of the Riccati type (usually referred to as the matrix differential Riccati equation)

$$\frac{d}{dt} K_o(t) = - K_o(t) A - A^T K_o(t) - Q$$

$$+ K_o(t) B R_o^{-1} B^T K_o(t) \qquad (55)$$

subject to the boundary condition at the terminal time T.

$$K_o(T) = G \qquad (56)$$

The proof of the above result can be found in many places in the literature in the field of optimal control. There are also several ways of proving this result. One way is using Pontryagin's maximum principle [26] and subsequent manipulations of the necessary conditions [27]. This procedure is also outlined in the original work by Kalman [28,29]. Another way is through the use of Hamilton-Jacobi-Bellman partial differential equations [27,29,30,31]. Yet another method is related to completing squares and proving that $\lim_{T\to\infty} K(t) = K_\infty(t)$ exists for all t, the limit being approached monotonically from below. The proof is completed by showing that the corresponding closed loop system is exponentially stable [32]. Another solution method assumes that the optimal control is linear and of the form (53) and carries out a parameter optimization to determine the matrix $G_o(t)$ [33].

The solution of the practical, constant gain problem (49) is given in the form

$$u(t) = -G\, x(t) . \qquad (57)$$

The feedback control gain matrix G is a constant (time invariant) matrix in this case, and its value is given by

$$G = -R^{-1} B^T K \qquad (58)$$

where the nxn constant, positive definite matrix K (Riccati matrix) is the solution of the nonlinear matrix algebraic Riccati equation:

$$-KA - A^T K - Q + KBR^{-1}B^T K = 0 \qquad (59)$$

subject to the terminal boundary condition

$$K(T) = 0 . \qquad (60)$$

In this case then, the optimal trajectory is the solution of the linear, time invariant homogeneous system

$$\dot{x} = (A - B\, G_o)\, x(t)$$
$$\triangleq A_c\, x(t), \quad x(o) = x_o \text{ (given)} . \qquad (61)$$

The existence and uniqueness of the solution stated above are guaranteed by the following assumptions:

a) $[A,B]$ is a controllable pair

b) $[A,Q^{\frac{1}{2}}]$ is an observable pair

The closed loop system

$$\dot{x}(t) = A_c\, x(t)$$

is asymptotically stable in the large, i.e., all of the eigenvalues of the matrix $A_c \triangleq (A - BG)$ lie in the left half complex

plane. The proof of this result can be found in the literature [27,30,34,35,36].

The main task in the solution of the optimal regulator design problem, therefore, is the computation of the constant symmetric, positive definite Riccati matrix K which is the solution of the algebraic matrix Riccati equation (59) with the boundary conditions (60). The Riccati equation (59) is equivalent to a system of $n(n+1)/2$ simultaneous scalar quadratic equations, and hence presents a formidable computational task even for moderately large values of n, the dimension of the state vector x(t). Until recently the equation was solved by direct integration of the corresponding differential Riccati equation (55),[37]. Anderson [38] has shown that the solution of the Riccati equation is equivalent to the solution of the spectral factorization problem which has been studied by Youla [39], Davis [40], and Amara [41]. An important result obtained is a theorem due to Potter [42] whereby the solution of the Riccati equation can be written down in terms of the eigenvectors of an associated Hamiltonian of the problem. MacFarlane [43] and O'Donnell [44] also proposed a similar technique. Fath [45] proposed a modified eigenvector solution for constant coefficient gain matrix by transforming the Riccati matrix into upper Hessenburg form (which has all the elements below the first subdiagonal equal to zero) and then to block diagonal form. This method was used to design controllers for systems up to the 25th

order with time reductions of the order 50 to 1 over earlier techniques using numerical integration of the Riccati equation. In most of these methods, numerical difficulties occur when the time step chosen for integration is too large. It has been shown by Vaughan [46, 47] that a very small time step is required when the real parts of the characteristic values of the system matrix Z [48] have a large spread, and very long computing times occur when the main interest is in the steady state solution.

An iterative procedure based on the Newton-Raphson method is found to be extremely useful in solving the algebraic matrix Riccati equation for the steady state case. The structure of the procedure is as follows [48]:

The steady state solution K of the Riccati equation (55) must satisfy the algebraic Riccati equation (59).

$$0 = Q - K S K + A^T K + KA$$

where

$$S = BR^{-1}B^T . \qquad (62)$$

Consider the matrix function

$$F(K) = Q - K SK + A^T K + KA . \qquad (63)$$

The problem is to find the non-negative definite symmetric matrix $\bar{K}$ that satisfies

$$F(\bar{K}) = 0 . \qquad (64)$$

The iterative procedure is derived as follows. Suppose that at the i-th stage, a solution K_i has been obtained, which does

not differ much from $\bar{K}$, i.e.,

$$\bar{K} = K_i + \tilde{K}$$

If $\tilde{K}$ is small, $F(\tilde{K})$ can be approximated by neglecting quadratic terms in $\tilde{K}$ to obtain

$$F(K) = Q - K_i S K_i - K_i S \tilde{K} - \tilde{K} S K_i - A^T (K_i + \tilde{K}) + (K_i + \bar{K}) A \quad . \qquad (65)$$

The basic idea of the Newton-Raphson method is to estimate K by setting the right hand side of (65) equal to zero. If this estimate is $\tilde{K}_i$, then

$$K_{i+1} = K_i + \tilde{K}_i \qquad (66)$$

Kleinman [49] and McClamroch [50] have shown that if the algebraic Riccati equation has a unique non-negative definite solution, K_i and K_{i+1} satisfy

$$K_{i+1} \leq K_i \qquad i = 0, 1, 2, 3, \ldots \qquad (67)$$

and

$$\lim_{i \to \infty} K_i = \bar{K} \qquad (68)$$

provided K_o is chosen such that

$$A_o = A - S K_o = A - B R^{-1} B^T K_o \qquad (69)$$

is asymptotically stable. Thus, an incorrect initial guess of K_o may lead to convergence to a different solution or no convergence at all. If the system coefficient matrix A is asymptotically stable, a safe choice would be $K_o = 0$. If it

is not, then the initial choice presents difficulties, thereby leading to numerical divergence or convergence to a wrong solution.

Although favorable experience using the Newton-Raphson method to solve Riccati equations has been reported in the literature [51], it is to be noted that the method does not provide conditions that will insure monotonic convergence of the solution. Kleinman [49] proposed an iterative scheme based on successive substitutions and by using the concept of a cost matrix proved that the iterations are monotonically convergent. The method is exactly similar to one obtained by applying Newton's method in function space [49]. The solution, in addition to being monotonically convergent, is also quadratically convergent in the vicinity of the true solution. This is unlike other iterative methods, where the schemes display only linear convergence near the true solution. Hence, the solution converges faster to the true solution.

In a later paper, Kleinman [52] also gave a method of constructing a stabilizing control law without the necessity of transforming variables or of specifying pole locations. The structure of Kleinman's iterative technique and the way to construct the stabilizing control law is outlined in Appendices [G,H] for the sake of completeness. The control gain matrix is constructed using these techniques.

All the methods described above, including Kleinman's iterative technique have a potential drawback. The existence of the set of stabilizing feedback gains assumes the complete controllability and the complete observability of the linear system (50) and (51). This means that

1) (A,B) is a completely controllable pair, and

2) (A,C) is a completely observable pair .

These restrictions as such are not serious restrictions when the technique is applied to systems that are naturally controllable and observable. This kind of situation arises when it is desired to control the attitude of a pointing device (a telescope) which is mounted on a stabilized inertial platform (a Shuttle). This problem has been discussed in great detail by Anderson and Joshi [53] as applied to the Annular Suspension and Pointing System (ASPS). As the platform is by itself inertially stabilized, the pointing system can be stabilized in inertial space (against this platform).

The present problem of stabilizing the LST in inertial space by torquing it against the spinning rim in the magnetic gaps, presents some difficulties. These difficulties arise due to the fact that the platform (spinning rim in this case) is not actively stabilized in inertial space. The only stabilizing effect on the rim is due to the inertial stiffness provided by its angular momentum vector H which is fixed in inertial space in the absence of any external torques. Since the small magnetic

forces, which control the LST-gimbal body are in effect external forces on the rim, the momentum vector of the rim will exhibit a small albeit definite, precessional motion. Thus, the LST-gimbal body is being forced to stabilize in inertial space by controlling it against a platform (spinning rim) which cannot resist these control torques. Mathematically, this difficulty shows up as failure of the solution to converge when the transverse angles θ_{a_2}, θ_{a_3} of the rim are included in the state variable vector. In fact, the study showed that the method fails to generate even the initial stabilizing gains when these transverse angles are included in the state vector.

Thus, the system is uncontrollable. The open loop eigenvalues are all zero, except for two eigenvalues at $\pm j\omega_o$, where ω_o is the nominal spin frequency of the rim. The spinning rim does not have any stabilizing mechanism of its own. Thus, the system is unstabilizable. However, since the state variables θ_{a_2}, θ_{a_3} are not of major importance, they can be excluded from the state vector, and a linear quadratic optimal regulator can be designed. In the estimator design, however, the complete state vector must be retained to preserve observability. The optimal input, therefore, is a linear feedback of a part of the optimal estimator.

Many problems of practical applications, including the present problem of fine pointing control, fall in this category.

Sandell [54] pointed out and proved that the assumptions of controllability and observability of Kleinman and others can be weakened to stabilizability and detectability. This important theorem with the proof is outlined in Appendix [K]. Thus, the Newton-Kleinman method [App. H] in conjunction with Kleinman's start up technique [App. G] represents a powerful and practical algorithm for computation of the Riccati equation solution, even for uncontrollable and unobservable system. The restrictions are now relaxed to include systems which are stabilizable and detectable.

3.5 Linear Gaussian Optimal Estimator Problem.- The stochastic, linear Gaussian optimal estimation problem, which is the estimator (filtering) part of the stochastic control problem defined in Section 3.2, is stated completely as follows:

Given the linear stochastic, time-invariant, dynamic system

$$\dot{x}(t) = A\,x(t) + B\,u(t) + \xi(t) \qquad (70)$$

$$\text{with } x(t_o) = x_o, \text{ and}$$

$$z(t) = C\,x(t) + \theta(t) \qquad (71)$$

where

1) $x(t)$ is a random variable, the initial state vector being Gaussian with known mean $\bar{x}_o$ and covariance matrix Σ_o ($\Sigma_o = \Sigma_o^T \geq 0$),

2) $\xi(t)$ the plant driving noise is white, Gaussian with zero mean and known covariance matrix, $\Xi(t)\ \delta(t-\tau)$, ($\Xi = \Xi^T \geq 0$ for $t \geq t_o$) and,

3) $\theta(t)$ the measurement noise is white, Gaussian with zero mean and known covariance matrix $\Theta(t)\ \delta(t-\tau)$, ($\Theta = \Theta^T > 0$ for $t \geq t_o$) find a vector $\hat{x}(t)$ which is an optimal state estimate of the true state $x(t)$.

There are a variety of ways to define the optimization criterion. Some of these are least square error criterion, minimum variance criterion, maximum likelihood of occurrence criterion, etc. However, the linear-Gaussian nature of the hypothesis developed for the problem lead all the above criteria to

the same "optimal" answer--that the optimal state estimate $\hat{x}(t)$ is generated by the Kalman-Bucy filter and is the mean of the true state $x(t)$.

The solution of the above seemingly complicated problem was made possible by Kalman and Bucy [55,56] who have shown that the dual of the optimal estimator problem is the optimal regulator problem. The dual problem is stated below.

Define a dynamical system which is the dual of

$$\dot{\hat{x}}(t) = A\,\hat{x}(t) + B\,\xi(t) \qquad (72)$$

$$z(t) = C\,\hat{x}(t) + \theta(t) \qquad (73)$$

by replacing above matrices as follows:

$$\begin{aligned} A(t) &\rightarrow A^T(t^*) \\ B(t) &\rightarrow C^T(t^*) \qquad t^* = -t \\ C(t) &\rightarrow B^T(t^*) \end{aligned} \qquad (74)$$

The dual dynamic system is then defined by

$$\frac{dx^*}{dt^*} = A^T(t^*)\,x^*(t^*) + C^T(t^*)\,u^*(t^*) \qquad (75)$$

$$z^*(t^*) = B^T(t^*)\,x^*(t^*). \qquad (76)$$

The dual optimal regulator problem is then to find a control law which minimizes

$$J = \tfrac{1}{2}\,||x^*(t_o^*)||^2_{\Sigma_o} + \tfrac{1}{2}\int_{t^*}^{t_o^*} [x^{*T}(\tau)\,Q\,x^*(\tau) + u^{*T}(\tau)\,R\,u^*(\tau)]\,d\tau. \qquad (77)$$

The complete mathematical details of this problem are

discussed by Sage [15]. Kalman [55] has shown that the results of the solution of this problem can be applied to the optimal state estimation problem because of the duality theorem which states that the two solutions are equivalent. This leads to the solution of the optimal state estimation problem by the well-known Kalman-Bucy filter as indicated below.

The duality theorem, along with another theorem due to Kalman [57], makes the solution of the optimal state estimation possible using an iterative technique for continuous time case (for time varying systems) by the Kalman-Bucy filter as follows:

The optimal state estimate $\hat{x}(t)$ of a general linear dynamic time-varying system of type (70) and (71) is generated by

$$\dot{\hat{x}}(t) = A\,\hat{x}(t) + B\,u(t) + H_o(t)\,[z(t) - C\,\hat{x}(t)] \qquad (78)$$

with initial conditions

$$\hat{x}(t_o) = \bar{x}_o \ .$$

The filter gain matrix $H_o(t)$ is given by

$$H_o(t) = \Sigma_o(t)\,C^T\,\Theta^T \qquad (79)$$

where Σ_o is the covariance matrix of the estimation error vector. It turns out that

$$E\left\{x(t) - \hat{x}(t)\right\} = 0 \qquad (80)$$

so that

$$\Sigma_o(t) = E\left\{\hat{x}(t) - x(t)(x(t) - \hat{x}(t))^T\right\} \qquad (81)$$

Furthermore, by a theorem [57] due to Kalman which gives the solution to the recursive estimation problem, the error covariance matrix $\sum_o(t)$ is the solution of the matrix Riccati differential equation

$$\dot{\sum}_o(t) = A \sum_o(t) + \sum_o(t) A^T + \Xi(t) - \sum_o(t) C^T \Theta^{-1} C \sum_o(t) \qquad (82)$$

with $\sum_o(t_o) = \sum_o$ (known initial covariance of x_o)

The solution of the practical constant gain, LG problem assumes a similar, but much simpler form. The filter gain matrix H_o is a constant (time invariant) matrix, and its value is given by

$$H_o = \sum_o C^T \Theta^{-1}. \qquad (83)$$

The constant, symmetric (at least) positive semidefinite matrix $\sum_o$ is the steady state estimation error covariance matrix and is the solution of the algebraic Riccati matrix equation,

$$0 = A \sum_o + \sum_o A^T + \Xi - \sum_o C^T \Theta^{-1} C \sum_o . \qquad (84)$$

The complete derivation of the Kalman-Bucy filter can be found in the original publications of Kalman [55] and Kalman-Bucy [56]. There are many different derivations of the above result since then, as well as extensions to nonlinear cases.

Comparing the steady state, LG problem (of calculating the filter gain matrix H_o and the algebraic Riccati equation

for error covariance matrix Σ_o) with the steady state LQ problem (of calculating the control gain matrix G and the algebraic Riccati equation for Riccati matrix K), it is seen that both problems are exactly equivalent with matrices A, B, Q, R, replaced by A^T, C^T, Ξ and Θ respectively. The discussion about the solution of the steady state Riccati equation in Section 3.4 holds for the LG problem also. The iterative procedure (outlined in Appendix H) is again used to calculate the Kalman-Bucy filter gains for the estimator.

The measurement vector, which consists of the magnetic gaps at the bearing stations, is a function of the transverse angles θ_{a_2} and θ_{a_3}. Therefore, to preserve observability, the angles θ_{a_2} and θ_{a_3}, which were neglected in the regulator problem, have to be considered in the estimator problem. The inclusion of these angles does not create any numerical difficulties in convergence of the solution, as it did in the regulator design.

With the design of the Kalman-Bucy filter and the estimator now complete, it is possible to discuss the dynamics of the closed loop LQG, which follows.

3.6 Stochastic Linear-Quadratic Gaussian (LQG) Control Problem.- After having formulated the solution of the linear quadratic optimal regulator (sec. 3.4) and of the linear Gaussian optimal filter (estimation problem) (sec. 3.5), it is now possible to cascade the two together (made possible by the separation theorem) to obtain the linear steady state, dynamic compensator.

The steady-state Linear Quadratic Gaussian (LQG) stochastic control problem can now be stated as follows:

Given the completely controllable and observable (these now being reduced to stabilizable and detectable) linear, time invariant system

$$\dot{x}(t) = A\,x(t) + B\,u(t) + \xi(t) \qquad (85)$$

where x is an n-state vector,

u is an m-control vector

and the time invariant measurement relation

$$z(t) = C\,x(t) + \theta(t) \qquad (86)$$

where z is an r-measurement vector

where

1) $\xi(t)$ the plant noise, is Gaussian, white, with zero mean and stationary,

2) $\theta(t)$ the measurement noise, is Gaussian, white, with zero mean and stationary, and

3) $\xi(t)$, $\theta(t)$ are uncorrelated,

find the control $u(t)$ for all $t \in (0,\infty)$ such that the cost functional

$$J = \lim_{T\to\infty} \frac{1}{T} \int_0^T [x^T(t)\, Q\, x(t) + u^T(t)\, R\, u(t)]dt$$

$$Q = Q^T \geq 0, \quad R\, R^T > 0 \qquad (87)$$

is minimized.

Solution: The optimal control correction vector $u(t)$ is given by

$$u(t) = - G\, \hat{x}(t) \qquad (88)$$

where $\hat{x}(t)$ is the optimal estimate of the state. The mxn constant matrix G is given by

$$G = R^{-1} B^T K \qquad (89)$$

where K, a constant, positive definite Riccati matrix is the solution of the (control) algebraic Riccati equation

$$0 = - KA - A^T K - Q + KB\, R^{-1}\, B^T K. \qquad (90)$$

The optimal state estimation vector $\hat{x}(t)$ is generated on line by the steady state Kalman-Bucy filter

$$\dot{\hat{x}}(t) = A\, \hat{x}(t) + B\, u(t) + H\, [z(t) - C\, \hat{x}(t)]. \qquad (91)$$

The constant, filter gain matrix H is given by

$$H = \Sigma C^T \Theta^{-1} \qquad (92)$$

where Σ, nxn constant matrix is the solution of the (filter) algebraic Riccati equation

$$0 = \Sigma A + A^T \Sigma + \Xi - \Sigma C^T \Theta^{-1}\, C \Sigma. \qquad (93)$$

Substituting for $u(t)$ from (88) in the equation for

$x(t)$ and $\hat{x}(t)$ and combining these two equations, the closed loop system satisfies the equation

$$\frac{d}{dt}\begin{Bmatrix} x(t) \\ \hat{x}(t) \end{Bmatrix} = \begin{bmatrix} A & -BG \\ HC & A-BG-HC \end{bmatrix}\begin{Bmatrix} x(t) \\ \hat{x}(t) \end{Bmatrix} + \begin{bmatrix} I & 0 \\ 0 & H \end{bmatrix}\begin{Bmatrix} \xi(t) \\ \theta(t) \end{Bmatrix} \qquad (94)$$

An alternate and a more clear state representation of the closed-loop system is obtained by the use of the state estimation error vector

$$\tilde{x}(t) = x(t) - \hat{x}(t). \qquad (95)$$

From the definition of $x(t)$ and (91), the modified closed-loop system now satisfies

$$\frac{d}{dt}\begin{Bmatrix} x(t) \\ \tilde{x}(t) \end{Bmatrix} = \begin{bmatrix} A - BG & BG \\ 0 & A - HC \end{bmatrix}\begin{Bmatrix} x(t) \\ \tilde{x}(t) \end{Bmatrix} + \begin{bmatrix} I & 0 \\ I & -H \end{bmatrix}\begin{Bmatrix} \xi(t) \\ \theta(t) \end{Bmatrix}. \qquad (96)$$

The eigenvalues of this system are given by the eigenvalues of the 2n x 2n matrix, whose characteristic polynomial is given by

$$\det \begin{bmatrix} A - BG - \lambda I & 0 \\ 0 & A - HC - \lambda I \end{bmatrix} \qquad (97)$$

$$= \det\ (A - BG - \lambda I) \det\ (A - HC - \lambda I).$$

From this, the following points follow:

1) Half of the eigenvalues can be independently adjusted by the value of G (which depends only on Q and R, the weighting matrices), while the other half can be independently adjusted by the value of H(which depends only on Ξ and Θ, the noise intensity matrices).

2) Since (A - BG) and (A - HC) are both strictly stable

matrices (this is individually assured in the regulator design and the estimator design), it follows that the overall closed loop system is stable.

The block diagram of the linear, time invariant, dynamic compensator is shown in Fig. 6. As is seen from the figure, the dynamics compensator is obtained by cascading the Kalman-Bucy filter designed in Section 3.5 with the optimal regulator design in Section 3.4. The design of the stochastic steady state linear quadratic Gaussian control is now complete for the fine pointing problem.

It is noted again here, that to retain observability, the state estimator vector $\hat{x}(t)$ contains the transverse angles of the spinning rim, viz., θ_{a_2} and θ_{a_3}. However, the inclusion of these angles in the state vector for the regulator problem, makes the system uncontrollable. Thus, only a part of the complete state estimator vector $\hat{x}(t)$ (without the transverse angles) is used to generate the optimal feedback control vector u(t).

It now only remains to prove the validity of the design by calculating the accuracy of the results. This is done by calculating the covariance of error of the states. The procedure to calculate the covariance matrix, which indicates the root-mean-square (RMS) error in the estimation of the states, is outlined in the next section.

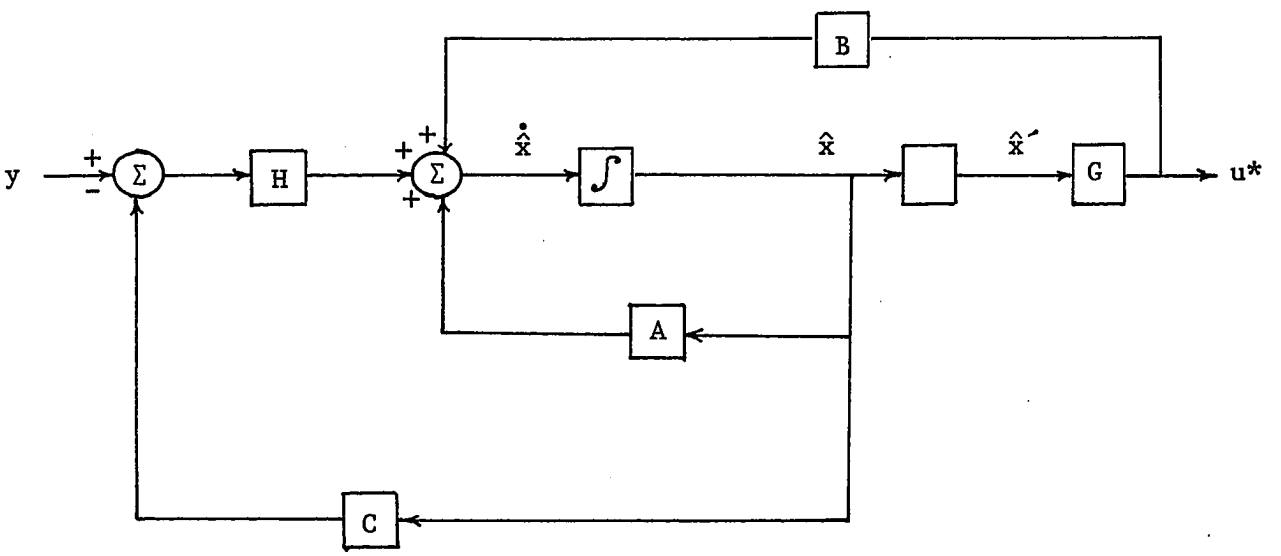

Figure 6. Dynamics Compensator

3.7 Covariance Analysis.- In order to evaluate the performance of the controller design using the procedure outlined in sec. 3.4-3.6, it is necessary to perform a covariance analysis of the equations governing the total system consisting of the optimal regulator and the optimal estimator (filter).

The system equations for the optimal regulator are

$$\dot{x} = Ax + BF, \tag{98}$$

$$\dot{F} = A_F F + B_F\ (v + \eta_v) \tag{99}$$

with the measurement equation

$$z = Cx + \theta\ , \tag{100}$$

The system equation for the time invariant Kalman-Bucy filter generating the optimal state estimate $\hat{x}$ for the above stochastic, time invariant state equations, is given by

$$\begin{aligned}\dot{\hat{\zeta}}(t) &= A_\zeta \hat{\zeta} + B_\zeta v + H\ [z - C\hat{\zeta}] \\ &= A_\zeta \hat{\zeta} + B_\zeta v + H\ [C\zeta - C\hat{\zeta} + \theta].\end{aligned} \tag{101}$$

Here, the state vectors x, F, ζ, the control vector v and the measurement vector z, are defined as follows

$$x = (\varepsilon_x, \dot{\varepsilon}_x, \varepsilon_y, \dot{\varepsilon}_y, \varepsilon_z, \dot{\varepsilon}_z, \theta_{g_2}, \dot{\theta}_{g_2}, \theta_{g_3}, \dot{\theta}_{g_3}, \omega_{a_2}, \omega_{a_3}, \theta_{g_1}, \dot{\theta}_{g_1})^T$$

$$F = (F_{a_1}, F_{r_1}, F_{a_2}, F_{r_2}, F_{a_3}, F_{r_3}, T_s)^T$$

$$v = (v_{a_1}, v_{r_1}, v_{a_2}, v_{r_2}, v_{a_3}, v_{r_3}, v_s)^T$$

and

$$\hat{\zeta} = (x^T, F^T, \theta_{a_2}, \theta_{a_3})^T$$

$$z = (g_{a_1}, g_{r_1}, g_{a_2}, g_{r_2}, g_{a_3}, g_{r_3}, \theta_{g_1}, \dot{\theta}_{g_1}, \theta_{g_2}, \dot{\theta}_{g_2}, \theta_{g_3}, \dot{\theta}_{g_3})^T$$

The solution of the Riccati equation for the optimal regulator problem (sec. 3.4) yields the optimal control vector v as a closed loop, time-invariant function of the state estimates $\hat{x}$, $\hat{F}$ as

$$v = [G]\begin{Bmatrix}\hat{x}\\ F\end{Bmatrix} \quad G \text{ is } 7\text{x}21 \text{ matrix} \qquad (102)$$

$$= G_1\hat{\zeta}$$

where G_1 is a 7x23 matrix obtained by adding two zero column vectors to G.

Now let

$$\tilde{\zeta} = \zeta - \hat{\zeta}$$

$$\therefore \hat{\zeta} = \zeta - \tilde{\zeta}$$

and $v = G_1\hat{\zeta} = G_1\zeta - G_1\tilde{\zeta}$.

But $G_1\zeta \equiv [G]\begin{Bmatrix}x\\ F\end{Bmatrix}$ (103)

Substituting for v from above in (99), we have

$$B_F v = B_F\, G\begin{Bmatrix}x\\ F\end{Bmatrix} - B_F\, G_1\tilde{\zeta} \qquad (104)$$

Now, let

$$G \equiv [G'\ G'']$$

where G' is a 7x14 matrix and G'' is a 7x7 matrix. Then,

$$B_F v = B_F G' x + B_F G'' F - B_F G_1 \tilde{\zeta} \qquad (105)$$

Also, the state equation can be written as

$$\dot{\zeta} = A_\zeta \zeta + B_\zeta v.$$

But, $\dot{\tilde{\zeta}} = \dot{\zeta} - \dot{\hat{\zeta}}$.

Thus, substituting for $\dot{\hat{\zeta}}$ from (101),

$$\dot{\tilde{\zeta}} = (A_\zeta - HC)\tilde{\zeta} + B_\zeta \eta_v - H\theta. \qquad (106)$$

Therefore, the equation for the total system of regulator and estimator can be expressed as

$$\begin{Bmatrix} \dot{x} \\ \dot{F} \\ \dot{\tilde{\zeta}} \end{Bmatrix} = \begin{bmatrix} A & B & 0 \\ B_F G' & A_F + B_F G'' & -B_F G_1 \\ 0 & 0 & A_\zeta - HC \end{bmatrix} \begin{Bmatrix} x \\ F \\ \tilde{\zeta} \end{Bmatrix}$$

$$+ \begin{bmatrix} 0 & 0 \\ B_F & 0 \\ B_\zeta & -H \end{bmatrix} \begin{Bmatrix} \eta_v \\ \theta \end{Bmatrix} \qquad (107)$$

The above equation can be expressed as

$$\dot{\chi} = A_\chi \chi + B_\chi V \qquad (108)$$

where

$$\chi = (x \; F \; \tilde{\zeta})^T \quad . \qquad (109)$$

For a system given by the above equation, the covariance matrix evolves according to the equation,

$$\dot{\Sigma} = A_\chi \Sigma + \Sigma A_\chi^T + B_\chi v \; B_\chi^T = 0 \qquad (110)$$

where

$$\Sigma = E\,[XX^T] \ .$$

The covariance matrix Σ is a 44x44 matrix and the diagonal elements of Σ give the variance of the state vector $\chi = (x\ F\ \tilde{\zeta})^T$. The RMS errors in the estimation of the states can be obtained by taking the square root of these diagonal elements. The matrix equation (110) is solved by using Smith's method [58,59] outlined in Appendix J.

Chapter 4

OPTIMAL LARGE ANGLE MANEUVER

CONTROLLER DESIGN - NUMERICAL RESULTS

A detailed qualitative analysis of the complex motion of the LST-gimbal-spinning rim body was undertaken in Chapter 2. The system was considered to be made up of two bodies, the LST-gimbal and the spinning rim, and the nonlinear equations governing the motion of these two bodies in inertial space were derived in sec. 2.4 and 2.5. A way to derive the expressions for the magnetic forces and torques acting on each of the two bodies was indicated in sec. 2.7 and the procedure to increase the computational time interval for integration of these equations was outlined in sec. 2.6. A complete analysis of the nonlinear equations is undertaken in this chaper. In sec. 4.1, the nonlinear equations (5)-(8) are reduced to the final form suitable for the optimization procedure described in sec. 3.1. The specific forms of hard constraints on the state and control variables are derived explicitly in sec. 4.2. The numerical results obtained by applying the optimization procedure to an LST of specific parameters are presented in sec. 4.3.

4.1 Final Form for Equations of Motion for Large Angle Maneuvers of the LST/AMCD.- The translational and rotational equations of motion for the LST-gimbal and spinning rim were derived in sec. 2.4 and 2.5 in equations (5)-(8).

The expressions for the external forces F's and torques τ's

in these equations consist of two parts. The first part is due to a spring-dashpot system assumed for the bearings and is termed "passive." The expressions for the "passive" forces are derived in Appendix C and those for the "passive" torques are derived in Appendix B. These expressions are given in terms of the state variables. The second part consists of additional perturbative control forces generated by the bearing servos (termed "active"), the torques at 0_{gs} due to the offset of 0_g (the point of application of the forces) from 0_{gs}, and the torques due to the spin motor and the gimbal torquer. The experessions for the total forces and torques on the spinning rim are derived in Appendix D and those for the LST-gimbal are derived in Appendix E. The control vector consists of eight control variables - F_{a_1}, F_{a_2}, F_{a_3}, F_{r_1}, F_{r_2}, and F_{r_3} the six (axial and radial) forces at the bearing stations and the two torques T_s and T_g, the spin motor torque and the gimbal torquer torque.

As was pointed out in sec. 2.6, the translational motion of the center of mass of the LST-gimbal, 0_{gs}, and the translational motion of the center of the spinning rim, 0_a, are not independent of each other. Also, it is noted that the small inertial motions of the center of mass of the LST-gimbal, 0_{gs}, and of the center of mass of the rim, 0_a, are not of interest but the magnitude of the gaps at the gimbal stations are of practical interest. These gaps (axial and radial) are seen to be functions of the relative displacement, ε, between the center of the gimbal ring

and spinning rim and their relative orientation given by the differences in Euler angles θ_g and θ_a. Since the "passive" forces between the two bodies were derived as functions of ε ($\equiv x_a - x_g$) in Appendix C, the inertial components of ε and its velocity are taken as state variables instead of the motion of the mass center of either rim or LST-gimbal. Equations (5)-(8) assume the following form:

$$m_a \ddot{x}_{1_a} = - 3 K_a \varepsilon_x - 3 K_a \dot{\varepsilon}_x - (F_{a_1} + F_{a_2} + F_{a_3}), \tag{111}$$

$$m_a \ddot{x}_{2_a} = - 1.5 K_R \varepsilon_y - 1.5 K_R \dot{\varepsilon}_y - [F_{r_1} \cos \delta_1 - F_{r_2} \cos \delta_2 - F_{r_3} \cos \delta_3 - F_t (\sin \delta_1 + \sin \delta_2 - \sin \delta_3)], \tag{112}$$

$$m_a \ddot{x}_{3_a} = - 1.5 K_R \varepsilon_z - 1.5 K_R \dot{\varepsilon}_z - [F_{r_1} \sin \delta_1 + F_{r_2} \sin \delta_2 - F_{r_3} \sin \delta_3 + F_t (\cos \delta_1 - \cos \delta_2 - \cos \delta_3)], \tag{113}$$

$$I_{xx_{gs}} \ddot{\theta}_{g_1} - I_{xz_{gs}} \ddot{\theta}_{g_3} = - T_{spin} - \ell_1 \sin \theta [-1.5 K_R \varepsilon_y - 1.5 K_R \dot{\varepsilon}_y] - \ell_1 \sin \theta [- \{ F_{r_1} \cos \delta_1 - F_{r_2} \cos \delta_2 - F_{r_3} \cos \delta_3 - F_t (\sin \delta_1 + \sin \delta_2 - \sin \delta_3) \}], \tag{114}$$

$$I_{yy_g}\ddot{\theta}_{g_2} = K_\lambda (\theta_{a_2} - \theta_{a_3}) + K_\lambda^{\bullet} (\dot{\theta}_{a_2} - \dot{\theta}_{a_3}) - T_g$$

$$+ \ell_1 \sin\theta \cos\theta_{g_1} [-3 K_A \varepsilon_x - 3 K_A^{\bullet} \dot{\varepsilon}_x]$$

$$- \ell_1 \cos\theta \sin\theta_{g_1} [-1.5 K_R \varepsilon_y - 1.5 K_R^{\bullet} \dot{\varepsilon}_y]$$

$$+ \ell_1 \cos\theta \cos\theta_{g_1} [-1.5 K_R \varepsilon_z - 1.5 K_R^{\bullet} \dot{\varepsilon}_z]$$

$$+ \ell_1 \sin\theta \cos\theta_{g_1} [-(F_{a_1} + F_{a_2} + F_{a_3})]$$

$$- \ell_1 \cos\theta \sin\theta_{g_1} [-\{F_{r_1} \cos\delta_1 - F_{r_2} \cos\delta_2 - F_{r_3} \cos\delta_3 - F_t (\sin\delta_1 + \sin\delta_2 - \sin\delta_3)\}]$$

$$+ \ell_1 \cos\theta \cos\theta_{g_1} [-\{F_{r_1} \sin\delta_1 + F_{r_2} \sin\delta_2 - F_{r_3} \sin\delta_3 + F_t (\cos\delta_1 - \cos\delta_2 - \cos\delta_3)\}], \qquad (115)$$

$$I_{zz_{gs}}\ddot{\theta}_{g_3} - I_{xz_{gs}}\ddot{\theta}_{g_1} = K_\lambda (\theta_{a_3} - \theta_{g_3}) + K_\lambda^{\bullet} (\dot{\theta}_{a_3} - \dot{\theta}_{g_3})$$

$$- \ell_1 \sin\theta \sin\theta_{g_1} [-3 K_A^{\bullet} \dot{\varepsilon}_x - 3 K_A \varepsilon_x]$$

$$- \ell_1 \cos\theta \cos\theta_{g_1} [-1.5 K_R^{\bullet} \dot{\varepsilon}_y - 1.5 K_R \varepsilon_y]$$

$$- \ell_1 \cos\theta \sin\theta_{g_1} [-1.5 K_R^{\bullet} \dot{\varepsilon}_z - 1.5 K_R \varepsilon_z]$$

$$- \ell_1 \sin\theta \sin\theta_{g_1} [-(F_{a_1} + F_{a_2} + F_{a_3})]$$

$$- \ell_1 \cos\theta \cos\theta_{g_1} \left[- \{ F_{r_1} \cos\delta_1 - F_{r_2} \cos\delta_2 - F_{r_3} \cos\delta_3 - F_t (\sin\delta_1 + \sin\delta_2 - \sin\delta_3) \} \right]$$

$$- \ell_1 \cos\theta \cos\theta_{g_1} \left[- \{ F_{r_1} \sin\delta_1 + F_{r_2} \sin\delta_2 - F_{r_3} \sin\delta_3 + F_t (\cos\delta_1 - \cos\delta_2 - \cos\delta_3) \} \right], \quad (116)$$

$$I'_{yy_s} \ddot{\theta} = T_g , \quad (117)$$

$$I_{xx_a} \ddot{\theta}_{a_1} = T_{spin} , \quad (118)$$

$$I_{yy_a} \ddot{\theta}_{a_2} + (I_{xx_a} \omega_o) \dot{\theta}_{a_3} = - K_\lambda (\theta_{a_2} - \theta_{g_2}) - K_\lambda^{\bullet} (\dot{\theta}_{a_2} - \dot{\theta}_{g_2}) + r [F_{a_1} \sin\beta_1 + F_{a_2} \sin\beta_2 - F_{a_3} \sin\beta_3] , \quad (119)$$

and

$$I_{zz_a} \ddot{\theta}_{a_3} - (I_{xx_a} \omega_o) \dot{\theta}_{a_2} = - K_\lambda (\theta_{a_3} - \theta_{g_3}) - K_\lambda^{\bullet} (\dot{\theta}_{a_3} - \dot{\theta}_{g_3}) + r [- F_{a_1} \cos\beta_1 + F_{a_2} \cos\beta_2 + F_{a_3} \cos\beta_3] . \quad (120)$$

It can be seen that (114) and (116) are simultaneous equations in $\ddot{\theta}_{g_1}$, $\ddot{\theta}_{g_3}$ and have to be solved together to get separate equations for $\ddot{\theta}_{g_1}$ and $\ddot{\theta}_{g_3}$. Denoting the right-hand side of (114) = (116) by τ_x, τ_y, and τ_z respectively, the equations for $\ddot{\theta}_{g_1}$ and $\ddot{\theta}_{g_3}$ can be reduced to the following form:

$$\left(I_{xx_{gs}} - \frac{I_{xz_{gs}}^2}{I_{zz_{gs}}}\right)\ddot{\theta}_{g_1} = \tau_{gs_x} + \frac{I_{xz_{gs}}}{I_{zz_{gs}}}\,\tau_{gs_z} \qquad (114a)$$

$$I_{yy_g}\,\ddot{\theta}_{g_2} = \tau_{gs_y} \qquad (115a)$$

$$\left(I_{zz_{gs}} - \frac{I_{xz_{gs}}^2}{I_{xx_{gs}}}\right)\ddot{\theta}_{g_3} = \tau_{gs_z} + \frac{I_{xz_{gs}}}{I_{xx_{gs}}}\,\tau_{gs_x}\,. \qquad (116a)$$

Theoretically, equations (111) - (120), with (114a) and (116a) replacing (114) and (116) are the complete set of nonlinear, coupled, second order, nonautonomous differential equations fully describing the motion of the LST-gimbal-rim in inertial space and can be solved by standard numerical techniques on a digital computer. In practice, however, these equations pose an enormous computational time requirement for the reason discussed in sec. 2.6.

Therefore, following the technique noted in that section, the computational time interval required to integrate these equations was increased by an order of magnitude. The procedure to achieve this is as follows.

First, the high precessional frequency roots, due to the large rotational acceleration of the rim, were eliminated by defining the transverse moments of inertia of the rim identically equal to zero. This has the effect of instantaneous transfer of rotational velocities $\dot{\theta}_{a_2}$, $\dot{\theta}_{a_3}$ to the rim. The equations (119) and (120) thereby reduce to

$$K_\lambda \dot{\theta}_{a_2} + H_o \dot{\theta}_{a_3} = - K_\lambda \theta_{a_2} + K_\lambda \theta_{g_2} + K_\lambda \dot{\theta}_{g_2}$$

$$+ r [F_{a_1} \sin \delta_1 + F_{a_2} \sin \delta_2 - F_{a_3} \sin \delta_3], \quad (119a)$$

and

$$- H_o \dot{\theta}_{a_2} + K_\lambda \dot{\theta}_{a_3} = - K_\lambda \theta_{a_3} + K_\lambda \theta_{g_3} + K_\lambda \dot{\theta}_{g_3}$$

$$+ r [F_{a_1} \cos \delta_1 + F_{a_2} \cos \delta_2 + F_{a_3} \cos \delta_3]. \quad (120a)$$

These equations can be solved simultaneously for $\dot{\theta}_{a_2}$, $\dot{\theta}_{a_3}$ to yield

$$(K_\lambda^2 + H_o^2) \dot{\theta}_{a_2} = - K_\lambda K_\lambda \theta_{a_2} + K_\lambda K_\lambda \theta_{g_2} + K_\lambda^2 \dot{\theta}_{g_2}$$

$$+ K_\lambda r [F_{a_1} \sin \delta_1 + F_{a_2} \sin \delta_2 -$$

$$F_{a_3} \sin \delta_3] + K_\lambda H_o \theta_{a_3} - K_\lambda H_o \theta_{g_3} -$$

$$K_\lambda H_o \theta_{g_3} - H_o r[-F_{a_1} \cos \delta_1 + F_{a_2} \cos \delta_2 +$$

$$F_{a_3} \cos \delta_3] \quad (119b)$$

and

$$(K_\lambda^2 + H_o^2) \dot{\theta}_{a_3} = - K_\lambda H_o \theta_{a_2} + K_\lambda H_o \theta_{g_2} + K_\lambda H_o \theta_{g_2}$$

$$+ H_o r [F_{a_1} \sin \delta_1 + F_{a_2} \sin \delta_2 - F_{a_3} \sin \delta_3]$$

$$- K_\lambda K_\lambda \theta_{a_3} + K_\lambda K_\lambda \theta_{g_3} + K_\lambda^2 \dot{\theta}_{g_3}$$

$$+ K_\lambda r [- F_{a_1} \cos \delta_1 + F_{a_2} \cos \delta_2 +$$

$$F_{a_3} \cos \delta_3] \quad (120b)$$

However, since the magnitudes of the angular gaps $\theta_{a_2} - \theta_{g_2}$ and $\theta_{a_3} - \theta_{g_3}$ are of greater importance than the magnitudes of θ_{a_2}, θ_{a_3}, the above equations can be rewritten with $\theta_{a_2} - \theta_{g_2}$ and $\theta_{a_3} - \theta_{g_3}$ as new state variables as follows:

$$\dot{\theta}_{a_2} - \dot{\theta}_{g_2} = \frac{1}{(K_\lambda^2 + H_o^2)} \Big[- K_\lambda^{\cdot} K_\lambda \theta_{a_2} + K_\lambda K_\lambda^{\cdot} \theta_{g_2} + (K_\lambda^2 - 1) \dot{\theta}_{g_2}$$

$$+ K_\lambda r [F_{a_1} \sin \delta_1 + F_{a_2} \sin \delta_2 - F_{a_3} \sin \delta_3] +$$

$$K_\lambda H_o \theta_{a_3} - K_\lambda H_o \theta_{g_3} - K_\lambda H_o \dot{\theta}_{g_3} - H_o$$

$$r [- F_{a_1} \cos \delta_1 + F_{a_2} \cos \delta_2 + F_{a_3} \cos \delta_3] \Big] \quad (119c)$$

and

$$\dot{\theta}_{a_3} - \dot{\theta}_{g_3} = \frac{1}{(K_\lambda^2 + H_o^2)} \Big[- K_\lambda H_o \theta_{a_2} + K_\lambda H_o \theta_{g_2} + K_\lambda^{\cdot} H_o \dot{\theta}_{g_2}$$

$$+ H_o r [F_{a_1} \sin \delta_1 + F_{a_2} \sin \delta_2 - F_{a_3} \sin \delta_3]$$

$$- K_\lambda K_\lambda^{\cdot} \theta_{a_3} + K_\lambda K_\lambda^{\cdot} \theta_{g_3} + (K_\lambda^2 - 1) \dot{\theta}_{g_3} + K_\lambda^{\cdot}$$

$$r [- F_{a_1} \cos \delta_1 + F_{a_2} \sin \delta_2 + F_{a_3} \cos \delta_3] \Big] . \quad (120c)$$

Elimination of the large negative roots due to the large linear acceleration of the system, is a straightforward procedure. These three roots are eliminated by defining the mass of the rim identically equal to zero. This has the effect of instantaneous transfer of linear velocities x_{1_a}, x_{2_a}, x_{3_a} to

the AMCD rim mass. The equations(111) - (113) then reduce to

$$\dot{\varepsilon}_x = -\frac{K_a}{K_a^{\bullet}}\,\varepsilon_x - \frac{1}{3K_a^{\bullet}}\,[F_{a_1} + F_{a_2} + F_{a_3}]\,, \qquad (111a)$$

$$\dot{\varepsilon}_y = -\frac{K_R}{K_R^{\bullet}}\,\varepsilon_y - \frac{1}{1.5K_R^{\bullet}}\,[F_{r_1}\cos\delta_1 - F_{r_2}\cos\delta_2 - F_{r_3}\cos\delta_3 - F_t\,(\sin\delta_1 + \sin\delta_2 - \sin\delta_3)]\,, \qquad (112a)$$

$$\dot{\varepsilon}_z = -\frac{K_R}{K_R^{\bullet}}\,\varepsilon_z - \frac{1}{1.5K_R^{\bullet}}\,[F_{r_1}\sin\delta_1 + F_{r_2}\sin\delta_2 - F_{r_3}\sin\delta_3 + F_t\,(\cos\delta_1 - \cos\delta_2 - \cos\delta_3)]\,. \qquad (113a)$$

Substituting for $\dot{\varepsilon}$ in τ_x, τ_y, and τ_z the expressions for these torques reduce to the following simpler forms:

$$\tau_{gs_x} = -T_{spin}\,, \qquad (114b)$$

$$\tau_{g_y} = K_\lambda(\theta_{a_2} - \theta_{g_2}) + K_\lambda^{\bullet}(\dot{\theta}_{a_2} - \dot{\theta}_{g_2}) - T_g\,, \qquad (115b)$$

$$\tau_{gs_x} = K_\lambda(\theta_{a_3} - \theta_{g_3}) + K_\lambda^{\bullet}(\dot{\theta}_{a_3} - \dot{\theta}_{g_3})\,. \qquad (116b)$$

Utilizing equations (111a), (112a), (113a), (114a), (115a), (116a), (119c) and (120c), (111) - (120) after elimination of high frequency roots can be rewritten in the form (9).

4.2 Explicit Form for "Hard" Constraints.- In the nonlinear, large angle maneuvering problem formulated above, the state variables and the control variables cannot assume unbounded values. The magnitude bounds on states and controls arise due to the following reasons.

It is easily seen that there are physical limits on the magnetic gaps in which the spinning rim is suspended. These limits impose an immediate constraint on the magnitude of the state variables ε_x, ε_y, ε_z, $\theta_{a_2} - \theta_{g_2}$ and $\theta_{a_3} - \theta_{g_3}$.

Under the assumption stated in sec. 2.1, the plane of the spinning rim remains nearly fixed in inertial space. Hence, magnitude bounds are imposed on the variables θ_{g_2} and θ_{g_3} due to the limits on the magnetic gaps. In addition, the state variable θ_{g_1} cannot assume values greater than 2π, since this would mean that the maneuver has been accomplished by passing through the final desired value of θ_{g_1} more than once, and, this would not be an optimal maneuver.

In practical situations, the momentum vector of the spinning rim is pointed away from the Sun and the LST is not targeted to any point within a cone of 45° around the Sun. This imposes bounds on the values θ can assume.

The constraints imposed on the magnitudes of the control variables are much more direct and are a result of the maximum force or torque that the electromagnetic actuators and torquer

motors are able to supply. Thus, it can be seen that all the control variables have "hard" magnitude constraints.

It is observed that there are no strict limits on the values the angular velocities $\dot{\theta}_g$, $\dot{\theta}_a$, and $\dot{\theta}$ can take; the only indirect constraint being that the values of θ_g, θ_a, and θ cannot exceed the "hard" constraints on them. This is achieved in the program by prescribing reasonably large saturation values to these velocities and checking the output to assure that the state variables θ_g, θ_a, and θ do not exceed their limits.

Thus, all the "hard" constraints on the state variables and the control variables are of the form

$$x_i(t) \leq x_{sat_i} \qquad i = 1, 2, \ldots n \tag{121}$$

$$u_j(t) \leq u_{sat_j} \qquad j = 1, 2, \ldots m \tag{122}$$

where the saturation values x_{sat} and u_{sat} are given in Table - 1. These inequalities can be rewritten in the following form

$$1 - \frac{x_i}{x_{sat_i}} \geq 0 \tag{123}$$

$$1 - \frac{x_j}{x_{sat_j}} \geq 0 . \tag{124}$$

Thus, all the "hard" constraints on the state variables x, and the control variables, u, are reduced to the following standard form of sec. 2.3.1.

$$g(u,t) \geq 0 \tag{125}$$

Gimbal Torquer (ft-lbs)	Actuator Forces (lbs)	Spin Motor Torque (ft-lbs)	Actuator Gaps (inches)
220	2.0	30	0.5
Note: The selection of these values is explained in Sec. 4.3.			

Table 1. Constraints on Absolute Values of Variables

$$h\ (x,t) \geq 0 \qquad (126)$$

where $$g_j(u,t) = 1 - \frac{u_j\ (t)}{u_{sat_j}}$$

$$h_i(x,t) = 1 - \frac{x_i(t)}{x_{sat_i}} \quad .$$

4.3 Numerical Generation of Optimal Control Law.- It is noted that the design objective in the synthesis of the maneuvering problem was 1) to reorient the LST pointing axis with the new target, having the known azimuth angle $\theta_{g_{1_f}}$ and the known declination angle θ_f, and 2) to achieve this retargeting with the minimum expenditure of energy. It is also to be noted that all the other state variables (relative displacement ε and all the velocities) must return to their steady state value of zero.

The requirement of achieving the maneuver with minimum expenditure of energyis incorporated in the integral penalty term. The energy expended is assumed to be proportional to the square of the forces and torques developed by the electromagnetic actuators and torquers.

The algorithm to solve a general nonlinear, optimal control problem of the above form was programmed on a CDC 6600 digital computer [60]. The program was written in FORTRAN and can handle systems of order up to $n = 25$ and $n + m = 30$. The storage space provided in the program can store up to 1000 points for both the forward trajectory of state equations and the backward trajectory of the costate equations. Provision is made to stop the iterative procedure with a user specified convergence criterion or maximum number of iterations criterion. In the event of the latter, provision is made to save the control history generated at the end of the last iteration (or in the case when the program encounters the time

limit), and to restart the iterative procedure from this point onward. This feature makes it necessary to repeat only one iteration, without repeating all the previous iterations. A complete description of the procedure to use this program by a general user is given in reference [60].

The above program was used to generate an iterative procedure for obtaining the time history of the optimal, open loop control law. The numerical results were obtained for an LST/Gimbal/Spinning rim having parameters specified in Table 2. The maneuver retargeted the LST from an initial target with $\theta_{g_1} = \theta = 10^o$ to a final target $\theta_{g_1} = 31.5^o$, $\theta = 28.6^o$. The example maneuver was restricted to this range because of the computer time requirements. In addition, the magnitude of forces and torques assumed available at the bearings were increased by a factor of 10 in order to complete the maneuver within a reasonable time. The assumed magnitude of forces and torques are shown in Table 1. The convergence results for this specified problem are shown in Figs. 7-13. The initial guess for the control law for this maneuver was assumed to be a linear law which is known to be the optimal for a simple second order system [27]. Thus, for starting the iterative procedure, both the spin torque and the gimbal torquer were assumed to be of the following linear forms

$$T_{spin}(t) = -\left(T_{spin}^{max} - 2\, T_{spin}^{max}\ \frac{t}{T}\right) \tag{127}$$

$$T_g\ (t) = \left(T_g^{max} - 2\, T_g^{max}\ \frac{t}{T}\right) \tag{128}$$

	Mass Slugs	Inertia (slug-ft^2)		
		I_x	I_y	I_z
Rim	3.105	77.71	38.85	38.85
LST	1,000	2,000	15,542	15,542
Gimbal	12.5	312.5	156.25	156.25
$r = 5'$, $\ell_1 = 21.73'$, $\beta_o = 30^o$, $\omega_o = 200$ rad/sec.				

Table 2. System Parameters

It can be seen from the converged value of the time history for T_g, Fig. 7, that the shape of this converged time history does not change very much from the initial guess. The initial assumed magnitude was oversufficient to maneuver the LST from $\theta_i = 0.17$ rad to $\theta_f = 0.5$ rad. Hence, the iterative procedure cuts back on the magnitude of $T_g(t)$ retaining the form of the linear law. This can be easily seen to be appropriate since the equation of motion in the θ direction (117) is indeed a simple, second order equation and is uncoupled from the other equations.

However, the equation of motion in the θ_{g_1}, direction (114a), is nonlinear and highly coupled with the other state variables present. The effect of this can be seen distinctly in the converged solution of the time history for the spin control, Fig. 8. The final time history differs drastically from the initially assumed simple, linear law. This indicates that the initial guess does not always work and that the iterative method is capable of overcoming a bad initial guess. It is seen from the time history plot for T_{spin} that the correction generated by the iterative procedure indicates the necessity of a torque magnitude (at a few points) greater than that allowed by the magnitude constraint on the spin motor. This is found to be the result of the arbitrary choice of elements in the penalty matrices. An additional run was performed by cutting off these violations. The terminal angle θ_{g_1} obtained was found to be within 0.01 rad of the terminal angle obtained without cutting off the violation.

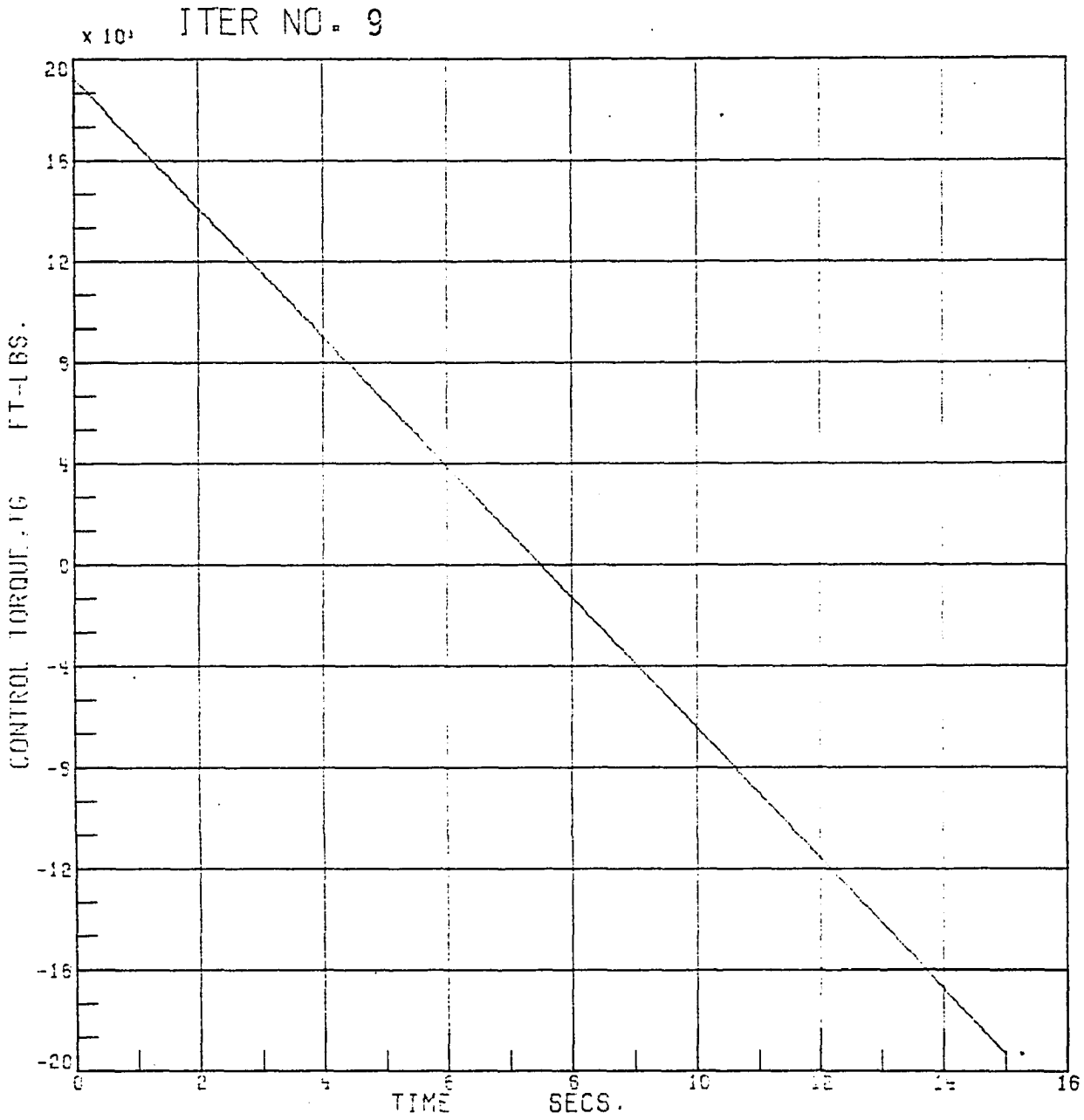

Figure 7. Optimal Control - Gimbal Torquer Torque

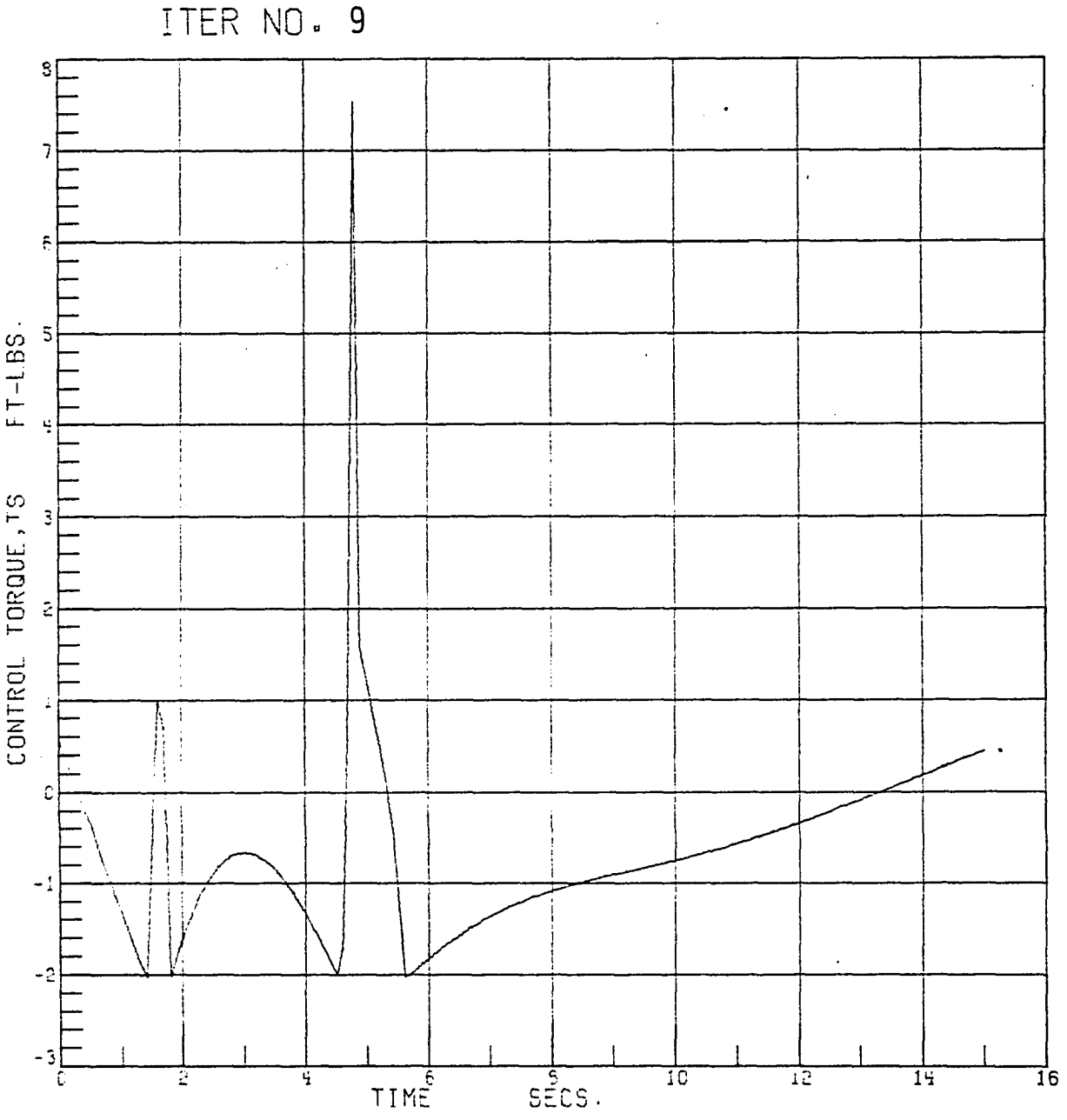

Figure 8. Optimal Control - Spin Torque

Figure 9 shows one of the components, ε_y, of the displacement of the rim center from the gimbal center, ε. It can be seen from the figure that the displacement is well below the maximum value of 0.5." Other components of ε exhibit similar behavior.

Figures 10, 11 show the time history of the two target angles of interest, θ_{g_1} and θ. It may be observed here that in the present case, saturation values were assigned only to the displacements, linear and angular, but not to the velocities. In spite of this absence of the saturation value on velocities (introduced by choosing very high magnitudes of the saturation values), it is seen that the terminal value of $\dot{\theta}$ is fairly low ($.84 \times 10^{-3}$ rad/sec = 173.2 arcsec/sec). This compares very well with the zero terminal velocity in the ideal case. However, it is found that the iterative procedure is unable to reduce the terminal value of $\dot{\theta}_{g_1}$ to a similar small value. The relatively high residual velocity θ_{g_1} (0.44×10^{-1} rad/sec = 9075 arcsec/sec) can be nulled by the fine pointing control as shown in Fig. 12. In practice, it will be nulled by the centering forces. Figure 13 shows one of the components of the relative angular displacement $\theta_{a_2} - \theta_{g_2}$, between the spinning rim and the gimbal plane. It can be seen that the angular displacement never exceeds the saturation value (0.833×10^{-2} rad = 1718 arcsec) during the maneuver, corresponding to 0.5" gap.

Thus, the iterative procedure successfully generates the time history of the control required to maneuver the LST with minimum expenditure of energy. The maneuver can be achieved

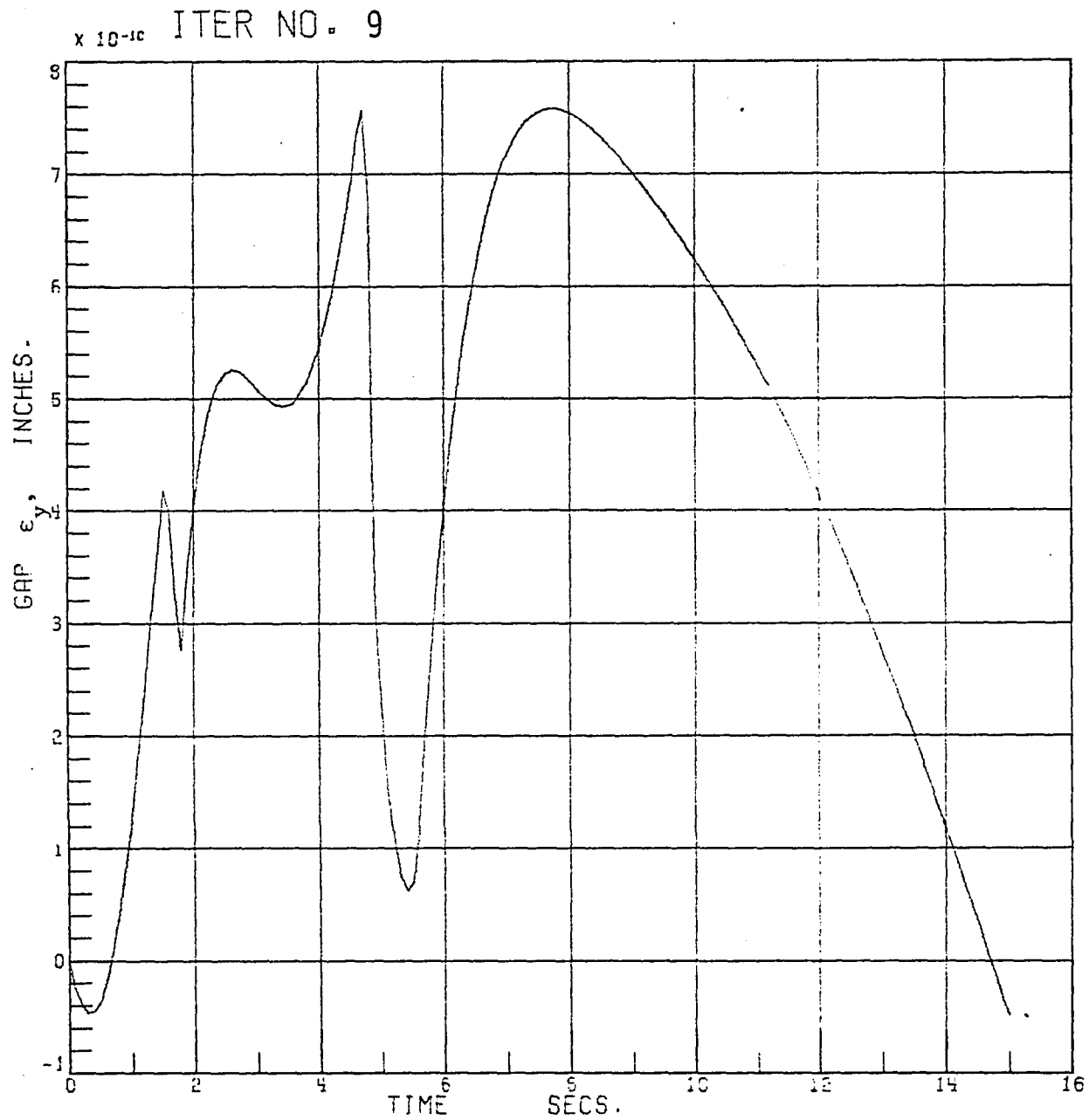

Figure 9. Converged Trajectory - Relative Displacement, ε_y

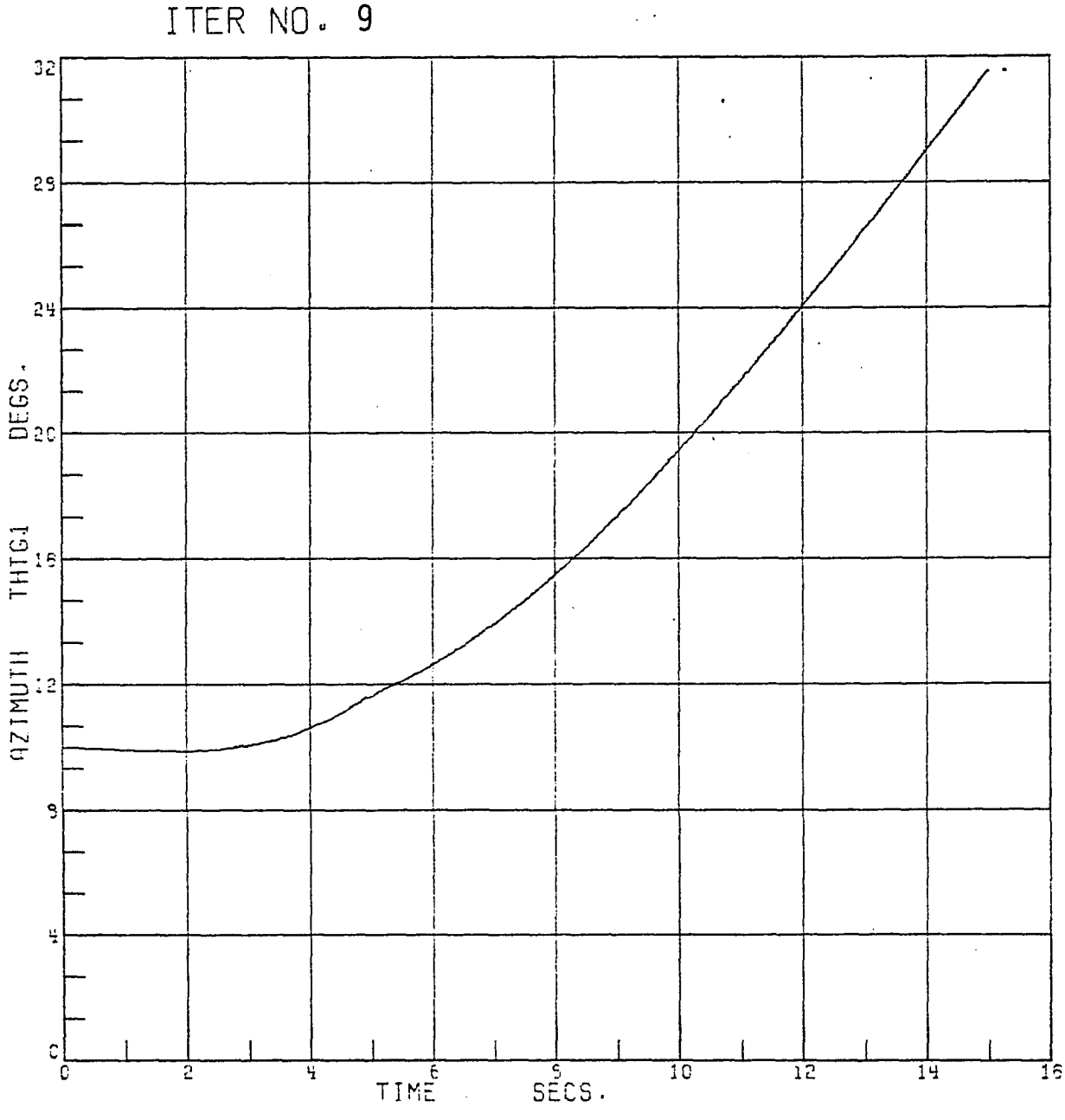

Figure 10. Converged Trajectory - Azimuth Angle, θ_{g_1}

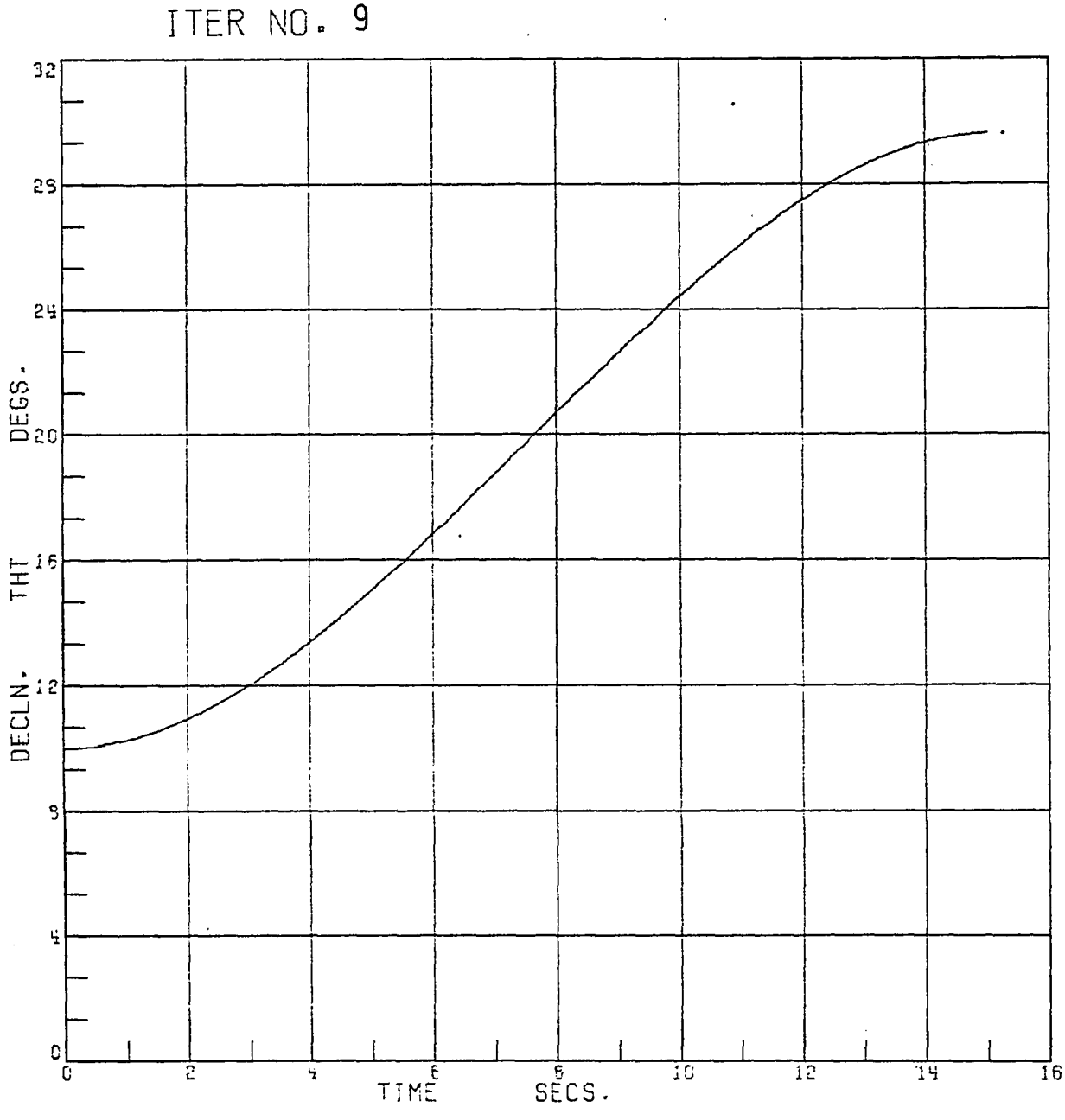

Figure 11. Converged Trajectory - Declination Angle, θ

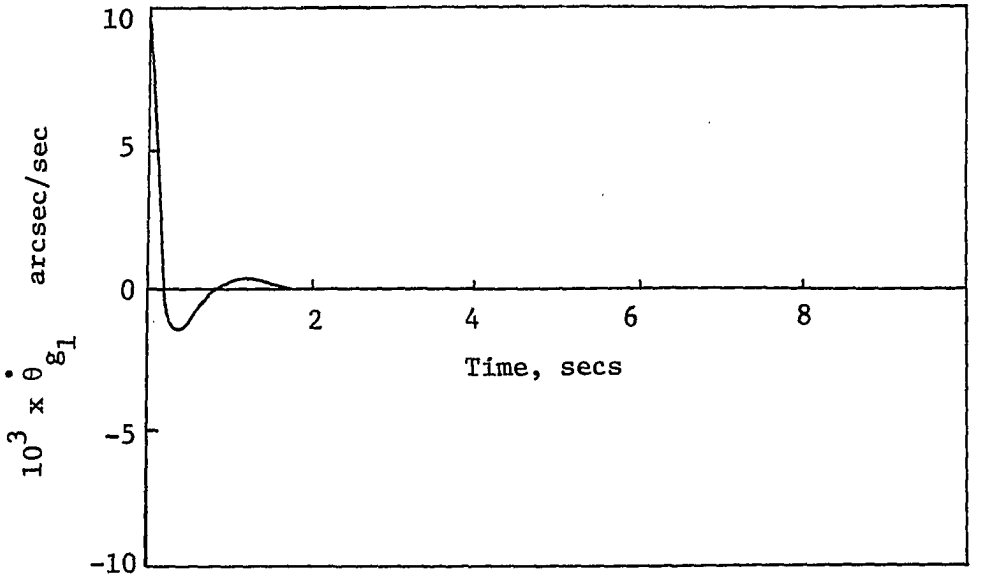

Figure 12. Linear Controller Response

NOTE: Full scale value represents gap of 0.233"

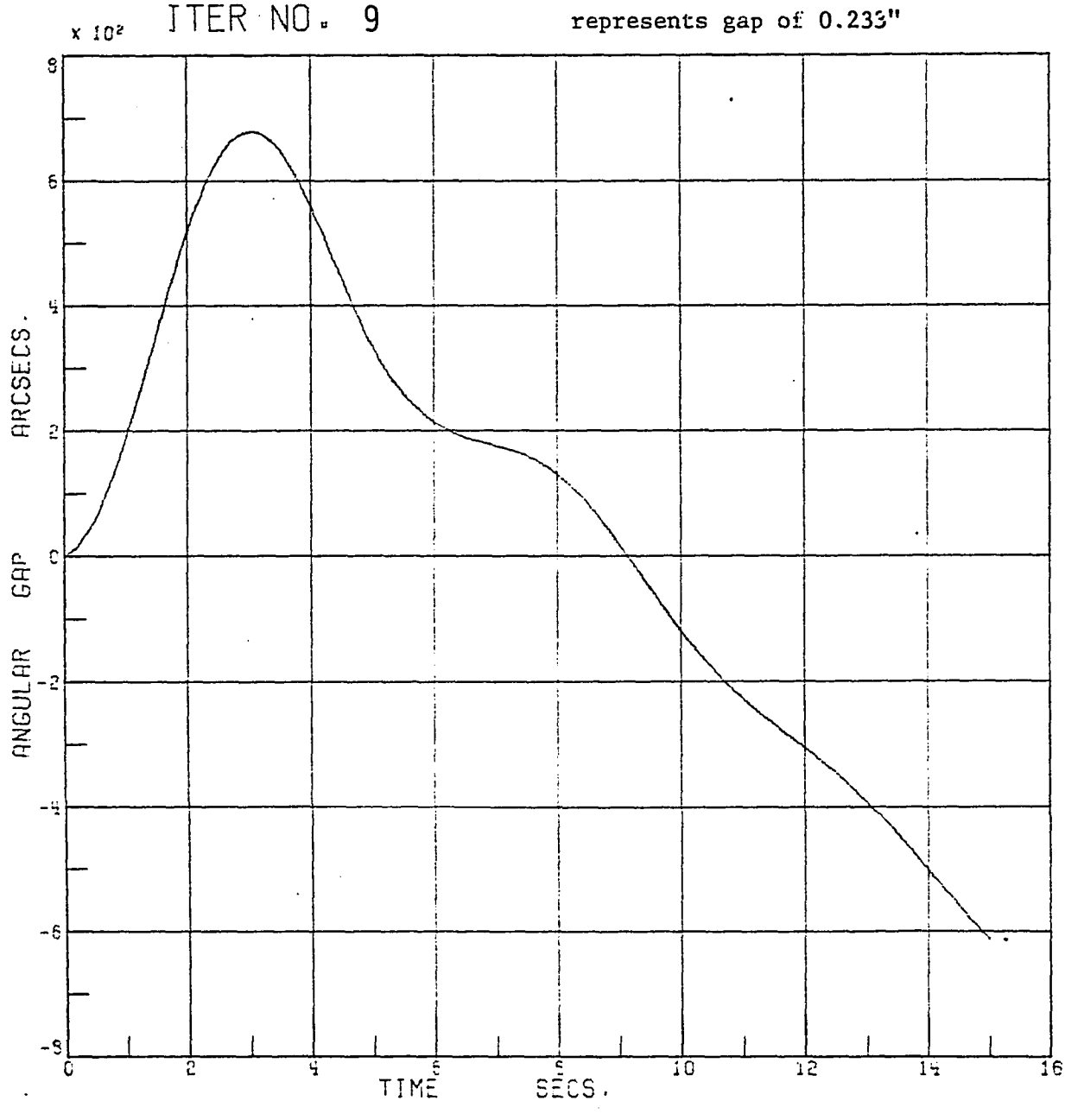

Figure 13. Converged Trajectory - Relative Orientation

without violating any of the hard constraints on the system. The residual errors in the pointing angles and velocities etc. may be corrected in the fine pointing mode.

The following general observations are made on the iterative procedure used to derive the open loop, time history of the control for a general, nonlinear, coupled, high order system. The rate of convergence of the iterative procedure, convergence to the (local) minima and the number of iterations required to converge to this minima, were found to be very sensitive to the following parameters:

a) The initial guess for the control time history to start the iterations,

b) The values of the elements of the weighting matrices G, Q, R and of Heaviside step functions K_{s_i} and K_{c_i}, and

c) Change in the value of a particular penalty during the iterative procedure.

The results for the iterative procedure with an assumed bang-bang control history as the initial guess are shown in Table 3 together with the converged value of the performance index. The results of the procedure with a linearly-varying time history (which is the optimal control history for a simple second order plant with the performance index to be minimized being the total energy), are shown in Table 4 together with the converged value of the performance index.

Iter. No.	θg_1	θ	cost(10^6)	ΔJ	Remarks
1	0.81	.76	0.3624	0.1	G(15,15) = 10^4
2	0.43	0.73	0.332	0.1	
3	0.76	0.73	0.329	0.1	
4	-0.031	0.73	0.48	0.05	
5	0.76	0.73	0.329	0.05	repeat of iter.3 "converged"

Note: $\theta_{g_{1_o}}$ = 0.1745 rad. θ_o = 0.1745 rad.

$\theta_{g_{1_f}}$ = 0.55 rad. θ_f = 0.5 rad.

Table 3. Convergence with Bang-Bang Law as Initial Guess

Iter. No.	θ_{g_1}	θ	cost(10^5)	ΔJ	Remarks
					First Run
1	0.5977	0.5655	1.999	0.1	$G(15,15) = 10^4$
2	0.3280	0.5464	1.087	0.1	
3	0.9508	0.5299	1.027	0.1	
4	0.8176	0.5298	0.9964	0.1	
5	-0.35	0.52	1.19	0.05	
6	0.8176	0.5298	0.9964	0.05	repeat of iter. 4
7	0.233	0.5257	0.9732	0.05	
8	0.6874	0.518	0.9338	0.05	
9	0.4775	0.517	0.9266	0.05	
10	0.44	0.51	1.257	0.025	
11	0.4775	0.517	0.9266	0.025	repeat of iter. 9
12	0.46	0.516	1.008	0.0125	
13	0.4775	0.517	0.9266	0.0125	repeat of iter. 11
					Second Run
1	0.4700	0.5169	1.266	0.1	$G(15,15) = 10^7$
2	0.4925	0.5169	1.111	0.1	
3	0.519	0.5169	0.9925	0.1	
4	0.5636	0.5168	0.9593	0.1	
5	0.499	0.5169	1.0950	0.05	
6	0.5636	0.5168	0.9593	0.05	repeat of iter. 4
7	0.5318	0.5168	0.97	0.05	
8	0.5636	0.5168	0.9593	0.025	repeat of iter. 6
9	0.5477	0.5168	0.9547		Convergence

Note: $\theta_{g_{1_o}} = 0.1745$ rad $\quad \theta_o = 0.1745$ rad

$\theta_{g_{1_f}} = 0.55$ rad $\quad \theta_f = 0.5$ rad

Table 4. Convergence with Linear Law as Initial Guess - Case 1

After the procedure converges to the neighborhood of θ_f, it is required to raise the penalty on the deviation of the final value of θ_{g_1} from $\theta_{g_{1_f}}$. However, it is seen from Table 5 that raising the value of G(15,15) (which penalizes the deviation in the terminal value of θ_{g_1}) from 10^4 to 10^6 does not facilitate convergence. However, raising G(15,15) to 10^7 makes the procedure converge faster as seen from Table 4.

A very high value of an element of the G matrix chosen initially may force the numerical procedure to converge to the terminal value of that particular state, even when other states are far from their desired terminal values. Again, the high penalty may or may not even force the particular state to its desired terminal value at a faster rate as was desired.

The value of a particular penalty may be required to be changed after a part of the iterative procedure, when all other states have converged to their final values but not this particular state. Thus, in summary, a good, near-optimal initial guess for the control history is required, and a judicious choice of the penalty matrices is required. It may be necessary to conduct a few test runs to assign the correct values for these matrices so that a fairly rapid convergence to the correct local minima is obtained.

It may be even necessary to change the values of the element(s) of the penalty matrices through the iterative procedure,

Iter. No.	θ_{g_1}	θ	cost(10^5)	ΔJ	Remarks
					Second Run
1	0.47	0.516	0.9785	0.05	G(15,15) = 10^6
2	0.50	0.516	0.9731	0.05	
3	0.518	0.516	0.99	0.025	
4	0.50	0.516	0.9731		"converged"

Table 5. Convergence with Linear Law as Initial Guess - Case 2

when the procedure indicates convergence of only some of the states to their final desired values, but not of others. Again, it may be necessary to conduct a few more test runs to assign proper new values to these elements.

Chapter 5

OPTIMAL FINE POINTING

CONTROLLER DESIGN - NUMERICAL RESULTS

A qualitative analysis of the motion of the LST-gimbal-spinning rim was done in Chapter 2. Assumptions made to linearize the complete nonlinear equations of motion, were outlined in sec. 2.8. A way to derive the expressions for the magnetic forces and torques acting at the bearing stations was indicated in sec. 2.7. The elements of the coefficient matrix B (premultiply the control vector u) are derived in Appendix F. A complete analysis of the linearized equations is undertaken in this chapter. In section 5.1, the linearized form of equations (5) - (8) is reduced to the final form suitable for optimization procedure described in sections 3.4 - 3.7. The numerical results obtained by applying this procedure to an LST of specific parameters are presented in sec. 5.2.

5.1 Final Form for Equations of Motion for Fine Pointing Control of the LST/AMCD.- The translational and rotation equations of motion for the LST-gimbal and the spinning rim were derived in sec. 2.4 and 2.5. As was pointed out in sec. 2.1, the gimbal torquer is locked during the fine pointing control and so, the relative degrees of freedom between the gimbal ring and the LST (i.e., θ and $\dot{\theta}$) are lost. Both the bodies move as a single rigid body. The equations derived in section 2.4 and 2.5, therefore, will have

to be modified slightly providing for the above changes.

Following the discussion in sections 2.6 and 2.8 concerning reduction in order and linearization, the above equations will have to be modified further as follows:

1) Combine equations (6) and (8) to get a single equation in the variable $x_a - x_g = \varepsilon$. Here, ε is the difference in the inertial positions of the center of the gimbal ring and the center of the spinning rim. This facilitates calculation of the air gaps at the bearing stations in terms of this difference and allows the magnetic forces and the spin torque (control vector components) to be expressed as a function of these difference, and

2) Drop equation (5a) since the small spin up (or slow down) of the spinning rim is of no direct interest to the problem.

Further, from the detailed discussion of the controllability of the system in Sec. 3.4, it was found necessary to ignore the transverse angles of the spinning rim, viz., θ_{a_2} and θ_{a_3} while designing the state feedback optimal regulator and calculating the gain matrix. It is, however, noted that, for the design of the Kalman-Bucy filter these two variables are included in the state vector to maintain observability. Thus the optimal regulator utilizes only a part of the state vector estimate from the filter, for feedback purposes.

Next, the explicit form for the equation of motion for ε, is developed utilizing the geometry of Fig. 14.

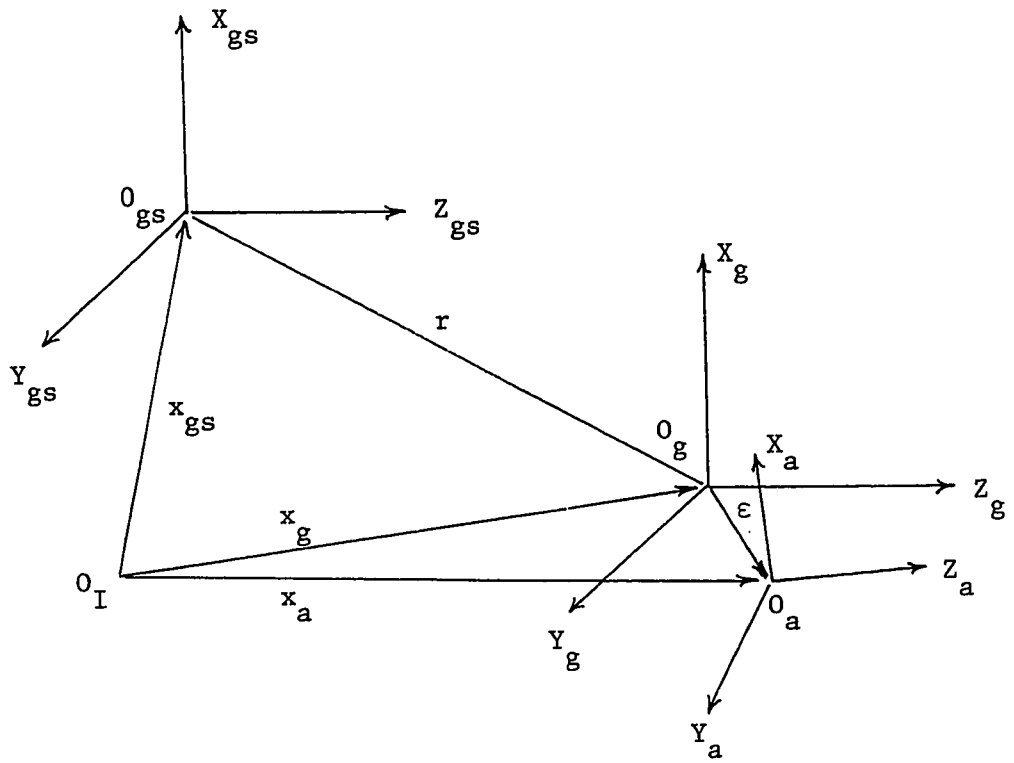

Figure 14. LST-Gimbal-Spinning Rim Geometry

Thus,

$$\varepsilon = x_a - x_g \tag{129}$$

$$\ddot{\varepsilon} = \ddot{x}_a - \ddot{x}_{gs} - \ddot{r} \tag{130}$$

Here r is a fixed vector in the reference coordinate-frame $O_{gs}\, x_{gs}\, y_{gs}\, z_{gs}$ which is rotating with the angular velocity $\omega_g^T = (\dot{\theta}_{g_1}, \dot{\theta}_{g_2}, \dot{\theta}_{g_3})$. Therefore, the velocity components of r in this reference frame are given by

$$\dot{r} = [\omega_g]\, r \tag{131}$$

where $[\omega_g]$ is the cross-product matrix defined earlier. Substituting for the components of r as

$$r_x = -\ell_1 \cos\theta,\quad r_y = 0,\quad r_z = \ell_1 \sin\theta \tag{132}$$

and simplifying, after substituting for $\ddot{x}_a$, $\ddot{x}_{gs}$, equation (130) reduces to the following vector form

$$\ddot{\varepsilon} = \left(\frac{1}{m_a} + \frac{1}{m_{gs}}\right) B_a\, u - \ddot{r} \tag{133}$$

Finally, dropping the equation for $\ddot{\theta}_a$ and considering only $\dot{\theta}_{a_2}$ and $\dot{\theta}_{a_3}$ as the state variables (but not θ_{a_2} and θ_{a_3}), the equations of motion for the system can be reduced to the final standard state variable form of sec. 3.4, viz.,

$$\dot{x}' = Ax' + Bu \tag{134}$$

where $x'^T = (\varepsilon_x\ \dot{\varepsilon}_x\ \varepsilon_y\ \dot{\varepsilon}_y\ \varepsilon_z\ \dot{\varepsilon}_z\ \theta_{g_2}\ \dot{\theta}_{g_2}\ \theta_{g_3}\ \dot{\theta}_{g_3}\ \omega_{a_2}\ \omega_{a_3}\ \theta_{g_1}\ \dot{\theta}_{g_1})$

and $u^T = (F_{a_1} \; F_{r_1} \; F_{a_2} \; F_{r_2} \; F_{a_3} \; F_{r_3} \; T_s)$.

Here x is a 14th order state vector and u is a 7th order control vector. The elements of the matrices A and B are given in Appendix F.

5.2 Controller Design and Numerical Results.- In the derivations of the equations of motion above, it was tacitly assumed that the control vector of magnetic actuator forces and torques was directly available and one could control the values of these forces and torques. However, in practice, these electromagnetic forces and torques are a result of the voltages in the actuator servo circuits. These forces and torques could be controlled only indirectly by controlling these voltages in the servo circuits. Thus, the differential equations of actuator dynamics governing the relations between the control voltages and the control forces and torques have to be included in the system equations as well. The actuator dynamics are represented by first order transfer functions (e.g., time lags due to inductances in the servo circuits). The control vector F, then, is obtained from the equation

$$\dot{F} = A_F F + B_F(V + \eta_V) \qquad (135)$$

where V is a 7x1 control voltage vector, and the zero-mean, white noise term η_V is included in order to represent actuator noise. The elements of the diagonal matrices A_F, and B_F are given in Appendix F.

The total system equations, therefore, can be written in the following vector matrix form

$$\begin{Bmatrix} \dot{x}' \\ \dot{F} \end{Bmatrix} = \begin{bmatrix} A & B \\ 0 & A_F \end{bmatrix} \begin{Bmatrix} x' \\ F \end{Bmatrix} + \begin{bmatrix} 0 \\ B_F \end{bmatrix} \{ v + \eta_v \} \qquad (136)$$

The above system of equations can be expressed in the standard form where

$$x' = (\varepsilon_x \ \dot{\varepsilon}_x \ \varepsilon_y \ \dot{\varepsilon}_y \ \varepsilon_z \ \dot{\varepsilon}_z \ \theta_{g_2} \ \dot{\theta}_{g_2} \ \theta_{g_3} \ \dot{\theta}_{g_3} \ \omega_{a_2} \ \omega_{a_3} \ \dot{\theta}_{g_1} \ \theta_{g_1})^T$$

$$F = (F_{a_1} \ F_{r_1}, \ F_{a_2}, \ F_{r_2}, \ F_{a_3}, \ F_{r_3}, \ T_s)^T$$

$$V = (V_{a_1}, \ V_{r_1}, \ V_{a_2}, \ V_{r_2}, \ V_{a_3}, \ V_{r_3}, \ V_s)^T$$

and η_V is zero-mean, white noise vector representing actuator noise.

It is assumed that the LST attitude and rate measurements are available via star trackers mounted (on hardware inside the LST) and rate gyros mounted on the LST. The axial and radial gap measurements are assumed to be available from the axial and radial proximity sensors mounted at each actuator station. Thus, the measurement equation is

$$y = Cx + \eta_y \qquad (137)$$

where

$$y = (\delta_{a_1}, \ \delta_{r_1}, \ \delta_{a_2}, \ \delta_{r_2}, \ \delta_{a_3}, \ \delta_{r_3}, \ \theta_{g_1}, \ \theta_{g_2}, \ \theta_{g_3}, \ \dot{\theta}_{g_1}, \ \dot{\theta}_{g_2}, \ \dot{\theta}_{g_3})^T$$

and η_y is a 12x1 zero-mean, white measurement noise vector. The elements of C matrix are given in Appendix F.

It is noted, however, that the state vector x in equation

(137) above, contains the two transverse angles θ_{a_2}, θ_{a_3} which are eliminated from consideration in the controller design for equation (136), due to the criterion on controllability. Thus, the state vector x in equation (137) is

$$x = (\varepsilon_x, \dot{\varepsilon}_x, \varepsilon_y, \dot{\varepsilon}_y, \varepsilon_z, \dot{\varepsilon}_z, \theta_{g_2}, \dot{\theta}_{g_2}, \theta_{g_3}, \dot{\theta}_{g_3}, \omega_{a_2},$$

$$\omega_{a_3}, \theta_{g_1}, \dot{\theta}_{g_1}, F^T, \theta_{a_2}, \theta_{a_3})^T$$

which is a 23x1 vector.

The procedure outlined in sections 3.4 to 3.7 can now be applied directly to the above problem for designing the stochastic optimal controller for fine pointing control. First, the deterministic optimal regulator problem is solved to get the optimal closed loop gains matrix G, so that the optimal control law is given by

$$u^* = G\,\hat{x}' \qquad (138)$$

where $\hat{x}'$ is the minimum-mean-square (MMS) estimate of the state vector x'. The state estimate $\hat{x}'$ used in the controller is a part of the complete state estimate $\hat{x}$ of the state vector x. This estimate $\hat{x}$ is generated by the Kalman-Bucy filter governed by the equation

$$\dot{\hat{x}}(t) = A\,\hat{x}(t) + B\,u(t) + H\,[z(t) - C\,\hat{x}(t)] \qquad (139)$$

with the initial condition $x_o\,(o) = \bar{x}_o$

The filter (or observer) problem is next solved to obtain the optimal filter gain matrix H.

As pointed out in sections 3.4 and 3.5, both the controller gain and estimator gain matrices are obtained via Newton-Kleinman iterations (Appendix H), using Kleinman's stabilizing (G), and Smith's method (J) for solving the Lyapunov matrix equation.

A complete block diagram of the dynamic compensator is shown in Fig. 6 . It is seen from that figure that only a portion ($\hat{x}'$) of the complete state estimate $\hat{x}$ is utilized for feedback purposes.

In order to investigate the performance of the above controller, a linear covariance analysis is performed as was outlined in sec. 3.7. The equations for the optimal regulator and the optimal controller were put in the form

$$\dot{\zeta} = A\zeta + B\, v \qquad (140)$$

where ζ is the state vector and v is the input noise vector with known covariance intensity (table 6). The covariance matrix evolves according to the equation

$$\dot{\Sigma} = A\Sigma + \Sigma A^T + B\, v\, B^T = 0 \qquad (141)$$

where $\Sigma = E\left\{\zeta\zeta^T\right\}$.

This matrix equation can be solved by Smith's method ([58] and Appendix J) and the steady state covariance matrix Σ can be obtained. The diagonal elements of Σ give the variance values of the state vector ζ.

The closed loop response with optimal gain, feedback control is plotted to observe the performance of the closed loop system.

The time history of the pointing angles θ_{g_1}, θ_{g_2}, and θ_{g_3} and one of the transverse angular velocity of the rim, ω_{a_2} are of particular interest and are plotted. Figure 15 shows the time response of the above variables for the LST-gimbal-rim configuration when the angle $\theta = 0^o$. This is the configuration when the inertial parameters have their least values. It is observed that the initial pointing errors are nullified in 5-6 seconds and the transverse velocity of the rim also is nullified.

Figure 16 shows the time response of these variables when $\theta = 45^o$. In this configuration the cross coupling effects between θ_{g_1}, θ_{g_2}, and θ_{g_3} are greatest in magnitude. It is again found that the initial pointing errors and the transverse angular velocity are nullified within the acceptable time interval.

The design of the optimal filter is done based on the procedure indicated in Sec. 3.5 and the optimal filter gain matrix was obtained.

To evaluate the validity of the design, covariance analysis of the regulator and the filter was conducted (Sec. 3.6-3.7) and the values of the RMS errors of the pointing angles θ_{g_1}, θ_{g_2}, and θ_{g_3} are tabulated in Table 7. The values of the sensor and actuator noise parameters used are shown in Table 6. The values of RMS errors in pointing are found to be less than 1 arcsecond. These could be reduced further by a proper choice of weighting matrices and noise parameters.

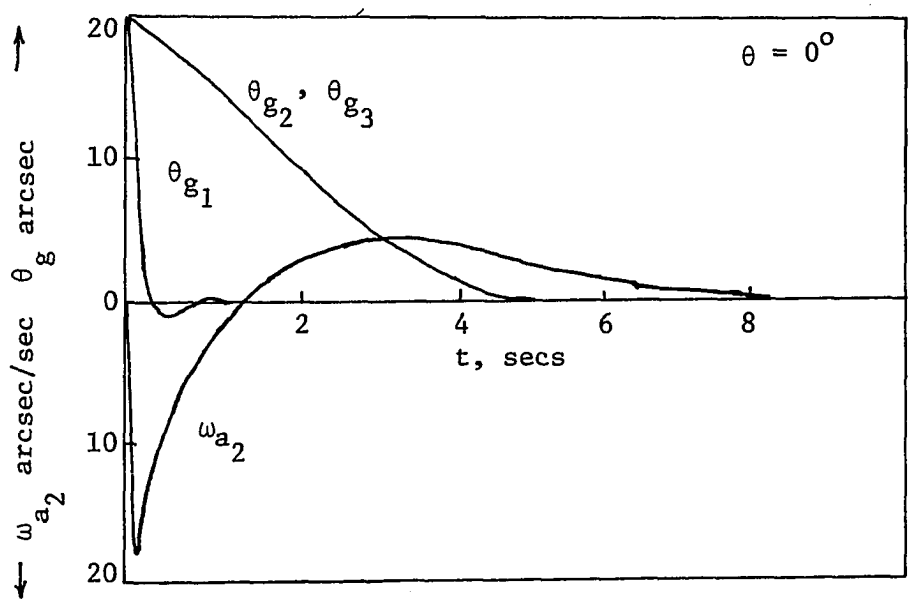

Figure 15. Linear Controller Response - $\theta = 0^{\circ}$ Case

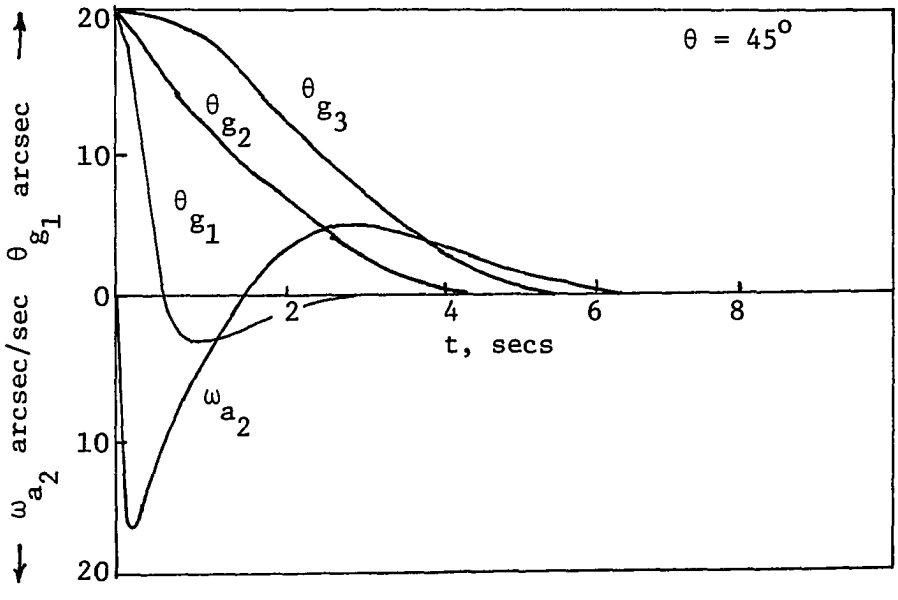

Figure 16. Linear Controller Response - $\theta = 45^{\circ}$ Case

Source	Standard Deviation
Proximity Sensors	0.0012 in.
Star Tracker	0.5 sec
Rate Gyros	0.031 sec/sec
Input Noise for Each Degree of Freedom	0.0001 (normalized)

Table 6. Noise Parameters

	$\sigma_{\theta_{g_1}}$	$\sigma_{\theta_{g_2}} = \sigma_{\theta_{g_3}}$
Proximity Sensor Noise	0.22	0.483
Star Tracker Noise	0.067	0.1
Rate Gyro Noise	0.71	0.508
Actuator Noise	0.0906	0.191
All Sources	0.76	0.73

Table 7. RMS Errors in Pointing Angles, arc sec., due to Various Noise Sources

Chapter 6

CONCLUSIONS

It has been demonstrated that both large angle maneuvers and fine pointing control of a Large Space Telescope can be effectively achieved using a single gimbal, single AMCD configuration.

A general user-oriented computer program was developed to compute an open loop optimal control law for a general, high-order, nonlinear system with "hard" constraints on state and control variables. The control history was generated using an iterative procedure utilizing a modified Gradient Method with penalty functions for handling the constraints. An optimal open loop, time varying control was computed for a nonlinear, large angle maneuvering problem, involving an LST reorientation of $\cong 20^{o}$. This optimal control law minimized the terminal pointing errors and the energy used for executing the maneuver. Convergence to a local minima was highly dependent on the initial control history chosen. Thus, for the minimum power (or energy) solution, it was desirable to choose the initial control history to be the linear law, which was known to be optimal for a simple second order system [27]. Other choices, e.g., the bang-bang control which is the optimal control for the minimum time problem, lead to a very low convergence rate or to a different local minima.

Choice of the weighting matrices G, Q, R and the Heaviside functions $H(h_i)$, $H(g_i)$ also affect the convergence rate. Too high a penalty on one or some of the state or control variables, may result

in the numerical procedure converging only those variables to their terminal values. The performance index converged to a minimum value, even though some of the variables had not yet reached their terminal value or some variables have exceeded their constraint limits. Several test runs were required to assign proper values to the elements of these weighting matrices. Also, it was necessary to change the weights after the iterative procedure indicates convergence of one or more of the variables to their desired terminal values, when values of others were still far from their desired values. Accordingly, the penalties on the states which were far from their desired values were increased, so that the errors in these states were minimized in the next stage of iterations.

Thus, the program was used successfully to generate an optimal control history for a specific nonlinear problem of large angle maneuvers of an LST. It was shown that the computation of the optimal control law for a high order, nonlinear system was an art rather than a science. Several test runs, along with a good initial guess and judicious selection of penalties are needed to obtain meaningful results.

A linear, time invariant, closed loop, optimal control law (as a state feedback) was obtained for providing fine pointing control for the LST. A powerful iterative technique due to Kleinman [49] was used to get the optimal controller gain matrix, using Smith's method [58] which has been proved useful for systems of high order. The procedure was extended, in the present problem, to a system which was only

stabilizable; thus, relaxing the requirements of controllability generally required by the above procedures.

The minimum mean square (MMS) error state estimate was obtained using the Kalman-Bucy filter and an optimal observer gain matrix was obtained using the same procedure as was used for the computation of the controller gains matrix above. Only a part of the estimated state vector was used for the feedback control law.

The covariance analysis of the total system of the regulator and the estimator (of the order 44) was performed to evaluate the fine pointing controller design. The RMS error in the estimates of the true pointing angles of the LST were found to less than 1 arcsecond. This can be reduced further, if desired.

A few suggestions for future work of interest are listed below.

The problem has severe requirements on computer storage. A large time interval is required to achieve any significant maneuver of more than 20^{o} - 30^{o}, due to the necessity of a very small step size (0.01 sec) for (forward) integration of the system equations and for (backward) integration of the adjoint system of order n^{2}, etc. These difficulties make a parametric study of the maneuvers all but impossible from the viewpoint of computer time required for each run and the number of runs required for even a moderate number of parameters. Since, it has been shown for the complete system that the maneuvers can be achieved without violating any constraints on linear and angular gaps, and other variables, these variables can be ignored and a much simpler system of

significantly reduced order (consisting of only target angles θ_{g_1} and θ for example) can be studied to conduct a parameter survey to get nondimensional design curves.

The linear, fine pointing control problem was solved to yield an optimal controller gain matrix which includes all cross feedbacks. This controller is complex to implement in practice. A preliminary design of a simplified controller, in which the axial position of the rim in the gaps and the LST pointing control was decoupled from the radial position control of the rim, was considered by Nadkarni, Groom, and Joshi [61]. Further work on that procedure is needed before the controller design may be simplified appreciably.

Appendix A

Transformation Matrices

The various transformation matrices are given by

$$\begin{Bmatrix} x_b \\ y_b \\ z_b \end{Bmatrix} = [E_{bI}] \begin{Bmatrix} x_I \\ y_I \\ z_I \end{Bmatrix} \tag{A.1}$$

$$\begin{Bmatrix} x_I \\ y_I \\ z_I \end{Bmatrix} = [E_{bI}]^{-1} \begin{Bmatrix} x_b \\ y_b \\ z_b \end{Bmatrix} \tag{A.2}$$

$$\begin{Bmatrix} \omega_x \\ \omega_y \\ \omega_z \end{Bmatrix} = [V_{bE}] \begin{Bmatrix} \ddot{\theta}_1 \\ \ddot{\theta}_2 \\ \ddot{\theta}_3 \end{Bmatrix} \tag{A.3}$$

$$\begin{Bmatrix} \dot{\theta}_1 \\ \dot{\theta}_2 \\ \dot{\theta}_3 \end{Bmatrix} = [V_{Eb}] \begin{Bmatrix} \omega_x \\ \omega_y \\ \omega_z \end{Bmatrix} \tag{A.4}$$

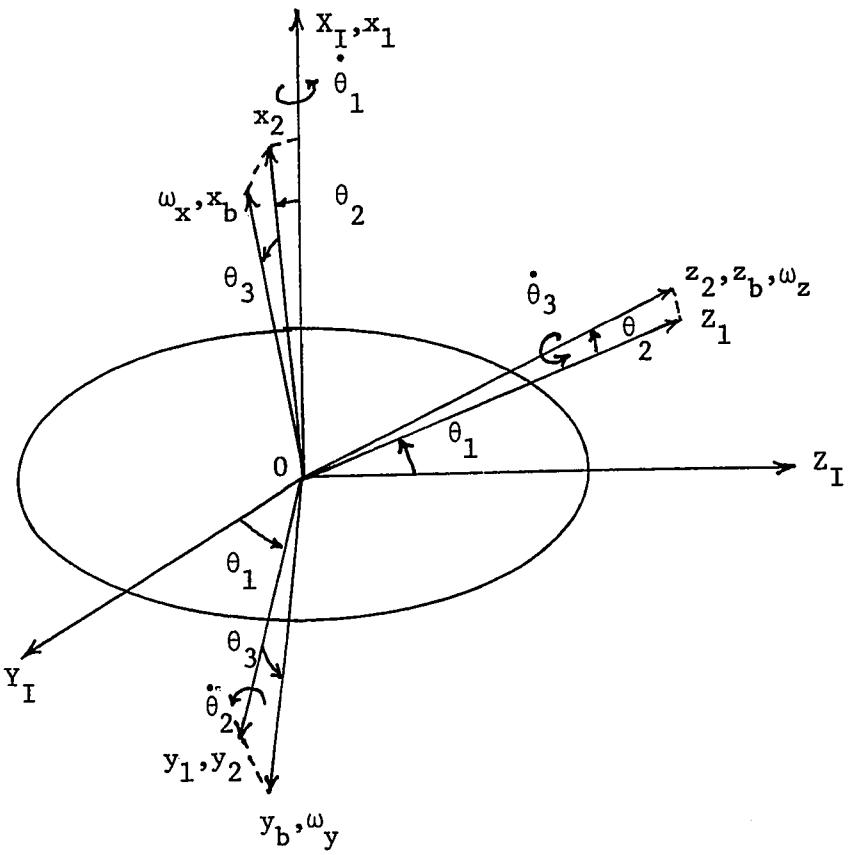

Figure A.1. Body Fixed Coordinate Frame

Appendix A (cont'd)

Transformation Matrices

where

$$[E_{bI}]=\begin{bmatrix} C\theta_2\ C\theta_3 & S\theta_1\ S\theta_2\ C\theta_3 + C\theta_1\ S\theta_3 & -C\theta_1\ S\theta_2\ C\theta_3 + S\theta_1\ S\theta_3 \\ -C\theta_2\ S\theta_3 & -S\theta_1\ S\theta_2\ S\theta_3 + C\theta_1\ C\theta_3 & C\theta_1\ S\theta_2\ S\theta_3 + S\theta_1\ C\theta_3 \\ S\theta_2 & -S\theta_1\ C\theta_2 & C\theta_1\ C\theta_2 \end{bmatrix}, \quad (A.5)$$

$$[E_{bI}]^{-1} = [E_{bI}]^T , \quad (A.6)$$

$$[V_{bE}] = \begin{bmatrix} C\theta_3\ C\theta_2 & S\theta_3 & 0 \\ -S\theta_3\ C\theta_2 & C\theta_3 & 0 \\ S\theta_2 & 0 & 1 \end{bmatrix}, \quad (A.7)$$

and

$$[V_{Eb}] = [V_{bE}]^{-1} = \begin{bmatrix} C\theta_3/C\theta_2 & -S\theta_3/C\theta_2 & 0 \\ S\theta_3 & C\theta_3 & 0 \\ -C\theta_3\ S\theta_2/C\theta_2 & S\theta_3\ S\theta_2/C\theta_2 & 1 \end{bmatrix}. \quad (A.8)$$

When the transverse angles θ_2, θ_3 are small ($<0.3^o$ in present problem), the Euler rates can be approximated by following relationships:

$$\dot{\theta}_1 \simeq \omega_x , \quad \dot{\theta}_2 \simeq \omega_y , \text{ and } \dot{\theta}_3 \simeq \omega_z \quad (A.9)$$

(Note: Here $S\theta = \sin\theta$ and $C\theta = \cos\theta$, etc.)

Appendix B

Expressions for "Passive" Torques

In the Figure B.1, the F_i's are acting in the positive $0_g x_g$ direction and on the rim are taken as positive forces.

$$F_1 = (K_a\lambda + K_a\dot{\lambda})\, r \sin\gamma + K_a\lambda\, r\, \dot{\gamma} \cos\gamma \quad (B.1)$$

$$F_2 = -(K_a\lambda + K_a\dot{\lambda})\, r \sin(60^o + \gamma) - K_a\lambda\, r\, \dot{\gamma} \cos(60^o + \gamma) \quad (B.2)$$

$$F_3 = (K_a\lambda + K_a\dot{\lambda})\, r \sin(60^o - \gamma) - K_a\lambda\, r\, \dot{\gamma} \cos(60^o - \gamma) \quad (B.3)$$

The components of torques due to these forces can be resolved into two components, one along the line of nodes, T, and the other normal to it, T_p, as follows:

$$T = r\,[\, -F_1 \sin\gamma + F_2 \sin(60^o + \gamma) - F_3 \sin(60^o - \gamma)] \quad (B.4)$$

$$T_p = r\,[\, -F_1 \cos\gamma + F_2 \cos(60^o - \gamma) + F_3 \cos(60^o - \gamma)] \quad (B.5)$$

Substituting for F_i's in above from (B.1) - (B.3), and simplifying

$$T = -(K_\lambda\lambda + K_\lambda\dot{\lambda}) \quad (B.6)$$

$$T_p = -K_\lambda\lambda\, \dot{\gamma} \quad (B.7)$$

where

$$K_\lambda = 1.5\, r^2\, K_a \quad (B.8)$$

$$K_\lambda = 1.5\, r^2\, K_a \quad (B.9)$$

These components can be expressed along the gimbal axes $0_g y_g$ and $0_g z_g$ as

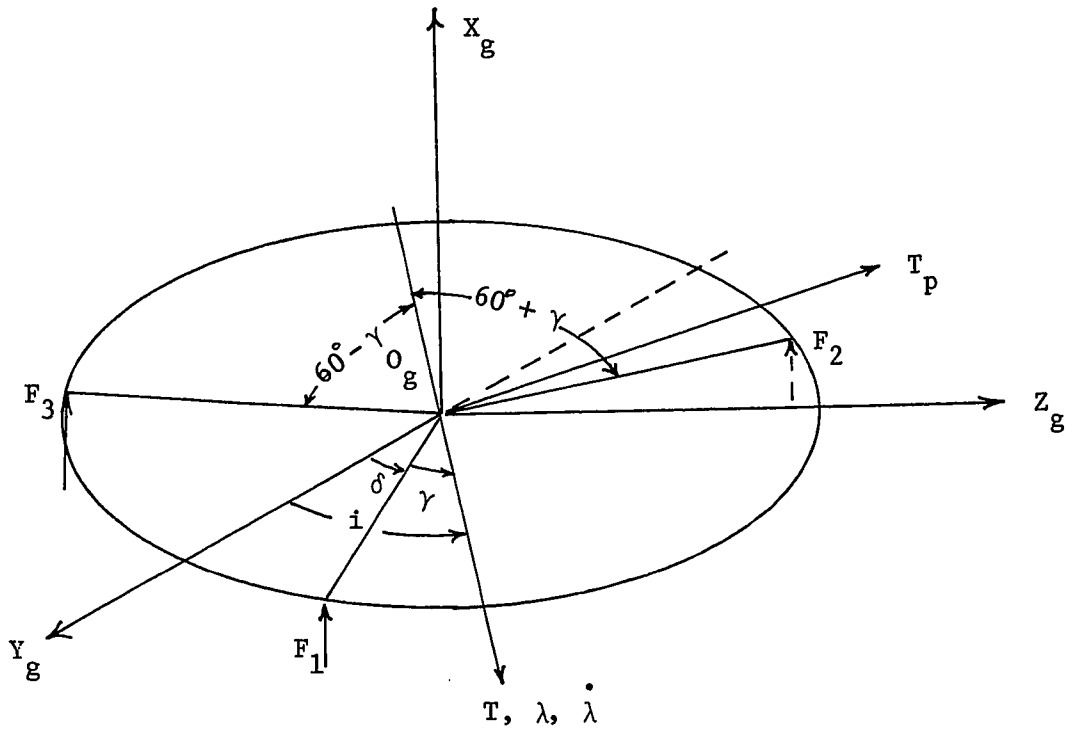

Figure B.1. Magnetic Bearing Forces and Resulting Torques

$$T_{y_g} = T \cos i - T_p \sin i \tag{B.10}$$

$$T_{z_g} = T \sin i + T_p \cos i \tag{B.11}$$

Following the derivation given in reference 6, and using Euler's Theorem on rotations, one can obtain the following expressions,

$$\lambda = (\Delta\theta_2^2 + \Delta\theta_3^2)^{\frac{1}{2}} \tag{B.12}$$

$$\dot{\lambda} = \Delta\dot{\theta}_2 \cos i + \Delta\dot{\theta}_3 \sin i \tag{B.13}$$

$$\sin i = \frac{\Delta\theta_3}{\lambda} = \frac{\Delta\theta_3}{\sqrt{\Delta\theta_2^2 + \Delta\theta_3^2}} \tag{B.14}$$

$$\cos i = \frac{\Delta\theta_2}{\lambda} = \frac{\Delta\theta_2}{\sqrt{\Delta\theta_2^2 + \Delta\theta_3^2}} \tag{B.15}$$

$$\dot{\gamma} = \dot{i} - \dot{\delta} \tag{B.16}$$

$$\Delta\theta_2 \equiv \theta_{a_2} - \theta_{g_2} \tag{B.17}$$

$$\Delta\theta_3 \equiv \theta_{a_3} - \theta_{g_3} \tag{B.18}$$

$$\Delta\dot{\theta}_2 \equiv \dot{\theta}_{a_2} - \dot{\theta}_{g_2} \tag{B.19}$$

$$\Delta\dot{\theta}_3 \equiv \dot{\theta}_{a_3} - \dot{\theta}_{g_3} \tag{B.20}$$

Substituting these in (B.10) - (B.11)

$$T_{y_g} = - K_\lambda (\theta_{a_2} - \theta_{g_2}) - K_{\dot{\lambda}} (\dot{\theta}_{a_2} - \dot{\theta}_{g_2}) - K_{\dot{\lambda}} \dot{\delta} (\theta_{a_3} - \theta_{g_3}) \tag{B.21}$$

$$T_{z_g} = - K_\lambda (\theta_{a_3} - \theta_{g_3}) - K_{\dot{\lambda}} (\dot{\theta}_{a_3} - \dot{\theta}_{g_3}) + K_{\dot{\lambda}} \dot{\delta} (\theta_{a_2} - \theta_{g_2}) \tag{B.22}$$

Now $\dot{\delta} = 0$ since δ is fixed in gimbal frame. Thus, the expressions for the components of passive torques in the gimbal-fixed frame are

$$T_{y_g} = - K_\lambda (\theta_{a_2} - \theta_{g_2}) - K_\lambda^{\bullet} (\dot{\theta}_{a_2} - \dot{\theta}_{g_2}) \qquad (B.23)$$

$$T_{z_g} = - K_\lambda (\theta_{a_3} - \theta_{g_3}) - K_\lambda^{\bullet} (\dot{\theta}_{a_3} - \dot{\theta}_{g_3}) \qquad (B.24)$$

These are the torques acting on the rim. The torques acting on the LST- gimbal at 0_g are opposite to these torques.

The above expressions are used in writing equations (111) - (120) for the nonlinear problem.

Appendix C

Expressions for "Passive" Forces

In the Figure C.1, the F_i's acting radially outwards on the rim are taken to be the forces following the procedure similar to that developed in Appendix B,

$$F_1 = - K_R \varepsilon \cos \gamma - K_{\dot{R}} [\dot{\varepsilon} \cos \gamma - \sin \gamma \dot{\gamma}],$$

$$F_2 = - K_R \varepsilon \cos(60^o + \gamma) + K_{\dot{R}} [\dot{\varepsilon} \cos(60^o + \gamma) - \varepsilon \sin(60^o + \gamma)\dot{\gamma}],$$

$$F_3 = - K_R \varepsilon \cos(60^o - \gamma) + K_{\dot{R}} [\dot{\varepsilon} \cos(60^o - \gamma) - \varepsilon \sin(60^o - \gamma)\dot{\gamma}],$$

where $\varepsilon = x_a - x_g$. (C1 - C4)

The components of the total force due to these bearing forces can be resolved into one along the relative displacement ε of the rim with respect to the gimbal and one normal to it.

Thus,

$$F = F_1 \cos \gamma - F_2 \cos(60^o + \gamma) - F_3 \cos(60^o - \gamma), \quad (C.5)$$

$$F_p = F_1 \sin \gamma + F_2 \sin(60^o + \gamma) - F_3 \sin(60^o - \gamma). \quad (C.6)$$

Substituting for F_i's from (C.1) - (C.3), and simplifying

$$F = - 1.5 K_R \varepsilon - 1.5 K_{\dot{R}} \dot{\varepsilon}, \quad (C.7)$$

$$F_p = - 1.5 K_{\dot{R}} \varepsilon \dot{\gamma}. \quad (C.8)$$

The components can now be expressed in inertial frame as follows:

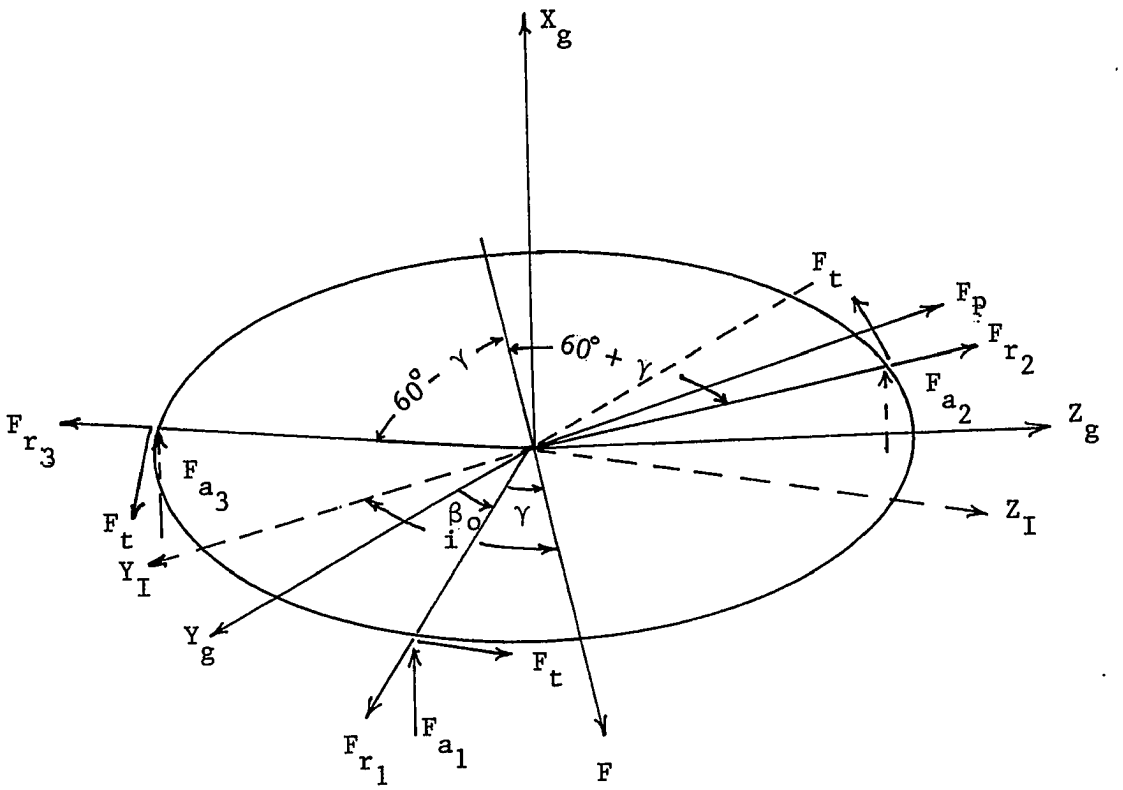

Figure C.1. Magnetic Bearing Forces and Resulting Forces

$$F_{y_I} = F \cos i - F_p \sin i \qquad (C.9)$$

$$F_{z_I} = F \sin i + F_p \cos i \qquad (C.10)$$

Substituting for F and F_p in (C.9), (C.10), and neglecting the product of small quantities, the expressions reduce to

$$F_{y_I} = - 1.5 K_R (x_{2_a} - x_{2_g}) - 1.5 K_{\dot{R}} (\dot{x}_{2_a} - \dot{x}_{2_g}), \qquad (C.11)$$

$$F_{z_I} = - 1.5 K_R (x_{3_a} - x_{3_g}) - 1.5 K_{\dot{R}} (\dot{x}_{3_a} - \dot{x}_{3_g}). \qquad (C.12)$$

These expressions are used in equations (111-120) for the nonlinear problem.

Appendix D

Total Forces and Torques on the Rim

In the Figure D.1, the F_{a_i}, F_{r_i}, F_t are control forces acting at the ith bearing station and are the forces exerted by the gimbal on the rim. These forces are given by:

$$F^c_{x_g} = F_{a_1} + F_{a_2} + F_{a_3}, \tag{D.1}$$

$$F^c_{y_g} = F_{r_1} \cos \beta_1 - F_{r_2} \cos \beta_2 - F_{r_3} \cos \beta_3 - F_t (\sin \beta_1 + \sin \beta_2 - \sin \beta_3), \tag{D.2}$$

and

$$F^c_{z_g} = F_{r_1} \sin \beta_1 + F_{r_2} \sin \beta_2 - F_{r_3} \sin \beta_3 + F_t (\cos \beta_1 - \cos \beta_2 - \cos \beta_3). \tag{D.3}$$

Similarly, the inertial components of the control forces $F^c_{x_I}$, $F^c_{y_I}$, and $F^c_{z_I}$ can be derived.

The torques on the rim due to these control forces are

$$T^c_{x_g} = 3\, r\, F_t, \tag{D.4}$$

$$T^c_{y_g} = r \left[F_{a_1} \sin \beta_1 + F_{a_2} \sin \beta_2 - F_{a_3} \sin \beta_3 \right], \tag{D.5}$$

$$T^c_{z_g} = r \left[- F_{a_1} \cos \beta_1 + F_{a_2} \cos \beta_2 + F_{a_3} \cos \beta_3 \right]. \tag{D.6}$$

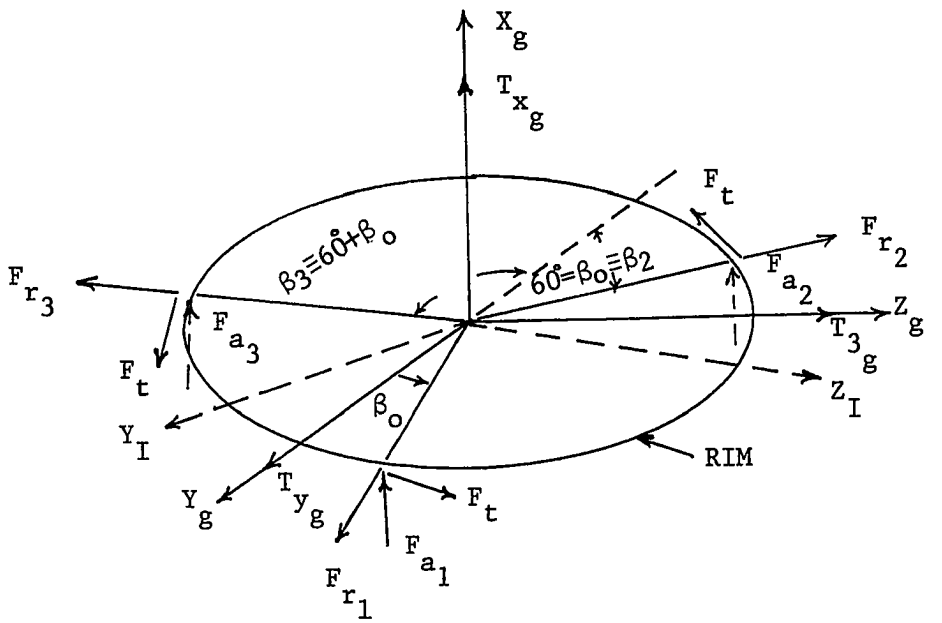

Figure D.1 Forces and Torques on the Rim

The components of "passive" torques acting on the rim are given in the gimbal-fixed frame as (Appendix B)

$$T_{y_g}^{p} = - K_\lambda (\theta_{a_2} - \theta_{g_2}) - K_\lambda^{\cdot} (\dot{\theta}_{a_2} - \dot{\theta}_{g_2}) \qquad (D.7)$$

$$T_{z_g}^{p} = - K_\lambda (\theta_{a_3} - \theta_{g_3}) - K_\lambda^{\cdot} (\dot{\theta}_{a_3} - \dot{\theta}_{g_3}) \qquad (D.8)$$

Thus, the torque on the rim is given by

$$\tau_a = T^c + T^p \qquad (D.9)$$

These expressions are used in equations (118)-(120). The total forces on the rim are given by

$$F_a = F_I^c + F_I^p \qquad (D.10)$$

where F_I^c is the component of F^c's along the inertial axes and F_I^p is given by expressions derived in Appendix. C.

Appendix E

Total Forces and Torques on LST Gimbal

The forces on the LST-gimbal are the reaction forces, which are equal and opposite to the forces exerted by the gimbal bearing stations on the rim. Therefore,

$$F_{gs} = - F_a \tag{E.1}$$

The expressions for F_a are given in Appendix D and the components of F_{gs} are shown in Fig. E.1.

The total torque acting on the LST-gimbal at the system center of mass 0_{gs}, consists of the following:

a) The reaction torque, τ_{gs}, which is equal and opposite to the bearing torque by the gimbal on the rim, τ_a,

b) The torque, τ_{gs}^{p}, due to the passive forces, F_{gs}^{p}, (equation C.11 and C.12) acting at 0_g, and

c) The torque, τ_{gs}^{c}, due to the control forces, F_{gs}^{c}, (equation D.1 - D.3) acting at 0_g.

The expressions for reaction torques are given by equations (B.23-24), with the signs of all the terms reversed. The expressions for torques due to forces at 0_g can be derived as follows.

If F_{x_I}, F_{y_I}, and F_{z_I} are the forces acting at 0_g, then the components T_1, T_2, and T_3 (Fig. E.1) are

$$T_1 = - F_{y_I} \ell_1 \sin \theta \tag{E.2}$$

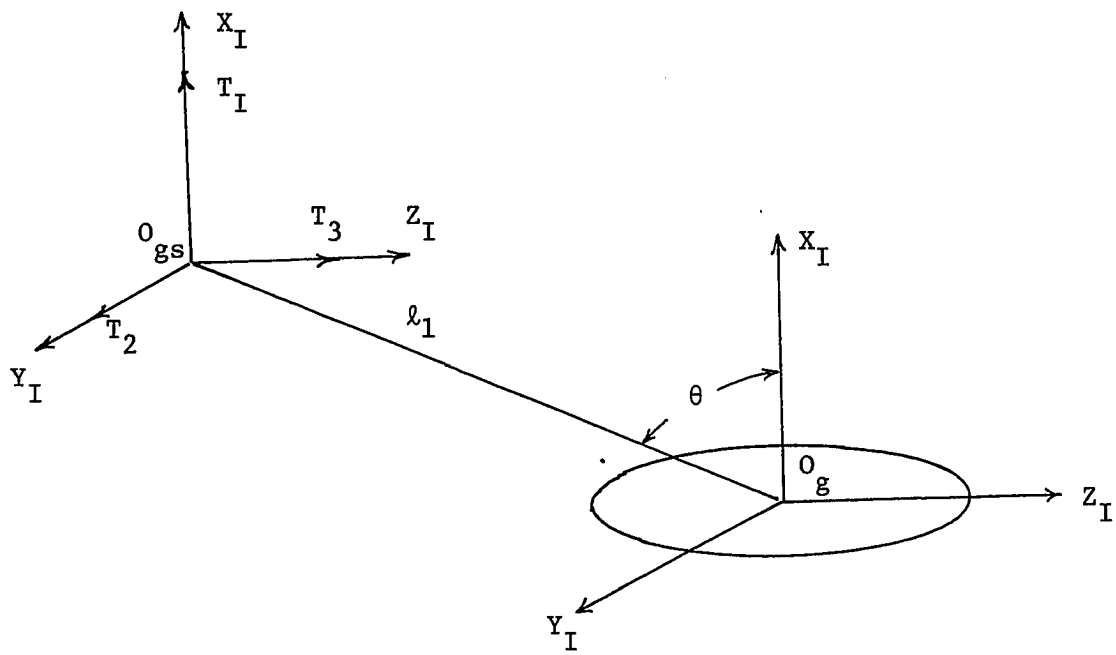

Figure E.1. Forces and Torques on the LST-Gimbal Ring

$$T_2 = F_{x_I} \ell_1 \sin\theta + F_{z_I} \ell_1 \cos\theta \qquad (E.3)$$

$$T_3 = - F_{y_I} \ell_1 \cos\theta \qquad (E.4)$$

These components can be expressed in reference frame $0_{gs}\ x_{gs}\ y_{gs}\ z_{gs}$ as

$$\tau_{gs_x} = T_1 \qquad (E.5)$$

$$\tau_{gs_y} = T_2 \cos\theta_{g_1} + T_3 \sin\theta_{g_1} \qquad (E.6)$$

$$\tau_{gs_z} = - T_2 \sin\theta_{g_1} + T_3 \cos\theta_{g_1} \qquad (E.7)$$

The components of τ_{gs}^{p} and τ_{gs}^{c} can obtained from equations (E.5) - (E.7) by substituting the values of F_{gs}^{p} (Appendix C) and F_{gs}^{c} (Appendix D) respectively. These expressions are used in equations (111)-(120).

Appendix F

Coefficient Matrices

The elements of the coefficient matrices A, A_F, B_F, B, and C are as follows:

$$A = [\, a_{i,j} \,] \qquad i, j = 1, 2, \ldots 14$$

where

$a_{i,j} = 0$ except for the following elements,

$$a_{1,2} = a_{3,4} = a_{5,6} = a_{7,8} = a_{9,10} = a_{13,14} = 1.0$$

$$a_{11,12} = - a_{12,11} = - H_o / I_{yy_a};$$

$$A_F = [\, a_{F_{i,j}} \,] \qquad i, j = 1, 2, \ldots 7$$

where

$$a_{F_{i,j}} = \begin{cases} 0 & i \neq j \\ -400 & i = j \end{cases};$$

$$B_F = [\, b_{F_{i,j}} \,] \qquad i, j = 1, 2, \ldots 7$$

where

$$b_{F_{i,j}} = \begin{cases} 0 & i \neq j \\ 400 & i = j \end{cases};$$

$$B = \begin{bmatrix} B_\epsilon - \ell_1 E(e) B_\ell \\ B_{\ell_2} \\ B_{\ell_3} \\ B_{\ell_2} \\ B_{\ell_3} \\ B_{\ell_1} \end{bmatrix}$$

where B_{ℓ_i} denotes ith row of B_ℓ etc., and B_ε, B_ℓ, and B_a are 3x7 matrices whose elements are listed below.

$$B_\varepsilon^T = \frac{1}{m_a} + \frac{1}{m_{gs}} \begin{bmatrix} 1 & 0 & 0 \\ 0 & c\delta_1 & s\delta_1 \\ 1 & 0 & 0 \\ 0 & -c\delta_2 & s\delta_2 \\ 1 & 0 & 0 \\ 0 & -c\delta_3 & -s\delta_3 \\ 0 & 0 & 0 \end{bmatrix},$$

$$B_\ell^T = \begin{bmatrix} 0 & -\ell s\theta + r s\beta_o & r c\beta_o \\ \ell s\theta c\beta_o & \ell c\theta s\beta_o & \ell c\theta c\beta_o \\ 0 & -\ell s\theta - r c\beta^- & -r s\beta^- \\ -\ell s\theta s\beta^- & -\ell c\theta c\beta^- & -\ell c\theta s\beta^- \\ 0 & -\ell s\theta + r c\beta^+ & -r s\beta^+ \\ -\ell s\theta s\beta^+ & \ell c\theta c\beta^+ & -\ell c\theta s\beta^+ \\ 1 & 0 & 0 \end{bmatrix},$$

$$B_a^T = \begin{bmatrix} 0 & -s\beta_o & -c\beta_o \\ 0 & 0 & 0 \\ 0 & c\beta^- & s\beta^- \\ 0 & 0 & 0 \\ 0 & -c\beta^+ & s\beta^+ \\ 0 & 0 & 0 \\ 1 & 0 & 0 \end{bmatrix},$$

and

$$E(\theta) = \begin{bmatrix} 0 & s\theta & 0 \\ -s\theta & 0 & -c\theta \\ 0 & c\theta & 0 \end{bmatrix},$$

and the elements of the coefficient matrix C are given as follows

$$C = [C_{i,j}] \qquad i = 1, 2, \ldots 12,$$
$$j = 1, 2, \ldots 23,$$

where $C_{i,j} = 0$ except for the following elements

$$c_{1,1} = c_{3,1} = c_{5,1} = c_{7,7} = c_{8,8} = c_{9,9} = c_{10,10} = c_{11,13}$$
$$= c_{12,14} = 1,$$

and

$$c_{1,7} = -c_{1,22} = rs\beta_o \ , \quad c_{1,9} = -c_{1,23} = rc\beta_o \ ,$$

$$c_{3,7} = -c_{3,22} = -rc\beta^- \ , \quad c_{3,9} = -c_{3,23} = -rs\beta^- \ ,$$

$$c_{5,7} = -c_{5,22} = rc\beta^+ \ , \quad c_{5,9} = -c_{5,23} = -rs\beta^+ \ ,$$

$$c_{2,3} = c\delta_1 \ , \quad c_{2,5} = s\delta_1 \ , \quad c_{4,3} = -c\delta_2 \ ,$$

$$c_{4,5} = s\delta_2 \ , \quad c_{6,3} = -c\delta_3 \ , \quad c_{6,5} = -s\delta_3 \ ,$$

where $\delta_1 = \theta_{g_1} - \beta_o \ , \quad \delta_2 = 60^o - \delta_1 \ , \quad \delta_3 = 60^o + \delta_1 \ ,$

$$\beta^- = 30^o - \beta_o \ , \quad \beta^+ = 30^o + \beta_o \ .$$

Appendix G

Computing the Stabilizing Gain for a Linear Constant System

It is required to find a control law of the form

$$u(t) = - L\, x(t) \qquad (G.1)$$

that stabilizes the linear constant controllable system

$$\dot{x}(t) = Ax(t) + Bu(t) \qquad (G.2)$$

without having to transform A to a canonical form and without regard to explicit closed loop pole assignments. Such situations exist in iterative methods for solving matrix quadratic equations of the following type (sec. 3.4)

$$- LA - A^{T}K - Q + KBR^{-1}\, B^{T}K = 0 \,. \qquad (G.3)$$

The following theorem presents a constructive method of finding a set of stabilizing feedback gain.

Theorem:

If the system (G.2) is completely controllable, then $u(t) = - L\, x(t)$ is a stabilizing control law with

$$L = B^{T}\, w^{-1}\, (T) \,, \qquad (G.4)$$

$$w(T) = \int_{0}^{T} e^{-A\tau}\, BB^{T}\, e^{A^{T}\tau}\, d\tau \,, \quad T = \text{arbitrary}$$

and

$$v(x) = x^{T}\, w^{-1} x$$

is a suitable Lyapunov function for the closed loop system.

The proof of this theorem is given by Kleinman [52].

Appendix H

Iterative Technique for Riccati Equation Computations

An iterative technique used for solving the linear regulator problem with infinite time (steady state problem) is outlined below. The method uses successive substitution methods developed by Kleinman [49].

Theorem:

Let V_k, $k = 0, 1, 2, \ldots$, be the (unique) positive definite solution of the linear algebraic equation

$$0 = A_k^T V_k + V_k A_k + C^T C + L_k^T R L_k , \qquad (H.1)$$

where, recursively,

$$L_k = R^{-1} B^T V_{k-1} , \quad k = 1, 2, \ldots , \qquad (H.2)$$

$$A_k = A - B L_k , \qquad (H.3)$$

and where L_o is chosen such that the matrix $A_o = B L_o$ has eigenvalues with negative real parts. Then

1) $K \leq V_{k+1} \leq V_k \leq \ldots\ldots, k = 0, 1, \ldots$

2) $\lim_{k \to \infty} V_k = K$

The proof of the above theorem is developed by Kleinman using the concept of a cost matrix.

The following advantages listed make the iterative technique very useful in applications to control problems.

1) Since the system is completely controllable, it is always possible to choose an L_o, such that Re $\lambda_i (A_o) < 0$.

This condition is necessary to insure the boundedness of the cost matrix V_o; otherwise the iterations may converge to an indefinite solution. It is noted here, that the initial L_o can be chosen using the stabilizing gains computed in Appendix G.

2) Kleinman [49] has shown that the above iterative scheme is precisely that which is obtained by applying Newton's method (in function space) to solve equations of the type (G.3). However, Newton's method above does not provide conditions that will insure monotonic convergence, whereas this method insures this.

3) In addition to being monotonically convergent, the method is also quadratically convergent and hence the convergence is rapid compared to other methods.

Appendix J

Numerical Solution of the Matrix Equation

$$Ax + xA^T + B = 0$$

A method of solving the nxn matrix equation

$$Ax + xA^T + B = 0 \qquad (J.1)$$

for systems of large order ($n \leq 146$), is outlined below:

Let q be a positive parameter, let I be the nxn identity matrix, and let

$$u = (gI - A)^{-1} , \qquad (J.2)$$

$$v = u(gI + A) , \qquad (J.3)$$

$$w = 2\,q\,UBU^T . \qquad (J.4)$$

If an eigenvalue of A has negative real parts,

$$y = \sum_{i=1}^{\infty} V^{i-1}\, w(V^{i-1})^T \qquad (J.5)$$

converges and is the solution of (J.1) for x, where A, B, and x are nxn matrices, B and x being symmetric. The rate of convergence can be improved by using the sequence of partial sum

$$y_\nu = \sum_{i=1}^{2\nu} V^{i-1}\, w(V^{i-1})^T \qquad (J.6)$$

which can be obtained recursively from

$$y_o = w , \qquad (J.7)$$

$$y_{\nu+1} = y_\nu + V^{(2\nu)}\, y_\nu\, V^{(2\nu)\,T} . \qquad (J.8)$$

The matrix recursion formula (J.8) works well for solving (J.1) even on large systems. The method is given by Smith [58] based on a method of solution suggested by Smith [59].

Appendix K

On Relaxation of Controllability and Observability Criteria for Solution of Riccati Equation

When Newton's method is applied to the solution of the algebraic matrix Riccati equation, two potential difficulties arise. One, the method may not converge, and secondly, it may not converge to the desired solution. Kleinman [52] has given a theorem (Appendix H) demonstrating that the difficulties do not arise if the initial guess is stabilizing. He has also given [49] a numerically appealing procedure for generating a stabilizing initial guess (Appendix G). However, this technique like other techniques, assumes the complete controllability and observability of the linear system. The theorem stated below due to Sandell [54] points out that the assumptions of controllability and observability can be weakened to stabilizability and detectability.

Theorem:

If the system

$$\dot{x} = Ax + Bu$$

is stabilizable, then

$u(t) = - L\, x(t)$ is a stabilizing control law with

$$L = B^T w\# (T)$$

where $w(T) \triangleq \int_0^T e^{A\tau} BB^T e^{-A^T\tau} d\tau$, T = arbitrary

where $\#$ denotes generalized inverse. The proof of the above is

is given by Sandell [54].

The relaxation of the controllability (observability) requirement to stabilizability (and detectability) is very important for applications. Kleinman's start up technique [52] and the Newton-Kleinman iterative procedure [49] can now be applied with confidence to systems that are not completely controllable (and/or completely observable) like the linear, fine pointing problem under study.

Appendix L

Survey of Numerical Methods

It is easier to analyze and visualize the finite dimensional optimization problem in the Euler n-space before analyzing the optimization problem in the function space as stated. The former problem is variously called "static" optimization, parameter optimization, or function minimization, etc. In its simplest form, it can be stated as follows:

Minimize $J = F(x, u)$

where F is a general nonlinear function of the state vector x and parameter vector u. Since near the minimum, the second order terms dominate, only those methods which will converge quickly for a general function are those which will guarantee to find a minimum of a general quadratic exactly (apart from numerical round off error) and speedily. It is well known that for a general quadratic, the direction of search is in the direction opposite to the gradient of the function to obtain maximum rate of decrease, which was the basic idea of the method of steepest descent [62]. It is possible to prove convergence under weak assumptions on $F(x)$ and to obtain bounds on the asymptotic rate of convergence. These bounds, however, demonstrate that the method is likely to perform unsatisfactorily on general functions, and the slow rate of convergence persists even in case of some quadratic functions. The difficulty arose because the method failed to utilize the curvature of the functions and hence the solution behaved in an

oscillatory manner near the minimum. The so-called Newton or Newton-Raphson method or other methods based on the second variation, overcame this difficulty by maintaining the step size of search along the gradient of the function inversely proportional to the second derivative (curvature) of the function. This, however, introduced two additional difficulties - one, to calculate the Hessian matrix (numerically for nondifferentiable functions) and, two, to invert the Hessian matrix at each iteration. The method completely breaks down when the Hessian matrix is locally singular at any step during the iterative procedure. Also, the generalized Newton-Raphson methods demanded a good initial guess. These serious disadvantages outweighed the fast convergence properties of the method near the minimum. [63]

A significant contribution to the field of function minimization was achieved when Hestenes and Steifel [64] proposed a method, now popularly called the method of conjugate gradients, for linear systems. The method was based on the fact that, to achieve conjugacy or search directions for quadratic functions, it is only necessary to force an orthogonality condition on successive search directions without evaluating the Hessian matrix [62]. The method was extended to general functions by Fletcher and Powell [65] with a modification of Davidon's metric method which has become popularly known as the Davidon-Fletcher-Powell(DFP) method. The method circumvented the necessity of evaluating the inverse of the Hessian matrix by replacing it with an arbitrary, positive definite symmetric matrix, which was initially an identity matrix. The iterative scheme pro-

yided a correction for this matrix and it was shown that this corrected matrix tends asymptotically to the inverse of the Hessian matrix. The method was very useful in handling functions of a large number of variables, required only first derivatives and could start from a poor initial guess. A slightly modified version of the DFP method was given by Fletcher and Reeves [66] to reduce the storage requirements. These methods developed algorithms having the capability of starting from a poor initial guess, sureness of convergence of steepest descent and fast convergence near minimum of the Newton-Raphson methods. The methods also assured that the minimum is reached in at most n steps (where n = number of variables). Myers [67] showed that both Davidon's method and the C-G (conjugate gradient) method search along the same line in the absence of numerical errors and that the direction vectors of both are positive scalar multiples of each other. However, the C-G method was less susceptible to error propagation due to numerical roundoff.

Soon many more variants of the steepest descent method and the conjugate gradient method began to appear in the literature. These methods however, were mostly developed for specific problems.

Although the methods described above primarily dealt with the problem of minimization of functions without any constraints on variables, linear constraints on the variables of the type

$$g(x) \geq 0 \qquad h(u) \geq 0$$

could be handled by these methods with slight modifications. The modifications involved essentially eliminating, or at least relaxing,

the constraints and solving the resulting problem as one of an unconstrained minimization problem or a sequence of such problems. This can be done in the simplest possible way by change or transformation of variables. However, this method is useful only when the number of variables is very small. Other ways of achieving this soon emerged. Roberts and Lyvers [68] proposed "hemstitching" where the point from which the steepest descent search was started, returned to the constraint boundary whenever the point violated the constraint. The method can handle large number of variables, but it breaks down for nonconvex objective function. More systematic methods with a theoretical backing in terms of existence and convergence theorems have been proposed. Prominent methods are the gradient projection, modified DFP method, approximation technique, or more commonly known as the penalty function method, or sequential unconstrained minimization technique.

The gradient projection method was introduced by Rosen [69] as a general nonlinear programing algorithm for problems with linear constraints and with nonlinear constraints [70]. The basic idea of the method is to search in a direction in which the function decreases, but which is also tangential to the constraint boundaries. Thus, the direction of search is given by the (negative) projection of the gradient on the constraint subspace. Attempts were made [71, 72, 73] to combine the gradient projection method with the DFP method. However, in the gradient projection method the gradient of the function is not orthogonal to the search direction (as in DFP method) at a

pointwhere it encounters a constraint. A new sequence of conjugate directions must therefore be started each time the constraint set is changed. Methods to update the inverse of the Hessian matrix for steps of arbitrary length and directions have to be included [71] and the computational requirements would increase tremendously for high order systems.

The approximation technique or the method of penalty functions was introduced by Kelley [74]to handle problems with equality or inequality constraints on the variables. The method essentially consisted of redefining the original performance index with the help of Heaviside unit step functions, so that the value of the index is penalized to be high whenever the constraint is violated. Kelley has shown that for increasingly large values of the penalty, the solution of the modified unconstrained minimum problem will tend towards the desired minimum problem with constraints. Butler and Martin [75] developed a penalty function method as an extension of Courant's method in Hilbert space and gave rigorous mathematical proof about the existence and convergence of the method. The penalty function technique is quite compatible with the successive approximation process provided by the gradient methods. Thus, the penalty function technique could be used in conjunction with the gradient procedure for ease of programing for problems involving a very large number of variables. The required computer logic is minimized; the influence of a particular violation is increasingly large if the constraint is violated, the influence being automatically nil if the constraint is satisfied.

The method, however, is not without its drawbacks. If the value of the unit function is chosen too small, the method converges to the minimum of performance index without paying any attention to constraint boundaries. On the other hand, too heavy penalties may result in convergence to the nearest point on the constraint boundary from the starting point. Hence, a judicious choice of the value for the unit functions must be made. This may not only involve different weights for different variables, but also some preliminary trial runs for establishing these weights.

A slight modification of the penalty function method, called the sequential unconstrained minimization technique (SUMT), was proposed by Carroll [76, 77] and developed by Fiacco and McCormick [78]. The method replaces a constrained minimization problem by a sequence of unconstrained minimization problems. By attaching different penalty functions to the given objective function, the successive optimal solutions (of unconstrained problems) approach the optimal solution of the given constrained problem.

Many attempts were made to extend the various methods of static or parameter optimization problems of Euler space into Banach space or the function space. The problem in general here is one of minimizing:

$$J = \theta(x_f, t_f) + \int_o^{t_f} \phi(x, u, t)\, dt$$

subject to

$$\dot{x}(t) = f(x, u, t), \quad x(o) = x_o$$

and

$$g(u, t) \geq 0, \quad h(x, t) \geq 0 .$$

One of the major difficulties faced in extending the methods of minimization of the functionals in Banach space was that the existence of the extremum (minimum or maximum) of a function which is assured in Euler space by the boundedness and continuity of the [illegible] function cannot be assumed anymore. In Banach space, the continuity of the space often has to be replaced by a weaker property of semi-continuity. Also, the convergence theorem of the Euler space does not hold if the elements of the set are not points on a line or in n-space, but functions, curves, or surfaces. Lagrange proposed to solve this problem with the multiplier method he had proposed earlier for ordinary problem of constrained maxima and minima in differential calculus. He proposed to include the above differential equality as an equality constraint in the function to be minimized and solve the problem as an ordinary extremum problem. However, this method does not take into account the inequality constraints on the control variables usually present in the optimal control problems. However, the method was very powerful and Pontryagin et al [26] finally succeeded in presenting the solution to the optimal control problem in a very elegant manner by formulating the necessary conditions or the so called "maximum (or minimum) Principle." The problem was reduced by the Maximum Principle to a two-point boundary value problem (TPBVP)of ordinary differential equations with split boundary conditions. The application of the Maximum Principle for linear problems

yields an ideal, linear, closed loop solution for the control vector. For a general nonlinear problem with state and control constraints, these set of equations may not be solved in a straightforward manner.

The difficulties in solving the two-point boundary value problems led to a search for variational methods of different kinds, known as direct methods or numerical methods useful for use of modern computers. The search developed broadly along three classes of techniques, Rayleigh-Ritz or finite difference, dynamic programing and gradient methods.

Rayleigh-Ritz techniques or finite difference methods are perhaps the earliest techniques used for the minimization problems. These methods are however, not too popular due to the difficulties in finding a suitable set of base functions. Another method, that of discrete dynamic programing was based on the Hamilton-Jacobi-Bellman partial differential equation, which is equivalent to Bellman's equation in function space. The method resembles closely the method of characteristics and is able to provide a nonlinear feedback control law. However, the method suffers from severe storage problems and is all but useless for problems involving more than three or four variables (the so called "curse of dimensionality" by Bellman himself). This prohibits its use in problems involving a large number of variables (such as the present one) even though the state and control constraints present can make the application to dynamic programing easier.

Hence, the only feasible straightforward direct numerical method

to be considered in the steepest descent or gradient method and its many variants and methods requiring second derivatives. Many proposals were put forward extending the steepest descent method, the conjugate gradient method and the DFP method to the function space [79-85]. These methods and their variants were proposed to handle problems with equality and inequality constraints in conjunction with the gradient projection [86-88], penalty function [89, 90], and sequential unconstrained problem [91-94]. McReynolds and Bryson [95] proposed a successive sweep method, which was essentially a unification and extension of steepest descent method and the second variation method. This method required, in addition to the usual integration of the adjoint vector differential equation, and additional integration of a matrix differential equation involving first and second derivatives of the performance index. It also required the second derivative of the Hamiltonian with respect to the control variables to be a nonzero matrix.

For the large angle maneuvering, nonlinear problem under consideration with added state and control inequality constraints, most of the methods described above posed potential difficulties. As was mentioned before, the problem consists of 20 ordinary, first order, differential equations. Also, the dominant translational frequencies of the spinning rim ($\approx 2\ \omega_o$) required extremely small step size for computing the trajectory. Even after certain approximations (sec. 2.6) the step size could be increased to only 0.01 sec. The high order of the system equations together with the very small computational

interval, rules out the methods based on second variation because of the tremendous storage problems and large computational time requirements even on the biggest computers available. Calculation and inversion of the Hession matrix of the performance index at each point along the trajectory will impose additional computational time requirements so severe that the advantage of the quadratic convergence of the method is certainly lost. The method may not also be able to handle the hard constraints efficiently.

The conjugate gradient methods are limited to lower order problems (less than 4) [62,96] and this method gets worse as the order increases. The modified DFP method (Fletcher-Reeves method) requires storage of, in addition to the gradient trajectory, one more trajectory of actual directions of search [82]. The method cannot handle the integral term in the cost function and the inequality constraints on states and controls.

The conjugate methods in addition require for a linear case, that the coefficient matrix A to be positive definite [63]. This requirement cannot be met in the present case, as is evident from the discussion of the linearized version of the present nonlinear problem in sec. 3.4. The gradient projection method, in conjunction with any of the minimization techniques above, can handle equality constraints very effectively, but cannot handle the hard inequality constraints. Even if the method can be modified, the expensive correction cycle required during each iteration, rule out this method for high order system as in present case.

References

1. Meirovitch, L.: Methods of Analytical Dynamics, McGraw-Hill Book Company, 1970.

2. Thomson, W. T.: Introduction to Space Dynamics, John Wiley and Sons, Inc., 1961.

3. Landon, V. D.; and Stewart, B.: Nutational Stability of an Axisymmetric Body Containing a Rotor. Journal of Spacecraft and Rockets, Vol. 1, No. 6, 1964, pp. 682-684.

4. Iorillo, A. J.: Hughes Gyrostat System. Proceedings of the Symposium on Attitude Stabilization and Control of Dual-Spin Spacecraft, Aug. 1-2, 1967, pp. 257-266.

5. Likins, P. W.: Attitude Stability Criteria for Dual Spin Spacecraft. Journal of Spacecraft and Rockets, Vol. 4, No. 12, 1967, pp. 1638-1643.

6. Mingori, D. L.: The Determination by Floquet Analysis of the Effects of Energy Dissipation on the Attitude Stability of Dual-Spin Satellites. Proceedings of the Symposium on Attitude Stabilization and Control of Dual-Spin Spacecraft, Aug. 1-2, 1967, pp. 25-36.

7. Stuhlinger, E.: Control and Power Supply Problems of Instrumented Satellites. Jet Propulsion, Vol. 26, No. 5, Part 1, 1956, pp. 364-368.

8. Anderson, W. W. and Groom, N. J.: The Annular Momentum Control Device (AMCD) and Potential Applications. NASA TN D-7866, 1975.

9. Anderson, W. W. and Groom, N. J.: Annular Momentum Control Device, U.S. Letters of Patent No. 3, 915, 416, Oct. 28, 1975.

10. Greenwood, D. T.: Principles of Dynamics, Prentice-Hall, Inc., 1965.

11. Speyer, J. L.; Kelley, H. J.; Levine, N.; and Denham, W. F.: Accelerated Gradient Projection Technique with Application to Rocket Trajectory Optimization. Automatica, Vol. 7, No. 1, 1971, pp. 37-43.

12. Kelley, H. J.: Gradient Theory of Optimal Flight Paths, ARSJ, Vol. 30, No. 10, 1960, pp. 947-954.

13. Valentine, F.A.: The Problem of Lagrange with Differential Inequalities as Added Side Conditions. Contributions to the Calculus of Variations 1933-1937, University of Chicago Press, 1937.

14. Berkovitz, L. D.: Variational Methods in Problems of Control and Programming. J. Math. Anal. and Appl., Vol. 3, No. 1, 1961, pp. 145-169.

15. Sage, A. P.: Optimum Systems Control, Prentice-Hall, Inc., 1968.

16. McGill, R.: Optimal Control, Inequality State Constraints, and the Generalized Newton-Raphson Algorithm. SIAM Journal Control, Vol. 3, No. 2, 1965, pp. 291-298.

17. Joseph, P. D. and Tou, J.: On Linear Control Theory, Trans AIEE Part II (Appl. and Industry), Vol. 80, September 1961, pp. 193-196.

18. Gunckel, T. L. II, and Franklin, G. F.: A General Solution for Linear Sampled-Data Control. Trans. ASME, Series D, J. Basic Engineering, Vol. 85, No. 2, 1963, pp. 197-203.

19. Lee, R. C. K.: Optimal Estimation, Identification, and Control MIT Press, 1964.

20. Tung, F.: Linear Control Theory Applied to Interplanetary Guidance, IEEE Trans. on Auto. Control, Vol. AC-9, No. 1, 1964, pp. 82-89.

21. Wonham, W. M.: On the Separation Theorem of Stochastic Control, SIAM Journal of Control, Vol. 6, No.2, 1968, pp. 312-326.

22. Wonham, W. M.: Random Differential Equations in Control Theory in Probabilistics Methods in Applied Mathematics, A. T. Bharucha-Reid, Ed., Academic Press, 1970, pp. 131-212.

23. Fleming, W. H.: Controlled Diffusions under Polynomial Growth Conditions in Control Theory and the Calculus of Variations, A. V. Balakrishnan, Ed., Academic Press, 1969, pp. 209-234.

24. Kushner, H. J.: Stochastic Stability and Control, Academic Press, 1967.

25. Kushner, Harold: Introduction to Stochastic Control, Holt, Rinehart, and Winston, 1971.

26. Pontryagin, L. S.; Bol'tanskii, V. G.; Gamkrelidze, R. S.; and Mischenko, E. F.: The Mathematical Theory of Optimal Processes, Pergamon Book, 1964.

27. Athans, M. and Falb, P. L.: Optimal Control, McGraw-Hill Book Co., 1966.

28. Kalman, R. E.: Contributions to the Theory of Optimal Control, Bol. Soc. Mat. Mex., Vol. 5, 1960, pp. 102-119.

29. Kalman, R. E.; The Theory of Optimal Control and the Calculus of Variations in Mathematical Optimization Techniques, R.Bellman Ed., Univ. of Calif. Press, 1963.

30. Bryson, A. E., Jr. and Ho, Y. C.: Applied Optimal Control, Blaisdell Publishing Co., 1969.

31. Anderson, B. D. O. and Moore, J. B.: Linear Optimal Control, Prentice-Hall, Inc., 1971.

32. Willems, J. C. and Mitter, S. K.: Controllability, Observability, Pole Allocation, and State Reconstruction, IEEE Trans. on Auto. Control, Vol. AC-16, No. 6, 1971, pp. 582-595.

33. Luenberger, D. G.: A New Derivation of the Quadratic Loss Control Equation, IEEE Trans. on Auto. Control, Vol. AC-10, No. 2, 1965, pp. 202-203.

34. Willems, J. C.: Least Squares Stationary Optimal Control and the Algebraic Riccati Equation, IEEE Trans. on Auto. Control, Vol. AC-16, No. 6, 1971. pp. 621-634.

35. Kleinman, D. L.: On the Linear Regulator Problem and the Matrix Riccati Equation, MIT Electronic Systems Lab. Rep. ESL-R-271, June 1966.

36. Brockett, R. W.: Finite Dimensional Linear Systems, John Wiley and Son, 1970.

37. Howerton, R. D. and Hammond, J. L., Jr.: A New Computational Solution of the Linear Optimal Regulator Problem, IEEE Trans, on Auto. Control, Vol. AC-16, No. 6, 1971, pp. 645-651.

38. Anderson, B. D. O.: Spectral Factorization by Algebra, Stanford Electronic Lab., Tech. Rep. 6560-6, Sept. 1966.

39. Youla, D. C.: On the Factorization of Rational Matrices, IRE Trans. Info. Theory, Vol. IT-7, 1961, pp. 172-189.

40. Davis, M. C.: Factoring the Spectral Matrix, IEEE Trans. on Auto. Control, Vol. AC-8, No. 5, 1963, pp. 296-305.

41. Amara, R. C.: Application of Matrix Methods to the Linear Least Square Synthesis of Multi-variable Systems, J. Franklin Inst., Vol. 268, No 1., 1959, pp. 1-16.

42. Potter, J. E.: Matrix Quadratic Solutions, J. SIAM on Appl. Math., Vol. 14, No. 3, 1966, pp. 496-501.

43. McFarlane, A. G. J.: An Eigenvector Solution of the Linear Optimal Regulator Problem, J. Electron. Contr., Vol. 14, 1963, pp. 643-654.

44. O'Donnell, J. J.: Asymptotic Solution of the Matrix Riccati Equation of Optimal Control, Proc. 4th Annual Allerton Conf. Circuit and System Theory, 1966, pp. 577-586.

45. Fath, A. F.: Computational Aspects of the Linear Optimal Regulator Problem, IEEE Trans. on Auto. Control, Vol. AC-14, No. 5, 1969, pp. 547-550.

46. Vaughan, D. R.: A Negative Exponential Solution for the Matrix Riccati Equation. IEEE Trans. on Auto. Control, Vol. AC-14, No. 1, 1969, pp. 72-75.

47. Vaughan, D. R.: A Nonrecursive Algebraic Solution for the Discrete Riccati Equation, IEEE Trans. on Auto. Control, Vol. AC-15, No. 5, 1970, pp. 597-599.

48. Kwakernaak, H. and Sivan, R.: Linear Optimal Control Systems, Wiley Interscience, 1972.

49. Kleinman, D.L.: On an Iterative Technique for Riccati Equations Computations, IEEE Trans on Auto. Control, Vol. AC-13, No.1, 1968, pp. 114-115.

50. McClamroch, N. H.: Duality and Bounds for the Matrix Riccati Equations, J. Math. Anal. and Appl., Vol. 25, pp. 622-627.

51. Blackburn, T. R.: Solution of the Algebraic Riccati Equation via Newton-Raphson Iteration, Preprints, 1968 Joint Auto. Control Conf., June 26-28, pp. 940-945.

52. Kleinman, D. L.: An Easy Way to Stabilize a Linear Constant System, IEEE Trans. on Auto. Control, Vol. AC-15, No. 6, 1970, p. 692.

53. Anderson, W. W. and Joshi, S. M.: The Annular Suspension and Pointing (ASP) System for Space Experiments and Predicted Pointing Accuracies, NASA TR R-448, 1975.

54. Sandell, N. R.: On Newton's Method for Riccati Equation Solution, IEEE Trans. on Auto. Control, Vol. AC-19, No. 3, 1974, pp. 254-255.

55. Kalman, R. E.: A New Approach to Linear Filtering and Prediction Problems, J. Basic Engineering, Trans. ASME, Vol. 82, Series D, March 1969, pp. 35-45.

56. Kalman, R. E. and Bucy, R. S.: New Results in Linear Filtering and Prediction Theory, J. Basic Engineering, Trans. ASME, Vol. 83, Series D, March 1961, pp. 95-108.

57. Luenberger, D. G.: Optimization by Vector Space Methods, John Wiley and Sons, 1969.

58. Smith, P. G.: Numerical Solution of the Matrix Equation $AX + XA^T + B = 0$. IEEE Trans. on Auto. Control, Vol. AC-16, No. 3, 1971, pp. 278-279.

59. Smith, R. A.: Matrix Equation $XA + BX = C$, SIAM J. Appl. Math. Vol. 16, No.1 1968, pp. 198-201.

60. Breedlove, W. J. and Nadkarni, A. A.: A General Computer Program for Computing Optimal Control Variable Histories for Nonlinear Vector-Matrix Equation in State Variable Form. Final Report prepared under NASA contract NAS1-14193-20, Old Dominion University Research Foundation, April 1977.

61. Nadkarni, A. A.; Groom, N. J. ; and Joshi, S. M.: Optimal Fine Pointing Control of a Large Space Telescope Using an Annular Momentum Control Device, IEEE 1977 Southeastcon, April 4-6, 1977.

62. Murray, W.: Numerical Methods for Unconstrained Optimization, Academic Press, 1972.

63. Gill, P. E. and Murray, W.: Numerical Methods for Constrained Optimization. Academic Press, 1974.

64. Hestenes, M. R. and Stiefel, E.: Methods of Conjugate Gradients for Solving Linear Systems, J. Res. Nat. Bur. Stand., Vol. 49, No. 6, 1952, pp. 409-436.

65. Fletcher, R. and Powell, M. J. D.: A Rapidly Convergent Descent Method for Minimization, Computer J., Vol. 6, April 1963 - June 1964, pp. 163-168.

66. Fletcher, R. and Reeves, C. M.: Function Minimization by Conjugate Gradients, Computer J., Vol. 7, No. 2, 1964, pp. 149-154.

67. Myers, G. E.: Properties of the Conjugate Gradient and Davidon Methods. J. Optimization Theory and Applications, Vol. 2, No. 4 1968, pp. 209-219.

68. Roberts, S. M. and Lyvers, H. I.: The Gradient Method in Process Control, Indust. and Eng. Chem., Vol. 53, 1961, pp. 877-882.

69. Rosen, J. B.: The Gradient Projection Method for Nonlinear Programming, Part I, SIAM J. Appl. Math., Vol. 8, 1960, pp. 181-217.

70. Rosen, J. B.: The Gradient Projection Method for Nonlinear Programming, Part II, SIAM J. Appl. Math., Vol. 9, 1961, pp. 514-532.

71. Murtagh, B. A. and Sargent, R. W. H.: A Constrained Minimization Method with Quadratic Convergence in Optimization, R. Fletcher, Ed., Academic Press, 1969.

72. Goldfarb, D.: Extension of Davidon's Variable Metric Method to Maximization Under Linear Inequality and Equality Constraints, SIAM J. Appl. Math., Vol. 17, No. 4, 1969, pp. 739-764.

73. Goldfarb, D. and Lapidus, L.: Conjugate Gradient Method for Nonlinear Programming Problems with Linear Constraints. Industrial and Engineering Chemistry Fundamentals, Vol. 7, No.1, 1968, pp. 142-151.

74. Kelley, H. J.: Methods of Gradients in Optimization Techniques, G. Leitmann, Ed., Academic Press, 1962.

75. Butler, T. and Martin, A. V.: On a Method of Courant for Minimizing Functionals. J. Math. and Physics, Vol. 41, 1962, pp. 291-299.

76. Walsh, G. R.: Methods of Optimization, John Wiley and Sons, 1975.

77. Carroll, C. W.: The Created Response Surface Technique for Optimizing Nonlinear, Restrained Systems. Operation Research, Vol. 9, No. 2, 1961, pp. 169-184.

78. Fiacco, A. V. and McCormick, G. P.: Nonlinear Programming - Sequential Unconstrained Minimization Techniques. John Wiley and Sons, 1968.

79. Miele, A.; Huang, H. Y.; and Heideman, J. C.: Sequential Gradient-Restoration Algorithm for the Minimization of Constrained Functions - Ordinary and Conjugate Gradient Versions. J. Optimization Theory and Appl., Vol. 4, No. 4, 1969, pp. 213-243.

80. Hestenes, M. R.: Multiplier and Gradient Methods. J. Optimization Theory and Appl., Vol. 4, No. 5, 1969, pp. 303-320.

81. Hestenes, M. R.: Multiplier and Gradient Methods in Computing Methods in Optimization Problems - 2, Zadeh, L. A.; Neustadt, L. W.; and Balakrishnan, A. V., Ed., Academic Press, 1969.

82. Lasdon, L. S.; Mitter, S. K.; and Waren, A. D.: The Conjugate Gradient Method for Optimal Control Problems, IEEE Trans. on Auto. Control, Vol. AC-12, No. 2, 1967, pp. 132-138.

83. Miele, A.: Recent Advances in Gradient Algorithms for Optimal Control Problems. J. Optimization Theory and Appl., Vol. 17, No.'s 5 and 6, 1975, pp. 361-430.

84. Miele, A.; Tietze, J. L.; and Cloutier, J. R.: A Hybrid Approach to Optimal Control Problems with Bounded State, Computers and Maths. with Appl., Vol. 1, No. 2, 14, pp. 175-194.

85. Pagurek, B. and Woodside, C. M.: The Conjugate Gradient Method for Optimal Control Problems with Bounded Control Variables, Automatica, Vol. 4, No.'s 5 and 6, 1968, pp. 337-349.

86. McCormick, G. P.: An Arc Method for Nonlinear Programming, SIAM J. on Control, Col. 13, No. 6, 1975, pp. 1194-1216.

87. Kelley, H. J.; Denham, W. F.; Johnson, I. L.; and Wheatley, P.O.: An Accelerated Gradient Method for Parameter Optimization with Nonlinear Constraints, J. Astro. Sciences, Vol. 13, No. 4, 1966, pp. 166-169.

88. Speyer, J. L.; Kelley, H. J.; Levine, N.; and Denham, W. F.: Accelerated Gradient Projection Technique with Application to Rocket Trajectory Optimization, Automatica, Vol. 7, No. 1, 1971, pp. 37-43.

89. Hewett, M. D. and Kirk, D. E.: Trajectory Optimization Using a Second Order Epsilon Method. J. Aircraft, Vol. 13, No. 3, 1976, pp. 174-179.

90. Balakrishnan, A. V.: On a New Computing Technique in Optimal Control, SIAM J. Control, Vol. 6, No. 2, 1968, pp. 149-173.

91. Luenberger, D. G.: A Primal-Dual Algorithm for the Computation of Optimal Control in Computing Methods in Optimization Problems-2, Sadeh, L. A.; Neustadt, L. W.; and Balakrishnan, A. V., Ed., Academic Press, 1969.

92. Pironneau, O. and Polak, E.: A Dual Method for Optimal Control Problems with Initial and Ginal Boundary Constraints, SIAM J. Control, Vol. 11, No. 3, 1973, pp. 534-549.

93. Bertsekas, D. P.: Combined Primal-Dual and Penalty Methods for Constrained Minimization. SIAM J. Control, Vol. 13, No. 3, 1975, pp. 521-544.

94. Bertsekas, D. P. and Mitter, S. K.: A Descent Numerical Method for Optimization Problems with Nondifferentiable Cost Functionals, SIAM J. Control, Vol. 11, No. 4, 1973, pp. 637-652.

95. McReynolds, S. R. and Bryson, A. E., Jr.: A Successive Sweep Method for Solving Optimal Programming Problems, Joint Auto. Control Conf., June 22-25, 1965, Preprints of Conf. Papers, pp. 551-555.

96. Fletcher, R.: Function Minimization Without Evaluating Derivatives - A Review. Computer J. Vol. 8, No. 1, 1965, pp. 33-41.

Biography

Name: Arun Anant Nadkarni

Personal Data: Born in Bombay on August 27, 1944

Education: Received the Bachelor of Engineering degree in Mechanical Engineering from Bangalore University, India, in 1966; received the Master of Engineering degree in Aeronautical Engineering from Indian Institute of Science, India, in 1968; received the Master of Science degree in Aerospace Engineering from Pennsylvania State University in 1975.

Publications:

1) "Teleoperator Control for Passivation of Satellites Possessing Angular Momentum" at 1974 Annual Conference of Virginia Academy of Science at Norfolk, May 1974.
2) "Control and Stability Problems of Remote Orbital Capture" at Second Conference on Remotely Manned Systems, June 9-11, 1975, at USC, Los Angeles.
3) "On Stability of a Future Generation Spacecraft Attitude Control System: at IEEE South East Conference, April 1976, at Clemson University, South Carolina.
4) "Optimal Maneuvering and Fine Pointing Control of Large Space Telescope with a New Magnetically Suspended, Single Gimballed Momentum Storage Device" at 1976 IEEE Conference on Decision and Control, at Clearwater Beach, Florida, December 1-3, 1976.

5) "Optimal Fine Pointing Control of a Large Space Telescope Using an Annular Momentum Control Device" presented at IEEE 1977 Southeastcon, April 4-6, 1977, at Williamsburg, Virginia.

Professional Experience: Worked as an Aerodynamics Engineer in Space Science and Technology Center, India, from 1968 to 1972.

Membership of Professional Organizations Fellowship:

Member of the Honor Society of Phi Kappa Phi (Pennsylvania State University Chapter)

Student Member of the American Institute of Aeronautics and Astronautics and of the Institute of Electrical and Electronics Engineers.

Graduate Fellowship under ODU-NASA Aeronautics Research Participation Program.